INVESTIGATION OF THE RELATIONSHIP BETWEEN SPHINGOLIPID AND INSULIN SIGNALING PATHWAYS

by

Kübra Büyükyanbolu Karagöz

B.S., Chemical Engineering, Marmara University, 2007

Submitted to the Institute for Graduate Studies in
Science and Engineering in partial fulfillment of
the requirements for the degree of
Master of Science

Graduate Program in Chemical Engineering

Boğaziçi University

2010

ACKNOWLEDGEMENTS

First and foremost, I would like to thank to my thesis advisor, Prof. Kutlu Ö. Ülgen, for the valuable guidance and advice. I also would like to thank my thesis jury; Prof. Zeynep İlsen Önsan and Prof. Dilek Kazan.

I am grateful to my friends, especially Aysun Eren, Burcu Özkaral, Celal Ceylan, İpek Paksoy, Yasemen Güngörmez, Pınar Kanlıkılıçer, Betül Kavun, Saliha Durmuş, Elif Dereli, Ceyda Kasavi. I must also acknowledge Esra Börklü Yücel for her suggestions on my experiments.

I would also like to thank my mother, Hüsniye Büyükyanbolu, my father, Ragup Büyükyanbolu and my brother, Burak Büyükyanbolu and my husband, Turgay Karagöz for their never ending support and encouragement.

I also acknowledge the financial supports provided by BAP 09A501P and TÜBİTAK 108M649 projects.

ABSTRACT

INVESTIGATION OF THE RELATIONSHIP BETWEEN SPHINGOLIPID AND INSULIN SIGNALING PATHWAYS

Sphingolipids are the membrane lipids which have significant roles in signal transduction as second messengers and in regulatory pathways including cell cycle arrest, apoptosis, senescence and differentiation. Ceramide functioning in sphingolipid metabolism is known to inhibit Akt/ protein kinase B (PKB) which is one of the core proteins of insulin signaling pathway. However, the mechanism of crosstalk between sphingolipid signaling pathway and insulin signaling pathway has not been elucidated completely. In this study, we investigated the proteins which play important roles in the association of sphingolipid and insulin signaling pathways. The deletion mutants of *PKH1*, *YPK1* and *YPK2* of *Saccharomyces cerevisiae* at 30g/l initial glucose concentration had reduced IPC percentages compared to wild type strain in agreement with the literature information. However, at 40 g/l initial glucose concentration, the deletion mutants resulted in higher percentages of lipid composition compared to wild type strain as well as higher amounts of remaining glucose in the medium as expected. When the initial glucose concentration in the medium was increased, the effect of other proteins having roles in glucose signal reception and transduction might be dominant. Nevertheless, the experimental results on the relation between glucose consumption and complex sphingolipid production were found to be in agreement with the literature. Then, Akt2 protein was further investigated from the aspect of drug discovery since Akt/PKB is the most significant protein that affects GLUT4 translocation, and it is also a critical target protein for anticancer drug discovery. Therefore, the pockets of Akt2 were identified by using both geometric and energetic approaches. SplitPocket (geometry-based program) identified all the residues whereas Q-SiteFinder (energetic-based program) detected only one residue that was reported as an inhibitor binding site in literature. Furthermore, solvation energy, electrostatics and druggability index of binding pockets were also estimated. These results can be used as a starting point for docking suitable ligands.

ÖZET

SFİNGOLİPİD VE İNSÜLİN SİNYAL İLETİM AĞLARI ARASINDAKİ İLİŞKİNİN İNCELENMESİ

Sinyal iletiminde, hücre döngüsünün durdurulması, apoptoz, hücre yaşlanması ve farklılaşmasını da içeren düzenleyici iletim ağlarında önemli rol oynayan hücre zarı lipidleri, sfingolipidlerdir. Sfingolipid mekanizmasında görevi olan seramidin, insülin sinyal iletim ağındaki ana proteinlerden biri olan Akt/Protein Kinaz B'yi inhibe ettiği bilinir. Fakat sfingolipid ve İnsülin sinyal iletimleri arasındaki ilişki tam olarak açıklanamamıştır. Bu çalışmada, sfingolipid ve İnsülin sinyal iletimleri arasında önemli rol oynayan proteinler incelenmiştir. *PKH1*, *YPK1* ve *YPK2* genlerinin silinmiş olduğu *Saccharomyces cerevisiae* hücrelerinde 30 g/l başlangıç glikoz konsantrasyonunda IPC miktarının doğal suşa göre literatürle uyumlu bir şekilde azaldığı görülmüştür. Ancak 40g/l başlangıç glikoz konsantrasyonunda delesyon mutantlarında doğal şuşa nazaran daha fazla lipid bileşimi elde edilmiş ve ortamda daha fazla glikoz kaldığı bulunmuştur. Ortamdaki başlangıç glikoz miktarı arttığında glikoz sinyal iletiminde yer alan proteinlerin etkilerinin de önemli olduğu söylenebilir. Genel olarak, deneysel sonuçlarda glikoz tüketimi ve kompleks sfingolipid üretimi arasındaki ilişki literatürle uyumlu olarak bulunmuştur. GLUT4 yer değiştirmesini etkileyen en önemli proteinlerden biri olan Akt/PKB, antikanser ilaç buluşları için kritik bir hedef proteindir. Bu yüzden, Akt2 proteini ilaç keşfi açısından incelenerek Akt2'nin cepleri hem geometrik hem de enerjik yaklaşımla tanımlanmıştır. Literatürde tanımlanmış inhibitör bağlanma amino asitlerinden, SplitPocket (geometrik yaklaşıma dayalı program) bitin amino asitleri tanımlarken, Q-SiteFinder (enerjik yaklaşıma dayalı program) sadece bir amino asit tanımlayabilmiştir. Bunun yanı sıra, bağlanma ceplerinin çözünme enerjisi, elektrostatik ve ilaç indeksleri gibi parametlerde incelenmiştir. Bu elde edilen sonuçlar, uygun ligand bulunmasında başlangıç noktası olara kullanılabilir.

TABLE OF CONTENTS

ACKNOWLEDGEMENT iii
ABSTRACT iv
ÖZET v
LIST OF FIGURES ix
LIST OF TABLES xvi
1. INTRODUCTION 1
2. BACKGROUND ASPECTS 3
2.1. Sphingolipid Signaling 3
2.1.1. Biosynthesis and Chemical Structure of Sphingolipids 4
2.1.2. Sphingolipid Metabolism in *Saccharomyces cerevisiae* 6
2.1.3. The Relation of Pkh1, Ypk1 and Ypk2 Proteins with Sphingolipid Pathway 8
2.2. Insulin Signaling 10
2.2.1. Pathways of Insulin Signaling 10
2.2.2. Glucose Transport 12
2.3. Sphingolipids in Insulin Resistance 12
3. MATERIALS AND METHODS 15
3.1. Homology Search 15
3.1.1. KEGG Pathway Database 15
3.1.2. BLAST (Basic Local Alignment Search Tool) 15
3.2. Experimental Materials 16
3.2.1. Deletion Mutant Strains Adopted 16
3.2.2. Storage of the Strains 16
3.2.3. Chemicals and Disposal Materials Used 16
3.2.3.1. Culture Media 16
3.2.3.2. Glassware Required for Analyses 17
3.2.3.3. Buffers and Chemicals Required for HPLC 17
3.2.4. Laboratory Equipments 18
3.3. Experimental Methods 19

3.3.1. Sterilization ……. 19
3.3.2. Cultivation Conditions ……..……. 19
3.3.3. Glucose Analyses …… 20
3.3.4. Lipid Extraction …….. 20
3.3.5. HPLC Analysis of the Extracted Lipids …….. 20
3.4. Computational Methods for Pocket Identification …… 21
3.4.1. Geometric Approaches …… 21
3.4.1.1. CAST/CASTp …… 21
3.4.1.2. SCREEN …… 23
3.4.1.3. SplitPocket ……. 24
3.4.2. Energetic Approaches: Using static 3D protein structures …..…….. 25
3.4.2.1. Q-SiteFinder ……... 25
3.4.2.2. Pocket-Finder ……. 26
3.4.2.3. SITEHOUND ……. 27
3.4.3. Analysis of the Physicochemical Properties of Binding Sites …… 29
3.4.3.1. Geometry ……..……. 29
3.4.3.2. Amino Acid Composition ……...……... 29
3.4.3.3. Solvation ……...……. 29
3.4.3.4. Electrostatics ……... 30
3.4.3.5. Chemical Fragment Interactions ……. 30
4. EXPERIMENTAL RESULTS AND DISCUSSION ……..…….. 31
4.1. Insulin and Sphingolipid Signaling Pathways ……..……..... 31
4.2. Batch Experiments with Yeast Cells (Wild Type and Deletion Mutants) …….. 34
4.3. Crosstalk Between Sphingolipid and Insulin Signaling Networks ……. 42
4.3.1. Regulation of Akt/Protein Kinase B by Sphingolipid Pathway Metabolites …… 42
4.3.2. The Physical and Genetic Interactions of *PKH1*, *YPK1* and *YPK2* ……. 46
5. AKT2 POCKET IDENTIFICATION FOR DRUG DEVELOPMENT …… 51
5.1. Structure of Akt2 ……..…….…….…..... 51
5.2. Ligand Binding Site Identification by Geometric Approaches …..…….…... 54
5.2.1. CAST/CASTp …..……..……..... 54
5.2.2. SCREEN ……..... 59
5.2.3. SplitPocket ……...……..... 64

5.2.4. Comparison of Geometry Based Web Servers ……..……... 67
5.3. Ligand Binding Site Identification by Energetic Approaches …….. 70
5.3.1. Q-SiteFinder …… 71
5.3.2. Pocket-Finder …….. 76
5.3.3. SITEHOUND …….. 81
5.3.4. Comparison of Energy Based Web Servers …… 86
5.4. Comparison of All Pocket Detection Servers ……. 88
5.5. Analysis of the Physicochemical Properties of Binding Sites …… 93
5.5.1. Geometry ……...……. 93
5.5.2. Amino Acid Residue Composition ……. 96
5.5.3. Solvation ……. 96
5.5.4. Electrostatics ……... 98
5.5.5. Chemical Fragment Interactions ……. 100
6. CONCLUSIONS AND RECOMMENDATIONS ……..... 101
6.1. Conclusions ……. 101
6.2. Recommendations..……..……..... 105
APPENDIX A: ANNOTATION-COLLECTION TABLES …….. 106
A.1. Process …… 106
A.2. Component ……. 124
A.3. Function …….. 135
APPENDIX B: THE CONSUMPTION OF GLUCOSE IN THE MEDIUM …… 150
REFERENCES ……... 151

LIST OF FIGURES

Figure 2.1.	Biological roles of sphingolipids ……..……	4
Figure 2.2.	Overview of sphingolipids structure ……..……..……	5
Figure 2.3.	The sphingomyelin cycle ……..……..……	6
Figure 2.4.	Sphingolipid metabolism in Saccharomyces cerevisiae ..…….....	7
Figure 2.5.	The signaling pathways controlled by Long chain Acid Bases in yeast	9
Figure 2.6.	The relation of Ypk2 and Pkh1 with ceramide and sphingolipid synthesis in yeast ……..……	9
Figure 2.7.	Insulin signaling pathway …….……....	11
Figure 2.8.	Glucose transport in muscle and fat cells …….....	13
Figure 2.9.	Regulation of Akt/PKB by ceramide	14
Figure 4.1.	Insulin signaling pathway ……..…….	31
Figure 4.2.	Growth profile of wild type and deletion mutants (20g/l glucose concentration) ……..…….....	35
Figure 4.3.	Growth profile of wild type and deletion mutants (30g/l glucose concentration) ..…….....	35
Figure 4.4.	Growth profile of wild type and deletion mutants (40g/l glucose concentration) ..…….	35

Figure 4.5. Time course of glucose remaining in the medium (for 20 g/l initial glucose concentration) …… ……. 36

Figure 4.6. Time course of glucose remaining in the medium (for 30 g/l initial glucose concentration) ……..... 36

Figure 4.7. Time course of glucose remaining in the medium (for 40 g/l initial glucose concentration) 37

Figure 4.8. Lipid analysis of wild type strain by HPLC (30 g/l initial glucose concentration) ……..... 38

Figure 4.9. Lipid analysis of the deletion mutant of by HPLC (30 g/l initial glucose concentration) 38

Figure 4.10. Lipid analysis of the deletion mutant of by HPLC (30 g/l initial glucose concentration) ……..... 39

Figure 4.11. Lipid analysis of the deletion mutant of . By HPLC (30 g/l initial glucose concentration) 39

Figure 4.12. Lipid analysis of wild type strain by HPLC (40 g/l initial glucose concentration) ……..... 40

Figure 4.13. Lipid analysis of the deletion mutant of by HPLC (40 g/l initial glucose concentration) 41

Figure 4.14 Lipid analysis of the deletion mutant of by HPLC (40 g/l initial glucose concentration) ……..... 41

Figure 4.15. Lipid analysis of the deletion mutant of . by HPLC (40 g/l initial glucose concentration) ……..…… 42

Figure 4.16. The regulation of insulin action by ceramide ……..…..…… 43

Figure 4.17. PHS activates AGC protein kinases ….……..…… 44

Figure 4.18. Torc2p and PHS activate Ypk2p for ceramide synthesis ……..... 45

Figure 4.19a. Physical interaction of Pkh1p ……..……... 47

Figure 4.19b. Genetic interaction of Pkh1p …..…… 47

Figure 4.20a. Physical interaction of Ypk1p ……...…..…….……..... 47

Figure 4.20b. Genetic interaction of Ypk1p ...……..... 47

Figure 4.21a. Physical interaction of Ypk2p 48

Figure 4.21b. Genetic interaction of Ypk2p ……..……. 48

Figure 4.22. Pyhsical interaction network of *PKH1, YPK1, YPK2, SCH9, PPH22* and *PKC1* ……..……..... 49

Figure 4.23. Pyhsical interaction network of *PKH1, YPK1, YPK2, SCH9, PPH22, PKC1, LCB1, LCB2, TSC3, TSC10, LAG1, LAC1* and *LIP1* 50

Figure 5.1. The structure of the protein kinase domain of Akt2 protein (PDB 1gzn)..... 52

Figure 5.2 The structure of PH domain of Akt2 protein (PDB 1p6s) …….. 52

Figure 5.3. The structure of protein kinase domain complex with inhibitor A-443654 (PDB 2jdr) ……..... 52

Figure 5.4. Jmol visualization of Akt2 (PDB 1gzn) by using CASTp 55

Figure 5.5. The areas and volumes of the protein kinase domain of Akt2 pockets' as a result of CASTp quest ……..... 55

Figure 5.6. Amino acid composition of the largest pocket and its mouth (PDB 1gzn) ……..……..…… 56

Figure 5.7. Jmol visualization of Akt2 (PDB 1p6s) by using CASTp 57

Figure 5.8. The areas and volumes of the PH domain pockets' as a result of CASTp quest ……...…… 58

Figure 5.9. Amino acid composition of PH domain of Akt2 by using CASTp results ……..……..... 58

Figure 5.10. MarkUs visualization of Akt2 (PDB 1gzn) ……... 60

Figure 5.11. Amino acid composition of the first ranked cavity …….. 61

Figure 5.12. Analysis of the role of cavity area on the predicting binding sites …... 61

Figure 5.13. MarkUs visualization of Akt2 (PDB 1p6s) ……..... 62

Figure 5.14. Amino acid composition of PH domain as a result of SCREEN 62

Figure 5.15. The connection between the area and the rank order of the pockets … 63

Figure 5.16. SplitPocket output window for Akt2 ……..……..……..... 65

Figure 5.17. Analysis of volume and area relation with pocket number (SplitPocket-protein kinase domain) ……. 66

Figure 5.18. Amino acid composition of functional surface of Akt2 protein kinase domain (PDB 2jdr) ……...……..… 66

Figure 5.19. The comparison of amino acid composition of mouth opening ……... 67

Figure 5.20. Overlap in ligand binding residues in the first predicted site of protein kinase domain ……..……... 69

Figure 5.21. Overlap in ligand binding residues in the first predicted site of protein kinase domain (all geometry based methods) ……. 69

Figure 5.22. Overlap in ligand binding residues in the first predicted site of pleckstrin homology domain ……..…..……..…… 70

Figure 5.23. The output of Q-SiteFinder for protein kinase domain……..... 72

Figure 5.24. Amino acid composition of the predicted site 1 of protein kinase domain of Akt2 ……..……...……...…… 73

Figure 5.25. Analysis of the role of predicted site volume of protein kinase domain on the predicting binding sites …...……... 73

Figure 5.26. The outputs of Q-SiteFinder for pleckstrin homology domain of Akt2 74

Figure 5.27. Amino acid composition of the predicted site 1 for PH domain of Akt2 ……... 75

Figure 5.28. Analysis of the role of predicted site volume on the predicting binding sites ……..... 75

Figure 5.29. The output of Pocket-Finder for kinase domain of Akt2 …..…… 77

Figure 5.30. Amino acid composition of the predicted sites 1 and 2 for kinase domain of Akt2 ……..……..……..... 78

Figure 5.31. The output window of Pocket-Finder for PH domain ……. 79

Figure 5.32. Amino acid composition of the predicted sites 1 and 2 for plekstrin homology domain of Akt2 80

Figure 5.33. Analysis of the role of predicted site volume on the predicting binding sites ……..……..... 80

Figure 5.34. SITEHOUND-web Carbon probe, average linkage clustering algorithm output example of kinase domain …….…….. 81

Figure 5.35. Comparison of the amino acid compositions of clustering algorithms (Protein kinase domain) ……..…….... 83

Figure 5.36. SITEHOUND-web Carbon probe, average-linkage clustering algorithm visualization of PH domain ……..... 83

Figure 5.37. The amino acid composition comparison of clustering algorithms (PH domain) ……...……..……..…… 84

Figure 5.38. Volume and rank relation of clusters ……..... 85

Figure 5.39. Overlap in the first ligand binding site (protein kinase domain) ……. 86

Figure 5.40. Overlap in ligand binding sites prediction in the first predicted site for protein kinase domain ……..…..... 87

Figure 5.41. Overlap in ligand binding sites (the second ranked site) for protein kinase domain ……... 87

Figure 5.42. Analysis of predicted residues in the first pocket related to PH domain ……...…… 88

Figure 5.43. Overlap in residues in the first predicted site for protein kinase domain by using CASTp, SITEHOUND, Pocket-Finder and Split Pocket ……... 91

Figure 5.44. Overlap of residues in ligand binding sites (first predicted site) for PH domain using CASTp, SCREEN, Q-SiteFinder, SITEHOUND and Pocket-Finder ……..…….... 92

Figure 5.45. Druggability index of protein kinase and PH domain of Akt protein ... 100

LIST OF TABLES

Table 3.1.	Parameters of the HPLC system	21
Table 4.1.	The results of BLAST analysis …….....	32
Table 4.2.	The sphingolipid pathway proteins in *S. cerevisiae* …….	34
Table 4.3.	The amounts of lipids measured by HPLC for 30g/l initial glucose concentration ……	37
Table 4.4.	The amounts of lipids measured by HPLC for 40g/l initial glucose concentration …….....	40
Table 4.5.	Physical interactions of Pkh1, Ypk1 and Ypk2 ……..	46
Table 4.6.	Genetic interactions of Pkh1, Ypk1 and Ypk2 ……	46
Table 5.1.	The residues of the pocket that interacts with inhibitors …….....	53
Table 5.2.	The comparison of the domains of Akt2 …….	59
Table 5.3.	The analysis of the largest pocket of protein kinase domain and pleckstrin homology domain of Akt2 ……..……	59
Table 5.4.	The features of Kinase domain and PH domain of Akt2 ……..	63
Table 5.5.	Comparison of the number of pockets detected by CASTp, SCREEN an SplitPocket ……	67

Table 5.6. The first ranked pocket comparison predicted by CASTp, SCREEN and SplitPocket ……...…….... 68

Table 5.7. The comparison of the predicted site 1 of protein kinase domain and pleckstrin homology domain of Akt2 76

Table 5.8. Pocket-Finder results comparison of predicted site 1 of protein kinase domain and pleckstrin homology domain of Akt2 ……..... 80

Table 5.9. The comparison of average-linkage and single-linkage clustering algorithm by using Carbon probe …….……..……. 82

Table 5.10. The comparison of average-linkage and single-linkage clustering algorithms in analyzing the PH domain …….…….. 84

Table 5.11. Comparison of first Clusters of Protein kinase domain and pleckstrin homology domain by using carbon probe and average-linkage clustering algorithm ……...……... 85

Table 5.12. The correlation of the ligand binding site prediction methods, Q-SiteFinder, Pocket-Finder and SITEHOUND for protein kinase domain ... 86

Table 5.13. The comparison of ligand binding site identification methods for protein kinase domain of Akt2 ……...……. 90

Table 5.14. The Ligand binding residues in literature ……..……..... 91

Table 5.15. The comparison of ligand binding site identification methods for pleckstrin homology domain of Akt2 ….……. 93

Table 5.16. The geometric features of the pockets given by CASTp (Top part kinase domain, bottom part PH domain) …….…… 94

Table 5.17. The geometric properties of the cavities identified by SCREEN …… 94

Table 5.18. The implementation of SplitPocket to assess geometric properties of kinase domain (PDB 2jdr) …….. 95

Table 5.19. Comparison of volumes of predicted ligand binding sites for kinase domain and PH domain of Akt2 protein ……...…….... 95

Table 5.20. Conservation scores of the first predicted binding sites……..…….. 96

Table 5.21. Solvation energy values belonging to protein kinase domain and PH domain of Akt2 protein..... 97

Table 5.22. Solvation energy values belonging to protein tyrosine phosphatase 1B (PDB 1l8g) and human factor Xa complexed with inhibitor RPR128515 (PDB 1ezq) ……..……..... 97

Table 5.23. Average charge, average electric potential and average electric field of protein kinase domain and PH domain of Akt protein ……..……. 98

Table 5.24. Average charge, average electric potential and average electric field of protein tyrosine phosphatase 1B (PDB 1l8g) and human factor Xa complexed with inhibitor RPR128515 (PDB 1ezq) ..…….. 99

Table A.1.1. Biological process terms of the significant proteins in insulin signaling pathway …….. 106

Table A.1.2. Biological process terms of the proteins in yeast found by BLAST …… 110

Table A.1.3. Biological process terms of the proteins that interact physically with Pkh1 112

Table A.1.4. Biological process terms of the proteins that interact physically with Ypk1 ……..…….. 114

Table A.1.5. Biological process terms of the proteins that interact physically with Ypk2 ……..……..... 116

Table A.1.6. Biological process terms of the proteins that interact genetically with Pkh1 ……..…….. 118

Table A.1.7. Biological process terms of the proteins that interact genetically with Ypk1 ……..…… 120

Table A.1.8. Biological process terms of the proteins that interact genetically with Ypk2 ……..... 123

Table A.2.1. Cellular component terms of the significant proteins in insulin signaling pathway ……..……. 124

Table A.2.2. Cellular component terms of the proteins in yeast found by BLAST …….. 126

Table A.2.3. Cellular component terms of the proteins that interact physically with Pkh1 ……..... 128

Table A.2.4. Cellular component terms of the proteins that interact physically with Ypk1 …..…….. 129

Table A.2.5. Cellular component terms of the proteins that interact physically with Ypk2 ……..…….. 130

Table A.2.6. Cellular component terms of the proteins that interact genetically with Pkh1 ……..……..... 131

Table A.2.7. Cellular component terms of the proteins that interact genetically with Ypk1 ……..…….. 132

Table A.2.8. Cellular component terms of the proteins that interact genetically with Ypk2 …….…… 134

Table A.3.1. Molecular function terms of the significant proteins in insulin signaling pathway ……..... 135

Table A.3.2. Molecular function terms of the proteins in yeast found by BLAST…..…. 139

Table A.3.3. Molecular function terms of the proteins that interact physically with Pkh1 ……..... 141

Table A.3.4. Molecular function terms of the proteins that interact physically with Ypk1 …….…….... 142

Table A.3.5. Molecular function terms of the proteins that interact physically with Ypk2 …...…….. 144

Table A.3.6. Molecular function terms of the proteins that interact genetically with Pkh1 ……. 145

Table A.3.7. Molecular function terms of the proteins that interact genetically with Ypk1 …….…….... 147

Table A.3.8. Molecular function terms of the proteins that interact genetically with Ypk2 …...…….. 149

Table B.1. The consumption of glucose in the medium (at 20 g/l initial concentration) …….. 150

Table B.2. The consumption of glucose in the medium (at 30 g/l initial concentration) …….. 150

Table B.3. The consumption of glucose in the medium (at 40 g/l initial concentration) …….. 150

1. INTRODUCTION

Sphingolipids are involved in membrane lipids which are structural components of the cell membrane. Sphingolipids play significant roles in signal transduction as second messengers and in regulatory pathways involving cell cycle arrest, apoptosis, senescence and differentiation. The recent studies show that bioactive sphingolipids are required for cancer therapeutics. Ceramide is a central molecule in sphingolipid pathway and a reasonable key metabolite in cancer therapy since ceramide induces antiproliferative and apoptotic responses (Ogretmen, 2006).

Insulin is known as the most potent anabolic hormone which promotes the synthesis and storage of carbohydrates, lipids and proteins and inhibits their degradation. Decreased secretion of insulin as well as insulin resistance leads to type 2 diabetes (Saltiel and Pessin, 2002). The insulin resistance is not only related with type 2 diabetes but also related with obesity, hypertension, polycystic ovarian syndrome, dyslipidemia and atherosclerosis. The diverse effects of insulin action are identified at the cellular level that includes changes in vesicle trafficking, stimulation of protein kinases and phosphatases, promotion of cellular growth and differentiation. Therefore, the insulin action and signaling pathway is involved in many signaling processes. Akt/PKB is a central mediator of insulin signaling pathway and it plays significant roles on glucose uptake and anabolic metabolism (Stratford et al., 2004).

The association between sphingolipid and insulin signaling pathway is revealed by the relation between ceramide and Akt/Protein kinase B (PKB). Two independent mechanisms explain the effects of ceramide on Akt/PKB. The common feature of these mechanisms is the inhibition of Akt/PKB action by ceramide. Protein phosphatase 2A (PP2A) is directly activated by ceramide and then PP2A dephosphorylates Akt/PKB in the first mechanism. Additionally, PKC is also activated by ceramide, then it phosphorylates the residue of Thr34 on PH domain of Akt; so Akt/PKB translocation from cytoplasmic store to the plasma membrane is blocked (Summers, 2006).

Despite considerable attention, the molecular mechanisms by which sphingolipid regulates insulin action are remained both elusive and controversial. Within the framework of this thesis, the homologs of proteins involved in insulin signaling of *H. Sapiens* were found in *Saccharomyces cerevisiae* by using Basic Local Alignment Search Tool (BLAST). Then Ypk1p, Ypk2p and Pkh1p were chosen for further investigation and their deletion mutants were used to clarify the relation of these proteins in sphingolipid pathway and glucose uptake. Additionally, Akt2 was determined as a drug target; so the pockets of Akt2 were identified by using both geometric and energetic approaches and the results were compared in detail.

Following this brief introduction, the second chapter gives more detail in sphingolipid and insulin signaling pathways and their relations. The third chapter gives information about the experimental methods for investigation of significant proteins related with these pathways in *S. cerevisiae* and computational methods for pocket identification used in this work. Moreover, the fourth and fifth chapters focus on the experimental results and discussion, and Akt2 pocket identification, respectively. The last chapter is "Conclusions and Recommendations" which gives a brief summary of the main results and contributions to the scientific literature including the recommendations for future work.

2. BACKGROUND ASPECTS

2.1. Sphingolipid Signaling

Sphingolipids are classified as membrane lipids and a family of important signaling molecules such as sphingosine, ceramide and sphingosine-1-phosphate are involved in sphingolipids. Sphingolipids effect on many regulatory pathways by regulating phosphates and kinases. Moreover, they play significant roles on many cell processes including differentiation, migration and apoptosis (Ogretmen and Hannun, 2004; Cowart and Obeid, 2007). Sphingosine and sphingosine bases direct actin cytoskeleton, the cell cycle, endocytosis and apoptosis whereas ceramide takes part in the regulation of cancer cell growth, differentiation, senescence and apoptosis (Hannun and Obeid, 2008; Hannun and Obeid, 2002). Additionally, sphingosine-1-phosphate is essential for regulation of proliferation, inflammation, vasculogenesis, and it provides resistance to apoptotic cell death as shown in Figure 2.1 (Payne *et al*., 2002).

Diabetes, many different types of cancers, Alzheimer's disease, heart disease and many neurological syndromes are related with sphingolipids; so the understanding of sphingolipid metabolism and signaling targets of the sphingolipids are very significant to know these diseases (Summers, 2006; Ogretmen and Hannun, 2004; Sawai *et al*., 2005; Park *et al*., 2006; Ginzburg *et al*., 2004).

Saccharomyces cerevisiae serves as a simple model system that contributes to the understanding of basic cell processes like cell cycle control. Furthermore, sphingolipid containing pathways between all eukaryotes are conserved; so yeast is suitable for studying biosynthesis, regulation and function of sphingolipids (Dickson *et al*., 2006).

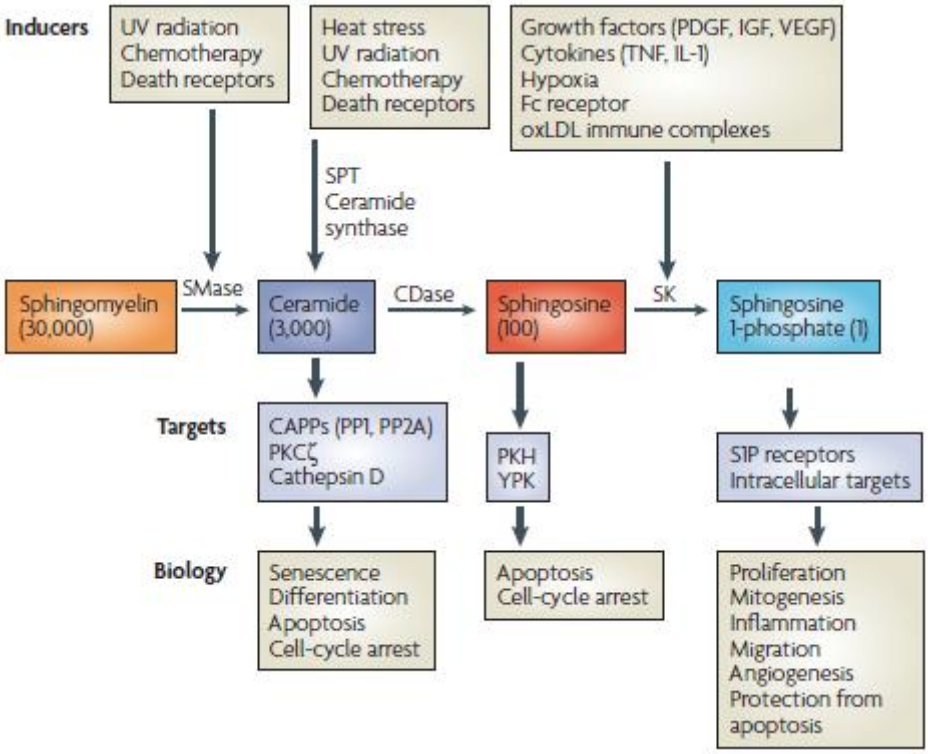

Figure 2.1. Biological roles of sphingolipids (Hannun and Obeid, 2008).

2.1.1. Biosynthesis and Chemical Structure of Sphingolipids

The term sphingolipids include more than hundreds of lipid compounds that differ in their chemical structure and biological functions; yet they are united by a common structural feature called sphingoid base (Dyatlovitskaya, 1999). A sphingoid base backbone is synthesized *de novo* from serine and a long-chain fatty acyl-coenzyme A, then converted into ceramides, phosphosphingolipids, glycosphingolipids and other species including protein adducts (Figure 2.2). These molecules compose the key structure of cell membranes and lipoproteins (Hirabayashi *et al.*, 2006).

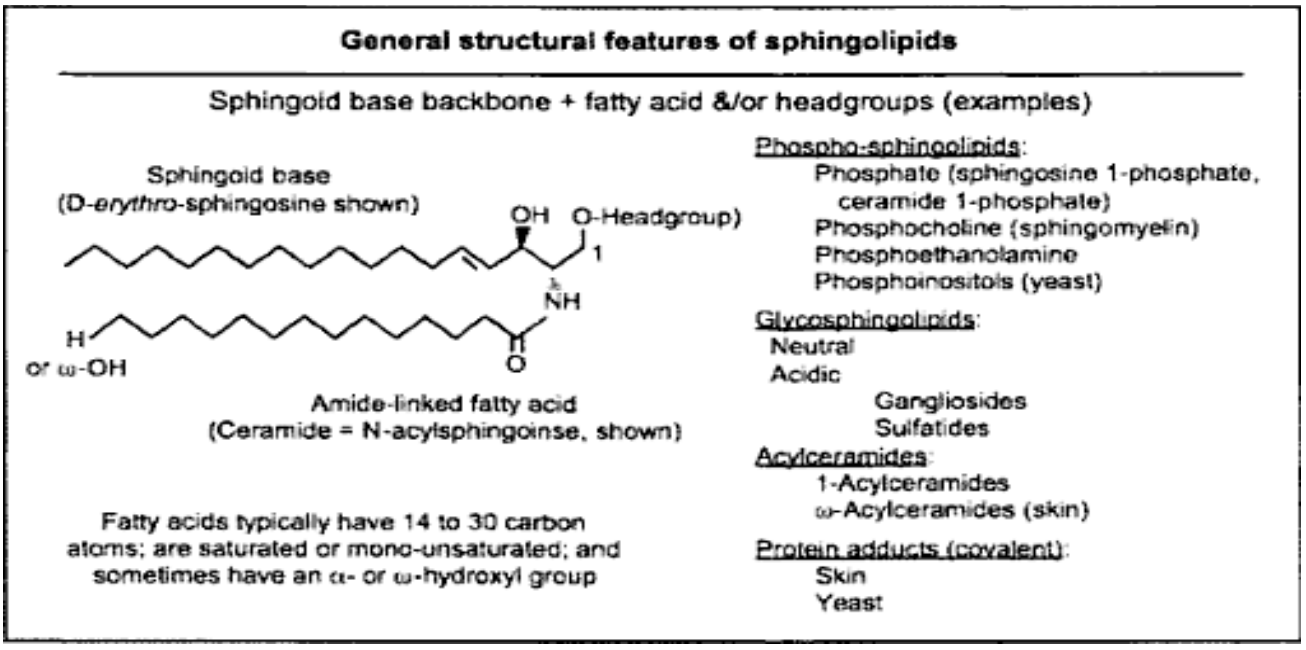

Figure 2.2 Overview of sphingolipids structure (Hirabayashi *et al*., 2006).

Sphingolipids can be classified into several major classes: **1.** *Long-chain bases (sphingoid bases)* are typical structural units of the sphingolipids that consist of long-chain aliphatic amines, containing two or three hydroxyl groups and differ in trans-double bond at position 4. The different derivatives of sphingoid bases are the 1-phosphates, lysosphingolipids (such as sphingosine 1-phosphocholine as well as sphingosine 1 glycosides), and N-methyl derivatives (N-methyl, N,N-dimethyl- and N,N,N-trimethyl-). The modification of functional groups permits the transformation of the sphingosine molecule into complicated sphingolipids. **2.** *Ceramides* consist of sphingoid base that are linked to a fatty acid by an amide bond. Ceramides are formed as the key intermediates in the biosynthesis of all the complex sphingolipids, in which the terminal primary hydroxyl group is linked to carbohydrate, phosphate. Predominantly saturated alkyl chains give ceramides high phase transition temperatures which favor the segregation of ceramides into specialized regions of membranes. **3.** *Phosphosphingolipids* are more complex sphingolipids with head groups that are attached by phosphodiester linkages, and the major phosphosphingolipids of mammals are sphingomyelins (ceramide phosphocholines).

4. *Glycosphingolipids* are also complex molecules and their head groups are attached by glycosidic bonds (Hirabayashi et al., 2006; Fahy *et al*., 2005).

De novo biosynthesis of sphingolipids is essential for many types of cells for membrane structure, cell-cell and cell-matrix interactions and numerous biological processes that are regulated by bioactive metabolites such as ceramide and sphingosine 1-phosphate (Hirabayashi *et al.*, 2006). Moreover, the biosynthesis and catabolism of sphingolipids include a large number of these intermediate metabolites whose biological activities are different from each other. Sphingomyelin cycle demonstrates the relationships between these metabolites in animals as shown in Figure 2.3 (Hannun and Obeid ,2008).

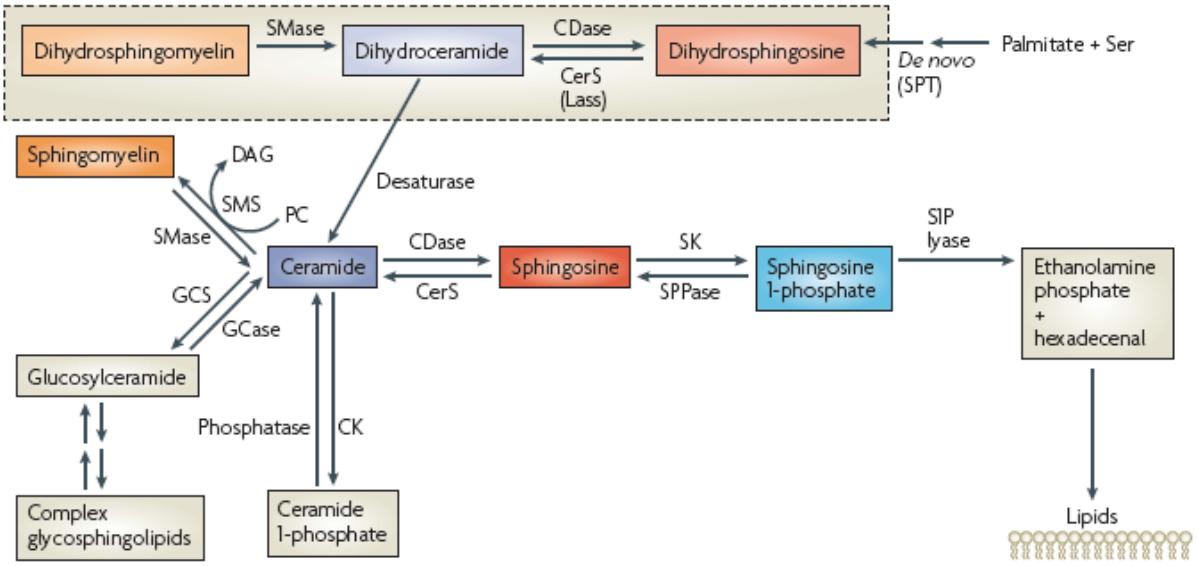

Figure 2.3 The sphingomyelin cycle (Hannun and Obeid, 2008).

2.1.2. Sphingolipid Metabolism in *Saccharomyces cerevisiae*

A long chain base (LCB), a fatty acid and a polar head group form sphingolipids. In *Saccharomyces cerevisiae*, dihydrsphingosine (DHS) and Phytosphingosine (PHS) are the LCBs which are necessary for cell viability (Dickson, 2008).

The initial step of sphingolipid synthesis occurs in the endoplasmic reticulum. Serine and a fatty acyl-CoA are condensed by serine palmitoyl transferase (SPT) to produce 3-ketodihydrosphingosine and CO_2. Lcb1, Lcb2 and Tsc3 proteins are required for SPT activity, and they are found in all organisms which contain sphingolipids. 3-ketodihydrosphingosine is converted to dihydrosphingosine (DHS) by the 3-ketodihydrosphingosine reductase which is also named as Tsc10 protein (Dickson, 2008).

In the next step of yeast sphingolipid synthesis, DHS yields dihydroceramide catalyzed by ceramide synthase enzyme encoded by Lag1 and Lac1. Furthermore, dihydroceramide is also hydroxylated to form phytoceramide by Sur2/Syr2 proteins. On the other hand, phytoceramide is also formed by hydroxylation of DHS producing PHS. Lip1 is another protein to form ceramide synthase; but its function is not known. In the endoplasmic reticulum, fatty acids are elongated from C_{14}-C_{18} to C_{26} by the very long chain fatty acid synthase which is described as elongation cycle (Figure 2.4) (Dickson, 2008).

Inositol phosphoceramide (IPC), mannose inositol phosphoceramide (MIPC) and mannose-(inositol-P)2-ceramide ($M(IP)_2C$) are the complex sphingolipids which are produced in Golgi by adding polar head groups to ceramides. Inositol phosphate is the first head group that is added to ceramide, and IPC synthase is used to catalyze this reaction to produce IPC. Then mannose is transferred from GDP-mannose onto the inositol 2-OH moiety of IPC to yield MIPC by mannosyl inositol phosphoceramide transferase. In the last step, a second inositol phosphate is transferred from phosphatidylinositol to MIPC to yield $M(IP)_2C$. The complex sphingolipids are broken down to ceramides and polar head groups by Isc1 protein (Dickson, 2008).

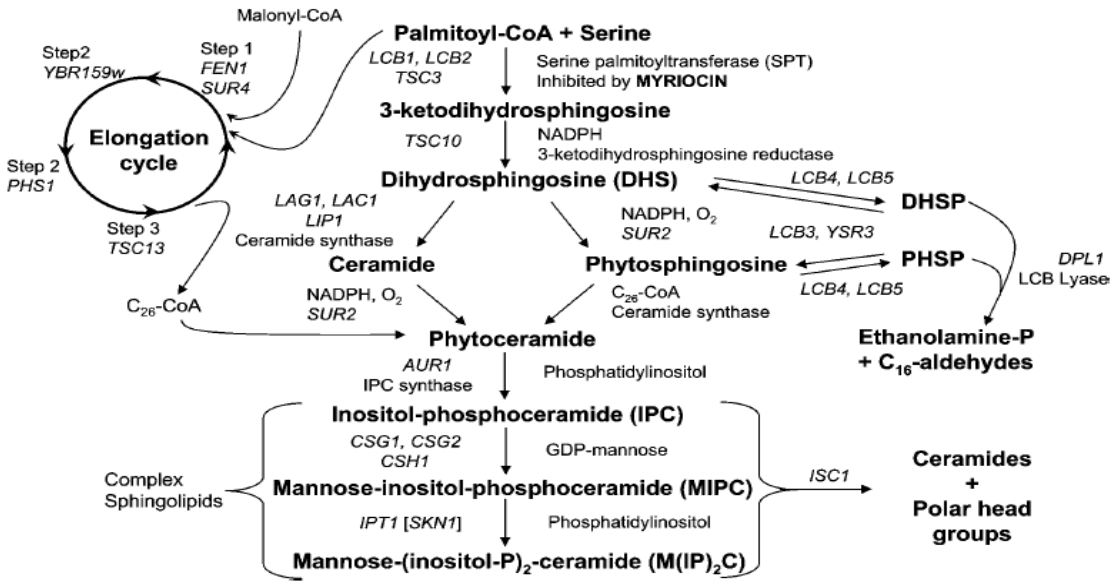

Figure 2.4. Sphingolipid metabolism in Saccharomyces cerevisiae (Dickson, 2008).

2.1.3. The Relation of Pkh1, Ypk1 and Ypk2 Proteins with Sphingolipid Pathway

Ypk1p and its paralog Ypk2p are both structural and functional homologs of mammalian serum- and glucocorticoid-inducible kinase (Casamayar *et al*., 1999). Ypk1p and Ypk2p are protein kinases that play significant roles in cell wall maintenance, actin cytoskeleton dynamics, and endocytosis (Schmelzle *et al*., 2002; Roelants *et al*., 2002; deHart *et al*., 2002). Although the losses of *YPK1* causes slow growth, double deletion mutant of *YPK1* and *YPK2* is lethal (Luo *et al*., 2008). YPK kinases also act as an effector of TORC2 and PKH kinases, and control actin cytoskeleton organization and endocytosis with MPK1-MAP kinase cascade and the type I myosins (Myo5) (Schemelzle *et al*., 2002; Grosshans *et al*., 2006).

PKH kinase, Pkh1p and Pkh2p, are yeast orthologues of the mammalian PDK1 protein kinase. The loss of Pkh1p or Pkh2p has little affect on cell growth although the deletion of both protein is lethal (Liu et al., 2005). Pkh1p and Pkh2p are required for actin cytoskeleton organization and endocytosis (Friant et al., 2001).

YPK kinases are phosphorylated by TORC2 and PKH kinases (Roelants *et al*.,2002; Kamada *et al*., 2005; Liu *et al*., 2005). After LCBs are increased by heat stress, they activate Pkh1p and Pkh2p. Moreover, LCBs also affect Ypk1p, Ypk2p and Sch9p by increasing their activities. Pkh1 and Pkh2 phosphorylate Ypk1, Ypk2, Sch9 and Pkc1 in their activation loop; but they are not enzymatically active. They are required to be phosphorylated in hydrophobic region, and TORC1 and TORC2 phosphorylate the hydrophobic region of Sch9 and Ypk2, respectively, as shown in Figure 2.5 (Liu et al., 2005; Dickson 2008).

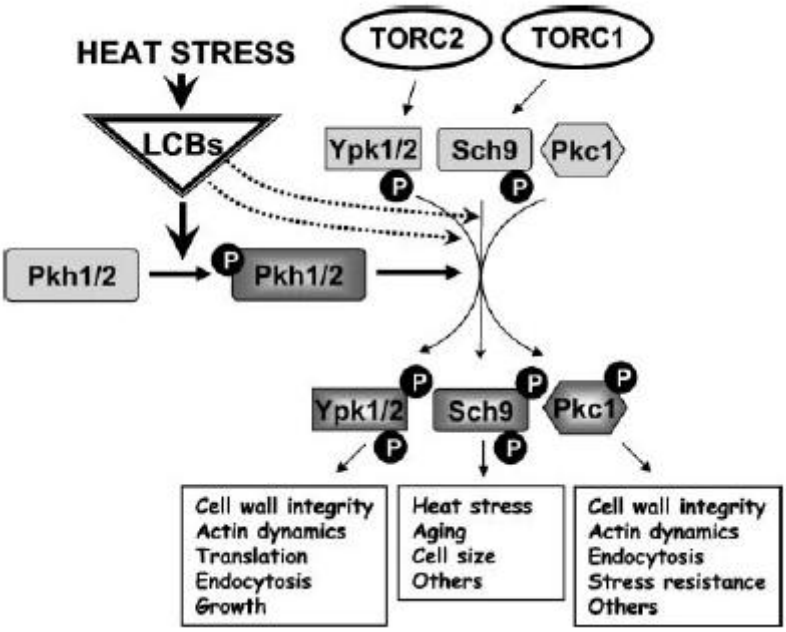

Figure 2.5. The signaling pathways controlled by long chain acid bases in *S. cerevisiae* (Dickson, 2008).

DHS and PHS activate Pkh1p and Pkh2p that further activate Ypk2p. DHS and PHS also directly activate Ypk2 (Liu et al., 2005). After that, Ypk2p activates ceramide synthase which affects the amount of complex sphingolipid synthesis as shown in Figure 2.6 (Dickson, 2008).

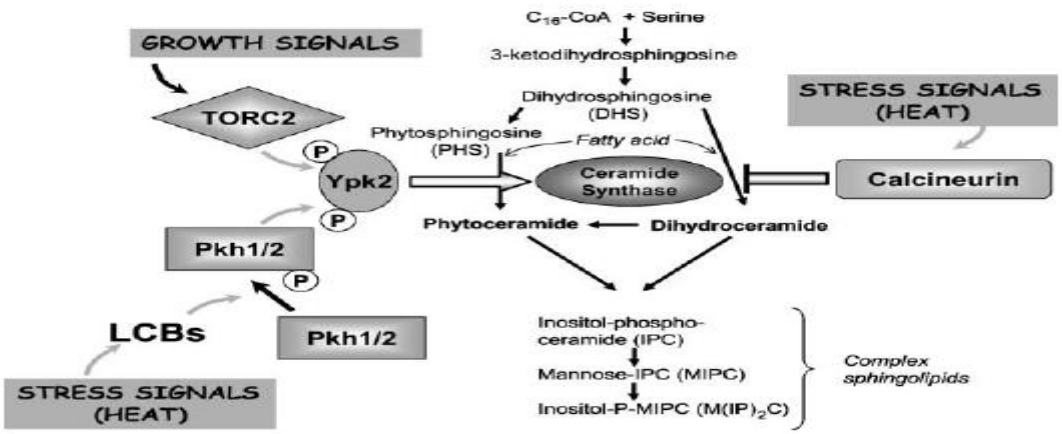

Figure 2.6. The relation of Ypk2 and Pkh1 with ceramide and sphingolipid synthesis in yeast (Dickson, 2008).

2.2. Insulin Signaling

Diabetes is caused by the defect of insulin responses, synthesis or secreting. There are two types of diabetes which are Type 1 and Type 2 diabetes. Autoimmune destruction of insulin producing beta cells causes Type 1 diabetes. Nevertheless, at least 75% of the diabetics are Type 2 diabetes (Cohen et al., 1997). The main characteristic of Type 2 diabetes is insulin resistance which is described by the failure of target tissues to increase whole body glucose disposal in response to insulin. Insulin-stimulated glucose uptake and metabolism are reduced in the fat and skeletal muscle tissues of people with Type 2 diabetes. Moreover, the importance of Type 2 diabetes is due to its association with obesity, hypertension, cardiovascular disease (Schmitz-Peiffer, 2000).

2.2.1. Pathways of Insulin Signaling

Insulin is a peptide hormone which maintains glucose homeostasis and regulates the metabolism of carbohydrate, lipid and protein. Insulin signaling network is a highly integrated and complex controlling many cell processes (Taniguchi et al., 2006).

The insulin signaling pathway contains hundreds of molecules; but the best-defined critical nodes are characterized as the insulin receptor (IR) / insulin receptor substrate (IRS), the phosphatidylinositol 3-kinase (PI3K) and Akt/protein kinase B (PKB) proteins that are required for insulin action. IR and IRS play roles in insulin resistant, hyperinsulinaemic state that includes Type 2 diabetes and obesity. Additionally, PI3K activates critical regulators in insulin signaling network. Akt controls the metabolic actions of insulin that is mediated by PI3K, and Akt is responsible for phosphorylation of kinases, signaling proteins and transcription factors (Taniguchi et al., 2006).

At the initial step of insulin signaling pathway, the IR phosphorylates IRS in the presence of insulin. Then IRS activates two main signaling pathways. The first one is the PI3K-Akt/PKB pathway that controls most of the metabolic actions of insulin. The second pathway is the Ras-mitogen activated protein kinase (MAPK) pathway which is

responsible for expression of some genes and cooperates with the PI3K pathway to control cell growth and differentiation (Taniguchi et al., 2006).

In PI3K/Akt pathway, IRS activates PI3 kinase that produces phosphatidylinositol (3,4,5)-triphosphate (PIP3). PIP3 contains the binding site which is for proteins containing pleckstrin homology (PH) domain. Serine/Threonine kinases, PKB and phosphatidylinositol-3-phosphate dependent kinase 1 (PDK1) have PH domain; which enables PIP3 and PKB or PDK1 interactions. PIP3 causes conformation changes in PKB; so it activates PKB. All these signaling events take place at plasma membrane. However, activated PKB relocates from plasma membrane to the cytosol. Furthermore, part of the activated PKB goes to the nucleus and provides the transcription of many target genes (Figure 2.7) (Li and Zhang, 2007; Langeveld and Aerts, 2009).

IR induces another signaling pathway called Ras/MAPK pathway that includes Growth factor binding protein 2 (Grb2)/ son of sevenless (Sos) and Ras, leading to the activation of MAPK isoforms, extracellular signal-regulated kinases ERK1 and ERK2. MAPK cascade is not associated with insulin stimulated glucose transport or glycogen synthesis. However, Ras/MAPK pathway regulates cell survival and proliferation (Figure 2.6) (Langeveld and Aerts, 2009).

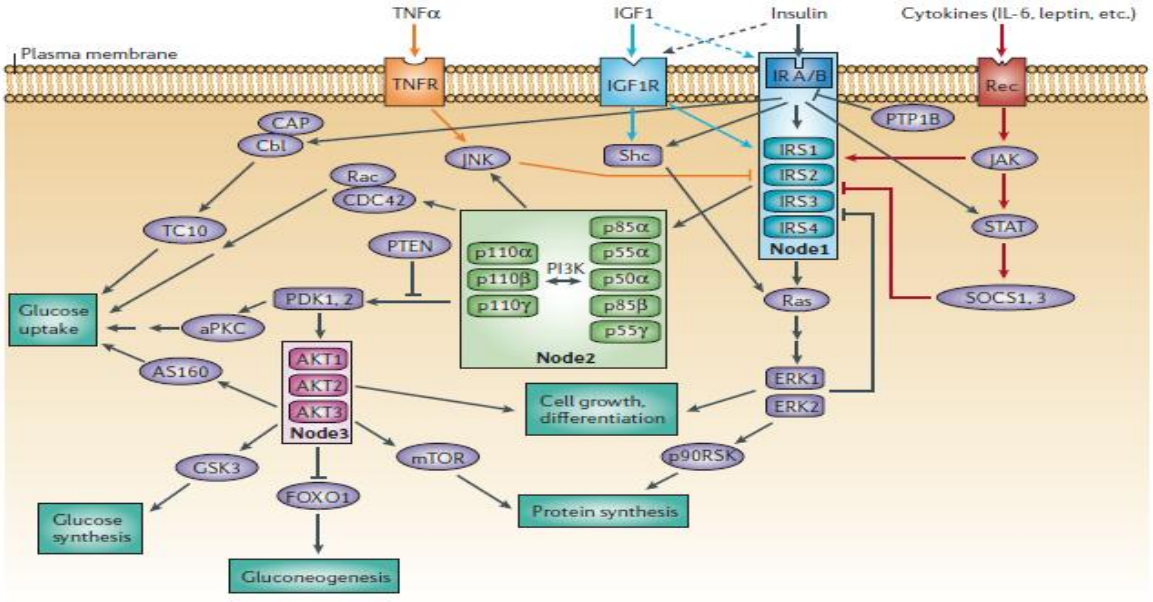

Figure 2.7. Insulin signaling pathway (Taniguchi et al., 2006).

2.2.2. Glucose Transport

Two different signaling pathways are involved in insulin-regulated GLUT4 translocation. The first one has the lipid kinase phosphatidylinositol 3-kinase (PI3K), and the second one has the proto-oncoprotein c-Cbl. Insulin binds to its receptor on the surface of target cells. This binding leads to a conformational change in the receptor and causes the activation of its tyrosine-kinase domain. Activated receptor phosphorylates many substrates such as the insulin-receptor substrates (IRS-1 and IRS-2) and c-Cbl (Bryant *et al*., 2002). The phosphorylated IRS proteins are held in close proximity to the plasma membrane through the association with the effector molecules such as PI3K. Furthermore, the serine/threonine kinase Akt/protein kinase B (PKB) and the typical protein kinase C (PKC) isoform, PKCζ, are the important targets of PI3K in muscle and fat cells that has a role in insulin-stimulated GLUT4 translocation. Activated Akt and PKCζ promote the translocation of GLUT4 to the plasma membrane, and GLUT4 allows glucose uptake as shown in Figure 2.8.

Akt has three isoforms; Akt1, Akt2 and Akt3. Akt1 controls cell and body size (Cho *et al*., 2001). Akt2 controls GLUT4 trafficking in adipose and muscle cells and mediate insulin signaling to control glucose output in liver (Cho *et al*., 2001; Jiang *et al*., 2003), and Akt3 controls brain size (Easton et al., 2005).

2.3. Sphingolipids in Insulin Resistance

Insulin resistance, which is a state characterized by impaired responsiveness of liver, muscle adipose tissue to insulin, is associated with Type 2 diabetes, obesity, hypertension and cardiovascular disease. The relation between lipid availability and insulin resistance is revealed by many studies (Schmitz-Peiffer, 2000; Summers, 2006).

Ceramide is a mediator in signaling cascades that control apoptosis, differentiation and cell cycle arrest (Ozbayraktar and Ulgen, 2009). Another role of ceramide is defined in insulin signaling pathway. It inhibits insulin stimulated glucose uptake, GLUT4 translocation and glycogen synthesis (Summers *et al*., 1998).

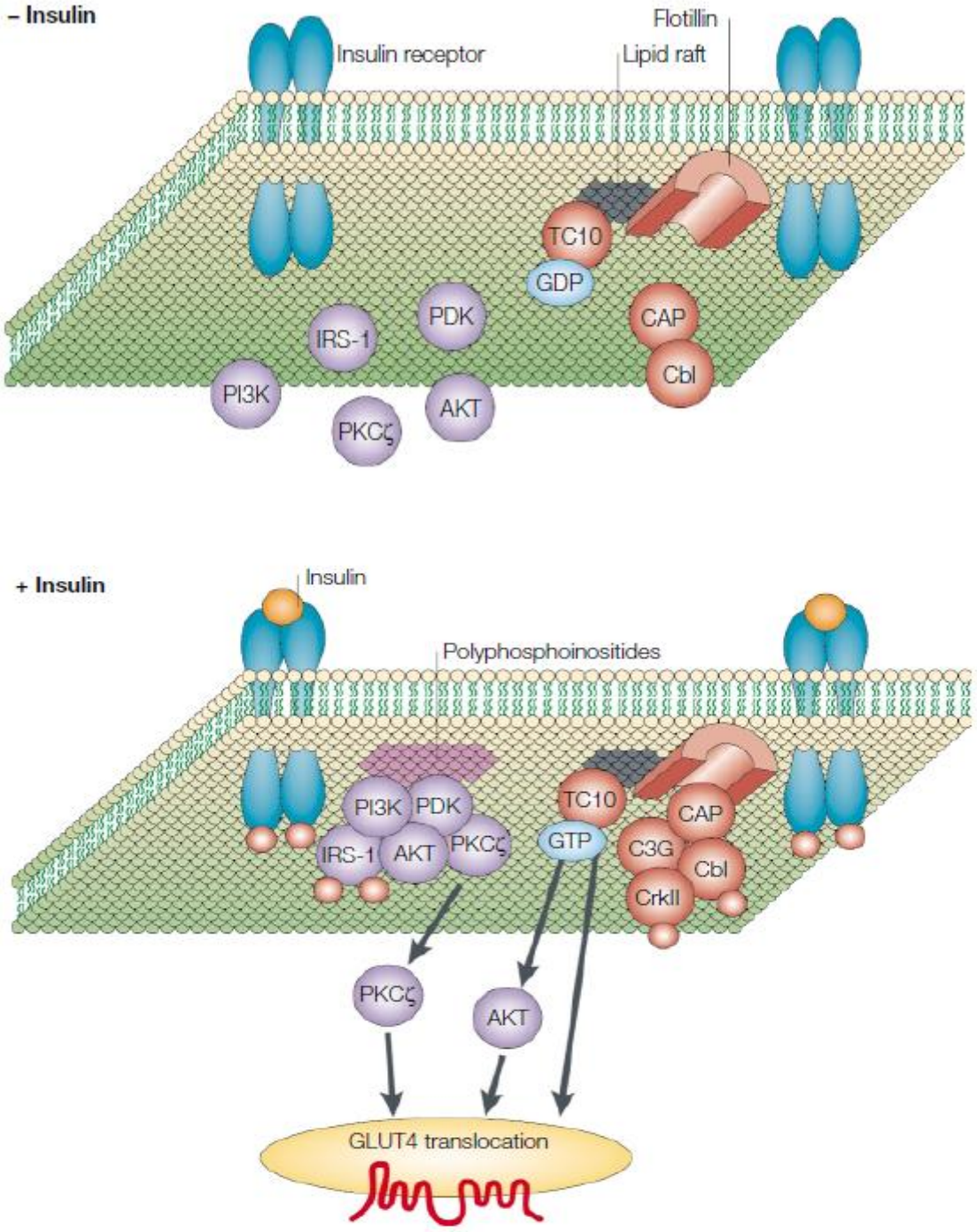

Figure 2.8. Glucose transport in muscle and fat cells (Bryant et al., 2002).

Although ceramide does not impair the phosphorylation of IR and IRS, it inhibits the activation of Akt/PKB (Stratford *et al*., 2004).

Two independent mechanisms are determined for inhibition of Akt/PKB by ceramide as shown in Figure 2.9 (Holland and Summers, 2008). Firstly, ceramide directly activate protein phosphatase 2A (PP2A) which promotes the dephosphorylation of Akt /PKB (Summers, 2006). Secondly, ceramide activate another enzyme PKCζ that inhibits the translocation of Akt/PKB by phosphorylation of Threonine-34 (Langeveld and Aerts, 2009; Summers, 2006).

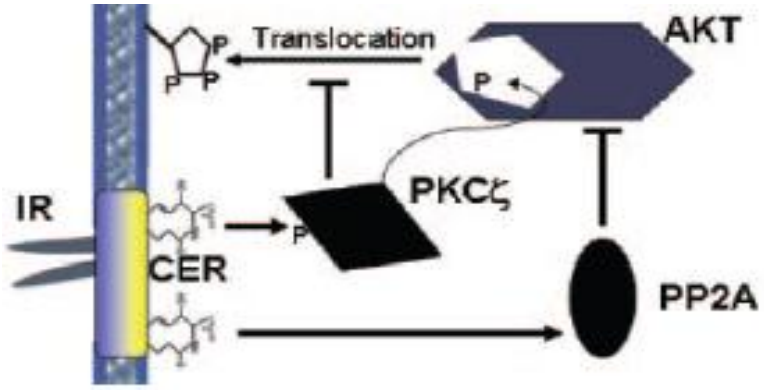

Figure 2.9. Regulation of Akt/PKB by ceramide (Holland and Summers, 2008).

Akt has many downstream targets that control tumor-associated cell processes including cell growth, cell cycle progression, survival and migration. If Akt signaling is blocked, it results in apoptosis and growth inhibition of tumor cells with elevated Akt level. Some tumors are dependent on Akt signaling for survival and growth; thus work on Akt signaling provides wide implications for cancer therapy (Cheng *et al*., 2005). The combinatorial chemistry, high-throughput and virtual screening, and traditional medicinal chemistry offer opportunities for discovering a number of inhibitors of the Akt pathway in last several years; thus Akt/PKB is an attractive therapeutic target in anticancer drug development (Lindsley *et al*., 2005; Saxty *et al*., 2007; Medina-Franco *et al*., 2009).

3. MATERIALS AND METHODS

3.1. Homology Search

3.1.1. KEGG Pathway Database

KEGG (Kyoto Encyclopedia of Genes and Genomes) is an integrated database which includes 16 main databases classified into 3 groups: systems information, genomic information and chemical information. The functional properties of biological systems are described by the class of system information. The cellular processes and organism behaviors are controlled by the molecular system and the data sources concerned with the molecular system are obtained manually from literature and they are presented as a graph called “pathway map” (Kanehisa et al., 2009).

KEGG Pathway is freely accessible through http://www.genome.jp/kegg/pathway.html. The pathway map displays information about different kinds of molecular networks: reaction/interaction networks for metabolism, genetic information processing, environmental information processing, perturbed reaction/interaction networks for human diseases and relation networks (chemical structure transformation networks) for drug development. KEGG Pathway map demonstrates the molecular network as a graph which is formed by nodes and edges. Nodes represent orthologs, genes, protein or small molecules, and edges display reactions, interactions or relations. Pathway maps also provide basic information about the nodes like name, definition, amino acid sequence and nucleotide sequence of the proteins, pathways and classes of the proteins. Moreover, PDB codes of proteins and the links related with the protein are given by the pathway maps (Kanehisa et al., 2009).

3.1.2. BLAST (Basic Local Alignment Search Tool)

The Basic Local Alignment Tool (BLAST) identifies similar residues/amino acids among the sequences. Nucleotide or protein sequences in different organisms can be compared to sequence databases and the statistics of matching are computed by the program of BLAST. It also gives information about functional and evolutionary

relationships between sequences and characterizes members of gene families. BLAST is available at http://blast.ncbi.nlm.nih.gov.

Two types of blast, protein and nucleotide blasts are used in this work. Protein blast searches protein database by using a protein query and nucleotide blast searches nucleotide database by using a nucleotide query. The homolog of the protein is selected with respect to E-values computed by BLAST. The lowest E-value infers that the match is significant.

3.2. Experimental Materials

3.2.1. Deletion Mutant Strains Adopted

EUROSCARF project enabled the production of the deletion mutant strains of *Saccharomyces cerevisiae*. A parent strain of *Saccharomyces cerevisiae*, BY4743 and three homozygous deletion mutant strains , and were used in experiments and they were kindly provided by Prof. Stephen Oliver, Manchester.

3.2.2. Storage of the Strains

Frozen stocks were prepared and kept at -80^{o}C. They include one ml of preculture and one ml of 30 per cent (v / v) glycerol. Moreover, the preparation of preculture is as follows; fifty ml of complex (YPD) medium was inoculated with a single colony of cells, and was incubated overnight at 30 ^{o}C and 180 rpm agitation.

3.2.3. Chemicals and Disposable Materials Used

3.2.3.1. Culture Media: Two types of culture media, yeast extract-peptone-dextrose medium (YPD) in liquid form and F1 (limited) medium, were used in this study.

- Composition of YPD Media : Yeast Extract 1 per cent (Lab M) and Bacteriological Peptone 2 per cent (Acumedia) were dissolved in distilled water. After sterilization of this medium, 40 per cent glucose, which was prepared as a stock previously, was added to the remaining medium.

- Composition of F1 Medium: D-Glucose 2.1 per cent (Merck), $(NH_4)_2SO_4$ 0.313 per cent (Merck), KH_2PO_4 0.2 per cent (Merck), $MgSO_4.7H_2O$ 0.055 per cent (Merck), NaCl 0.01 per cent (Merck), $CaCl_2.2H_2O$ 0.009 per cent (Merck), Uracil 0.002 per cent (Fluka), Histidine 0.002 per cent (Lifco), Leucine 0.01 per cent (Merck), Trace Element Solution 1 0.01 per cent, Trace Element Solution 2 0.01 per cent, Vitamin Stock Solution 0.17 per cent volume/volume of distilled water.
- Composition of Trace Element Solution 1: $ZnSO_4.7H_2O$ 0.07 per cent (Merck), $CuSO_4.5H_2O$ 0.01 per cent (Merck), H_3BO_3 0.01 per cent (Merck), KI 0.01 per cent (Merck) in distilled water.
- Composition of Trace Element Solution 2: $FeCl_3.6H_2O$ 0.05 per cent (BDH) in distilled water.
- Composition of Vitamin Stock Solution: Inositol 3.72 per cent (Merck), Thiamine / HCl 0.84 per cent (Sigma), Pyridoxine 0.24 per cent (Fluka), Ca-panthothenate 2.4 per cent (Fluka), Biotin 0.018 per cent (Merck) in distilled water.

Filter was used to sterilize the vitamin stock solution. 0.22 m filters were attached to the tip of the syringes and vitamin stock solution was added by syringes to the remaining part of the medium.

3.2.3.2. Glassware Required for the Analyses: When lipids contact with surfaces other than glass, metal or teflon, they are corrupted. Therefore, glass pipettes were used for pipetting purposes. Pasteur pipettes and micropipettes of volumes of 1-5, 10 and 20 l were obtained from Hirschmann Laborgerate. Pyrex centrifuge tubes of 100 ml were bought from DuPont.

3.2.3.3. Buffers and Chemicals Required for HPLC: All standards of sphingolipids were bought from Sigma and Avanti Polar Lipids. Furthermore, HPLC grade chloroform, methanol, ethanol and n-hexane were purchased from Sigma.

HPLC analysis required mobile phase which included HPLC grade Chloroform ($CHCl_3$)/Ethanol (EtOH)/Triethylamine (TEA)/Formic Acid(FA) (90:10:1:1 v/v). The concentrations of TEA and FA were 70 and 220 mM, respectively.

3.2.4. Laboratory Equipments

- Autoclave — ALP Model CL-40M (Japan)
- Balance — Precisa 80A-200M (Switzerland)
- Centrifuge — Avanti J-26 XPI Refrigerated Superspeed Centrifuge, Beckmann Coulter (USA)
- Deep freezers — -80^{o}C, New Brunswick Scientific U410 (England)
  -20^{o}C, BOSCH (Germany)
- HPLC System — 1515 Binary HPLC Pump, Waters (USA)
  717 plus Autosampler, Waters (USA)
  2420 ELSD, Waters (USA)
- Incubators — NÜVE EN500 (Turkey)
- Orbital Shakers — GFL 3032, GFL (Germany)
  INNOVA 4340 Illuminated refrigerated Incubator Shaker, New Brunswick Scientific (USA)
  EXCELLA E1 Open air shaker, New Brunswick Scientific (USA)
- Ovens — Incucell, MMM Group (Germany)
  VO 400 vacuum oven, Memmert (Germany)
- Refrigerators — +4^{o}C Arçelik (Turkey)
- Spectrophotometer — DU 640 Beckman (USA)
- Water Purification Systems — Millipore, Milli Ro Plus (USA)
  Millipore, Milli-Q UF Plus (USA)

3.3. Experimental Methods

3.3.1. Sterilization

Sterilization was required during the experiments due to contamination problem. The autoclave at 15 psig pressure and 121^{o}C was used for steam sterilization. Moreover, the sterilization of instruments was also required, and all sterile equipments were maintained by using sterile gloves and a sterile fume hood.

The culture medium and glucose stock solution were steam sterilized for 15 min and 3 min, respectively. All the equipments used in the experiments such as plastic tips and tubes, glass pipetting material, Erlenmeyer flasks were steam sterilized for 15 minutes at 15 psig and 121 °C. Filter sterilization was also used for vitamin solution while it was transferred from its stock to F1 medium.

3.3.2. Cultivation Conditions

Precultures were prepared by using YPD medium. Frozen stock which contained preculture and glycerol was added to 20 ml YPD medium and incubated at 30^{o}C and 180 rpm in orbital shakers. The optical density of the preculture was measured and when it was between 0.9 and 1.1, it was assumed that the culture reached its late exponential phase and could be used in experiments. The UV spectrophotometer was employed to determine the optical density where a wave length of 600 nm was used.

500 ml Erlenmeyer flasks were used in batch cultivations. 1-2 ml of preculture was inoculated into 200 ml F1 medium and incubated at 30^{o}C and 180 rpm in orbital shakers. The optical density of the samples was measured on hourly basis to control whether the culture was at steady state. When the state steady phase was reached, the samples were collected. This part of the experiment took approximately 24 h.

3.3.3. Glucose Analysis

The samples were taken at different times while the yeast cells were growing. Then, the samples were centrifuged and the supernatants were taken and the pellet samples were discarded. The supernatants were put into water bath at 80°C for 15 min. After that, D-Glucose (UV Method) kit of Roche was used to compute the amount of glucose in the medium. The calculation procedure was also given by D-Glucose kit so the results were obtained easily.

3.3.4. Lipid Extraction

The cells were washed by deionized water and then harvested by centrifuging for 5 min at 3000 rpm and 25°C and the supernatants were discarded. The pellets were resuspended in deionized water, and they were centrifuged again. Then the pellet sample was left to freeze at -20°C overnight.

For sphingolipid analysis, the washed pellet was extracted with 5 ml of ethanol-water 4:l at 100°C for 15 min and centrifuged. The upper phase was taken with a Pasteur pipette and saved in another glass tube. The pellet was extracted twice in identical fashion. All centrifugations were performed using Avanti J-26 XPI, Beckman-Coulter centrifuge with JA-14 rotor.

3.3.5. HPLC Analysis of the Extracted Lipids

In this work, a normal phase HPLC which separates analytes according to their polarities was used. The polar stationary phase and the nonpolar mobile phase were silica and a mixture of $CHCl_3$/EtOH, respectively. The polar stationary phase retained the polar analytes which were the lipids of interest.

A 3 m C_{18} Silica column (4.6x150 mm) and a guard column of the same material (4.6x25 mm) of Waters were employed in HPLC analysis of lipids. The parameters used (McNabb *et al.*, 1999) are listed in Table 3.1. The mobile phase, the composition of which was explained in section 3.2.3.3, was prepared and degassed under helium sparging for

about 20 min. Before injection, the column and the guard column were washed with mobile phase at about 15 min. ELSD detector was used with nitrogen gas at high pressure. Isocratic elution procedure was adopted in HPLC analysis.

Table 3.1. Parameters of the HPLC system.

Flow rate (ml/min)	0.5
Column Temperature (^{0}C)	25
Gain	6
Gas Pressure (bar)	1.9
Drift Tube Temperature (^{0}C)	70

3.4. Computational Methods for Pocket Identification

3.4.1. Geometric Approaches

The pockets or crevices on the protein surface or cavities in the protein are the binding sites for small molecules so the identification of pockets and cavities is used as a starting point for protein function annotation, protein-ligand docking and protein structure-based drug design. Many computational methods are generated to find out protein pockets by using the geometric characteristics of protein shape. Some instances are POCKET, LIGSITE, SURFNET, CAST, PASS and PocketPicker and none of them need the knowledge of the ligands (Henrich et al., 2009).

3.4.1.1. CAST / CASTp: Protein surfaces have complex shapes which include many concavities and protrusions and that specific environment provide ligand binding sites and catalytic sites. Ligands which function biologically, usually bind one or a few pockets at the active site. CAST is a program that identifies pockets and cavities in the protein structures and quantifies their size. It is based on alpha shape theory and discrete flow theory. CAST characterizes the pockets and cavities by computing volume, surface area and atoms, area and circumferences of pocket mouth(s) (Liang et al., 1998).

Active site analysis and structure based ligand design require shape and size parameters of pockets and cavities. CAST has a unique feature that computes mouth parameters. Mouths are analyzed by calculating the area of the mouth openings, identifying the “rim” atoms and the surrounding residues of the mouths. Mouth parameters are necessary to analyze molecular recognition and binding since pocket mouth number and size indicate the accessibility of ligand to the pocket interior (Liang et al., 1998).

The atomic van der Waals radii and the radius of the probe sphere are the only parameters that are required for CAST calculation. The probe sphere is necessary since it is used to define molecular surface. Probe radius is not adjusted by CAST and there is no generation of spheres of varying size to fill the pocket although many other programs employ variable sized probes (Liang et al., 1998).

The computational procedure of CAST involves many steps. Firstly, the atomic radius of each atom is accessed through PDB2ALF program by using PDB file. Secondly, three-dimensional weighted Delaunay triangulation is calculated by using DELCX program. Thirdly, MKALF program is used to compute the alpha shape. After these initial steps, the outputs of these three programs are assessed by using additional programs, RASMOL, VOLBL and ALVIS. Molecular visualization of pockets is produced by RASMOL. Moreover, the area and the volume of the each atom and also the whole molecule is computed by using VOLBL. Finally, Delaunay tetrahedral visualization of pockets can be generated by using ALVIS (Liang et al., 1998).

CASTp (http://cast.engr.uic.edu) is the new version of CAST and it includes annotated functional information of specific residues on the protein structure. The sequence mapping between entries in Swiss-Prot, OMIM and entries in PDB are obtained by a semi-global pair-wise sequence alignment method. The updated CASTp web server can be used to study surface features, functional regions and specific roles of key residues of proteins (Dundas et al., 2006).

The only input of CASTp is the 4 letter PDB code of protein structure. The number of pockets and their areas and volumes are given as outputs. Furthermore, Jmol visualization of the protein is presented as an output. The corresponding sequence map is

also shown and residues of the pocket can be highlighted in the same color as in structural visualization. The PDB structure of protein can be demonstrated in cartoon, wireframe, strands or ribbons and the color of pockets can be changed (Dundas et al., 2006).

3.4.1.2. SCREEN: SCREEN, **S**urface **C**avity **Re**cognition and **E**valuatio**n**, is a new method to find surface cavity of proteins. Surface cavities are defined geometrically by SCREEN. Cavity volume and area are estimated accurately. Each surface cavity is identified not only by measures of the surface shape but also by various properties of the residues on the cavity's floor. Thus, this definition generates a cavity property profile (Nayal and Honig, 2006).

SCREEN is unique to report the physicochemical properties of surface cavities. Many physical, chemical and structural properties have been considered, including various measures of cavity size, electrostatics, hydrogen bonding, hydrophobicity and polarity, amino acid composition, rigidity, secondary structure and cavity shape (Nayal and Honig, 2006).

SCREEN uses Random Forests, machine learning technique. It uses computed cavity profile to distinguish drug-binding cavities from non-drug binding cavities. The main reasons to choose Random Forests are that higher-order interactions can be detected, prior scaling of input variables is not required and the presence of a large number of irrelevant variables is not matter. These characteristics play a significant role in computing the properties because some calculated features may not be related to drug binding although combination of some of them makes sense (Nayal and Honig, 2006).

The algorithm of SCREEN is formed by several steps. Two molecular surfaces, a conventional molecular surface (MS) and the low-resolution envelope surface (ME), are firstly constructed by using GRASP. ME determines a ceiling for surface cavities. Furthermore, the contiguous MS surface regions are used to identify surface cavities. The second step is the clustering of MS surface vertices by using single-link clustering. After clusters are found, contraction operation is employed to remove all boundary vertices from the clusters. The last step is one-step expansion operation where vertices that pass the

depth criteria and are removed in the previous step, are re-enrolled in the contracted cluster (Nayal and Honig, 2006).

To sum up, the summation of the areas of the cavity surface triangles gives the surface area of the cavity. The volume of the cavity is described by the space between the cavity surface floor and its corresponding molecular envelope ceiling. Every surface vertex is corresponding with a protein atom during the construction of the molecular surface. Therefore, various physicochemical properties can be mapped from the protein on the cavity surface (Nayal and Honig, 2006).

SCREEN requires only PDB code of protein structure as an input. The output file includes physicochemical properties of cavities. SCREEN is accessed through MarkUs web server.

3.4.1.3. SplitPocket: A functional surface of a protein is defined by local regions where ligands, substrates or proteins interact with the protein; so the identification of the functional surfaces of a protein is significant to understand the binding features of the protein (Tseng et al., 2009).

SplitPocket is an online tool that identifies functional surfaces of a protein by using structure coordinates. To predict functional surfaces, SplitPocket uses information about geometric, physicochemical and evolutionary characteristics of protein. Furthermore, SplitPocket models the shape of binding surface whereas many other methods model the shape of a ligand (Tseng et al., 2009).

Alpha Shape Theory is used to describe molecular surfaces, and geometric measurements are calculated by the theory. The shape of the protein is modeled by using customized probe radii. A protein is divided into regions, protein cores and surfaces, by using the weighted-Delaunay triangulation. While a protein is dividing into parts, discrete flow algorithm is used with customized probes to get the pockets. Each pocket's length, solvent accessible area and volume are computed. Additionally, a mouth of the pocket, its sequence and solvent accessible area are obtained. SplitPocket only detects the functional surface(s) of an unbound structure. Conservation index of each pocket is also computed to

investigate its evolutionary conservation by the entropy measure of sequence variability (Tseng et al., 2009).

The coordinates of the protein structure is required by the SplitPocket thus PDB code is the only input. PDB file can be uploaded instead of PDB code. The output window of SplitPocket includes 3 levels: Profile, Predicted Pockets and The Functional Surface. The fundamental structural information is given by Profile window. Predicted Pockets window includes the sequence information of each pocket. It is important to emphasize that the predicted pocket is putative binding site and it can or cannot be a functional surface. The Functional Surface window displays the amino acid sequence of functional surface and mouth, and their solvent accessible areas and molecular volume (Tseng et al., 2009).

3.4.2. Energetic Approaches: Using Static 3D Protein Structures

The energy calculations can be used to locate small ligand binding sites on the protein surface. The interaction energy between the protein and a probe or chemical group is computed by positioned probe appropriately close to protein surface atoms or at a grid points surrounding the protein. Q-SiteFinder, Pocket-Finder and SITEHOUND are the web servers for ligand binding sites prediction by using energetic approaches (Henrich et al., 2009).

3.4.2.1. Q-SiteFinder: A protein interacts with other proteins and ligands on a specific site which is described by functional surface. The detection of functional site plays a significant role to address particular sites in structure-based drug design to help the discovery of new therapeutic agents. Therefore, the analysis of protein surface for pocket provides ligand binding site prediction. The largest pocket is usually the ligand binding site (Laurie and Jackson, 2005).

Q-SiteFinder (http://www.bioinformatics.leeds.ac.uk/qsitefinder) is a method to identify pockets of a protein by using energetic approach. The van der Waals interaction energies of a methyl probe with the protein is computed to define pockets. Probes with appropriate interaction energies are ascertained; then these probes are clustered to rank

according to their interaction energies. The first ranked cluster is the energetically most favorable cluster. It is important to state that the first ranked cluster may not be the largest one geometrically (Laurie and Jackson, 2005).

Q-SiteFinder uses some pre-processing steps to predict ligand binding site. Firstly, LigandSeek program is employed to separate ligand coordinates from other atom coordinates. Secondly, all HETATM records are changed into ATOM records, and water molecules are separated from the protein file. Thirdly, hydrogen atoms are added to the protein. Finally, the volume of the box enclosing the protein is minimized by rotating the coordinates around geometric centre. The non-bound interaction energy of probe type with the protein on each 3D grids, which employs GRID force field parameters, is computed by the program Liggrid. The definition of the interaction between the protein and methyl probe ($-CH_3$) at grid resolution of 0.9 A° on a 3D grid enclosing the whole protein is made up by Q-SiteFinder (Laurie and Jackson, 2005).

Individual probe energy is calculated and probes with the most favorable binding energy are saved; then a range of energies are tested (-1.0 to -1.9 kcal/mol). After that, each probe according to probes' spatial proximity are clustered, and total interaction energies of clusters are computed. Moreover, cluster with the most favorable total interaction energy is characterized as the first predicted binding site. Each cluster volume is also computed by Q-SiteFinder (Laurie and Jackson, 2005).

PDB code of protein structure is entered or uploaded to Q-SiteFinder as the only input. The volume and the residues of the predicted site, the binding box around the predicted site coordinates are obtained as outputs of Q-SiteFinder. Jmol visualization of the protein is displayed by output window. The predicted sites are also shown in different colors and the representation of protein can be changed as cartoon or wireframe.

3.4.2.2.Pocket-Finder:Pocket-Finder (http://www.bioinformatics.leeds.ac.uk/pocketfinder) used to detect pockets is based on Ligsite written by Hendlich *et al* (1997). Pocket-Finder works by searching a probe radius 1.6 A° along all gridlines of a grid resolution 0.9 A° around the protein. The probe also considers cubic diagonals. When the probe is within range of protein atoms followed by free space protein atoms, grid points are defined to be

part of a site. Each grid point can be defined as a part of a site up to seven times because the protein is scanned in seven directions. Grid points are only retained if they are defined to be part of a site at least five times. The Pocket-Finder program ranks the sites according to the number of probes in the site instead of probe energy (Laurie and Jackson 2005).

Pocket-Finder requires PDB code of protein structure or PDB file of protein can be also uploaded as an input. The users can select the output type of Pocket-Finder as Chime or Mage. The outputs are similar to Q-SiteFinder. The volume and the residues of the predicted site, the binding box around the predicted site coordinates are computed as outputs of Pocket-Finder. Jmol visualization of the protein is displayed by output window. However, there is not any option to change the representation of protein.

3.4.2.3. SITEHOUND: SITEHOUND (http://sitehound.sanchezlab.org) is a web server to identify ligand binding sites in protein structures. An energy-based method is used to characterize the regions which can be potential binding sites with ligands. The major difference of SITEHOUND compared to other ligand binding site prediction servers is that it provides two different probes to identify protein structure. Thus, as various types of binding sites are defined, introductory definition of their interaction properties are stated (Hernandez et al., 2009).

The algorithm of SITEHOUND analyzes possible ligand binding sites by describing the regions which are identified by a chemical probe. Two different probes, Carbon probe and Phosphate probe, can be used to characterize different types of sites. Carbon probe plays a significant role for identification of ligand binding sites for drug-like molecules. On the other hand, Phosphate probe can be chosen to analyze the sites for phoshorylated ligands like ATP and phosphopeptides (Hernandez et al., 2009).

The interaction of the probe and the protein is described by Affinity Maps (Molecular Interaction Fields) which are computed by AutoGrid and Easy MIFs program. Although both AutoGrid and Easy MIFs programs are used for Carbon probes, only Easy MIFs program is used for phosphate probe. Affinity map points are then filtered according to unfavorable interaction energies (Hernandez et al., 2009).

Input of SITEHOUND web is PDB code of protein. Moreover, a probe type and clustering algorithm are also required to be chosen for calculation. It is important to note that SITEHOUND removes the ligand from the PDB file automatically so users do not require any preprocessing. The clustering algorithm defines the way how clusters are combined from individual affinity map points by SITEHOUND. There are two clustering algorithms; average and single. The average-linkage clustering algorithm is for spherical clusters and single-linkage clustering algorithm is for larger elongated binding sites (Hernandez et al., 2009).

The output screen includes five sections: The 'Cluster Data' table, Jmol molecular viewer, the 'Cluster Selection' panel, the 'Cluster Details' panel, the 'Download Data' panel. The 'Cluster Data' table demonstrates the top 10 ranking interaction energy clusters and it includes the rank, TIE, coordinates, and volume for each cluster. The TIE is used to rank the clusters and it indicates the strength of the clusters. The cluster coordinates correspond to the x, y and z coordinates of the center of each cluster. It can be useful to set up a docking box centered on a putative binding site. The volume of the cluster in $A^{\circ 3}$ is shown in the last column of the Cluster Data table. Another window represents 3D interactive view of the protein structure and the clusters, and it is provided by the Jmol molecular viewer. The 'Cluster Selection' panel interacts with the Jmol molecular viewer, and it is used to toggle the demonstration of any of the top 10 clusters on and off. The coloring of the clusters is related with the rank in the Cluster Data table. A list of protein residues in the vicinity of a selected cluster is provided by the Cluster Detail panel. Users can click on the corresponding rank in the Cluster Data table to change the selected cluster. The last panel is the 'Download Data' panel which provides links to various data files: the 'Cluster Data' file , the DX file, the Cluster PDB file and MAP file. The 'Cluster Data' file gives the same information as the Cluster Data table, but for all established clusters. The DX file includes cluster data in the DX format which is useful for display in programs such as PyMOL and Chimera. The Cluster PDB file stores the coordinates of the cluster points in PDB format; it is useful for displaying the clusters in any molecular viewers. The MAP file is the affinity map that is used for the identification of binding sites. It can be used with the offline version of SITEHOUND (Hernandez et al., 2009).

3.4.2. Analysis of the Physicochemical Properties of Binding Sites

The shape and physicochemical complementary between the receptor and the ligand is the fundamental of molecular recognition. Thus the binding site and the ligand are analyzed and characterized to design ligands with high affinity and specificity. Some of the significant features of the binding sites are geometry, amino acid residue composition, solvation, hydrophobicity, electrostatic, chemical fragment interactions (Henrich et al. 2009).

3.4.2.1. Geometry: Geometric approaches give basic information about size, shape, surface and atoms lining the concavity of the pockets. Some methods which employ geometric approaches define the shape of binding site and compute the solvent accessible area and molecular surface area. Geometric approaches are straightforward and give a first impression of the pockets. SCREEN and CAST are the examples of the web servers that use geometric approach (Henrich et al. 2009).

3.4.2.2. Amino Acid Residue Composition: Functionally important residues on the ligand binding sites are conserved (Pupko et al. 2002). Catalytic residues are generally charged residues (Bartlett et al., 2002). Soga and coworkers identified that the occurrence of tryptophan is higher at the ligand binding sites (Soga et al., 2007). Moreover, there are differences between the enzyme and non-enzyme sites with high affinity ligands. The occurrence of Glycine residues are higher on enzyme sites but the occurrence of Leucine residues followed by tyrosine is higher on non-enzyme sites (Carlson et al, 2008). ConSurf (http://consurf.tau.ac.il) accessed freely, aims to analyze amino acid residue composition of proteins. Conservation score of each residue is given by color score from 9 (the most conserved position) to 1 in Consurf (the most variable position) (Landau et al. 2005).

3.4.2.3. Solvation: Proteins are embedded in solvent, generally in water molecules, and the displacement of water molecules is required since water molecules affect the thermodynamics of ligand binding. Solvation energy is the energy released when ions associate with proteins in a solvent. Hence, the identification of the sites at which water molecules bind is significant to characterize the properties of protein binding pockets. One of the methods for prediction water binding sites on protein is done with WatCH software

which identifies conserved sites in series of structures of the same protein (Sanschagrin and Kuhn 1998). GRID method is the another approach which uses a water probe and computes the interaction energy between probe and protein (Wade and Goodford 1993). SCREEN computes the solvation energy, and the solvation energy of the first predicted site is expected to be highest among the others.

3.4.3.4. Electrostatics: The calculation of the electrostatic potential of the protein is required to assign the position of hydrogen atoms that are not resolved in protein crystal structure and depend on the pKa value. GRASP, UHBD, DelPhi and APBS are the programs which compute the electrostatic potential of proteins by using Poisson-Boltzmann equation (Henrich *et al*., 2009). SCREEN also provides information about the electrostatics properties of predicted ligand binding sites. Average charge, electric potential and electric field are computed by SCREEN.

3.4.3.5. Chemical Fragment Interactions: Different ligands bind different parts of the binding site and these can be detected by different kinds of small organic molecules (Henrich *et al*., 2009). A method is developed to use molecular dynamics simulations of a constrained protein in a mixture of isopropyl alcohol and water molecules to compute interaction free energies between the protein and the organic molecules. As a result, binding sites are identified and their corresponding maximal affinity of a drug-like molecule are estimated by obtaining a druggability index (Seco *et al*., 2009). A druggability index is also computed by SCREEN.

4. EXPERIMENTAL RESULTS AND DISCUSSION

4.1. Insulin and Sphingolipid Signaling Pathways

The map of the insulin signaling pathway which is categorized in Organismal Systems under the subgroup of Endocrine Systems was obtained from KEGG database and shown in Figure 4.1. Therefore, all the proteins (62 proteins) involved in insulin signaling pathway and their features including the amino acid sequences were accessed through this database.

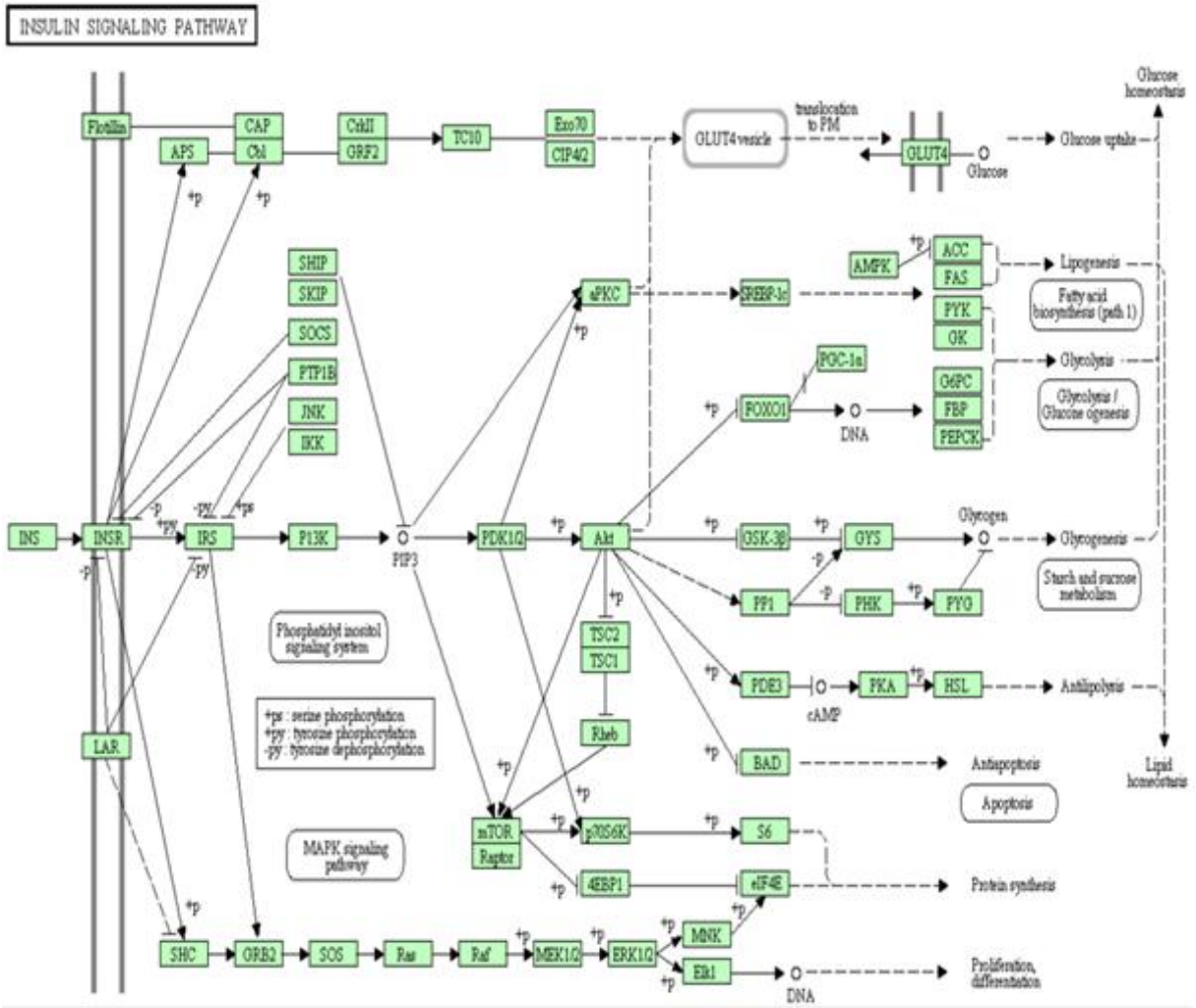

Figure 4.1. Insulin signaling pathway.

The homologs of the proteins involved in *Homo sapiens'* insulin signaling pathway were found in *Saccharomyces cerevisiae* by using Basic Local Alignment Search Tool (BLAST). Table 4.1 displays the BLAST results with E-values of the proteins below E-50. According to BLAST results, some proteins in *H. Sapiens* were found to match with proteins in *S. cerevisiae*. 5 proteins in Table 4.1 have E-values smaller than e-100, and 10 proteins have E-values between e-67 and e-98.

After the homologs were determined in *S.cerevisiae*, it was investigated which of these proteins have also roles in sphingolipid pathway. Sphingolipid signaling network was previously reconstructed within the framework of a research project supported by BU-BAP. Sphingolipid signaling network contains 8 core proteins, Pkh1p, Pkh2p, Pil1p, Lsp1p, Pkc1p, Ypk1p, Ypk2p, and Sch9p (Yücel et al., 2008). Five of them (Pkh1p, Pkc1p, Ypk1p, Ypk2p and Sch9p) were found in BLAST results. Moreover, three primary neighbors (Snf1p, Tor2p, and Hog1p), three secondary neighbors (Fus3p, Glc7p, Tpk2p) and two tertiary neighbors (Kogp and Rim11p) of these core proteins in sphingolipid pathway were obtained from the evaluation of the sequence alignment results (Table 4.2).

Pkh1p, Ypk1p and Ypk2p were selected for the investigation of the relationship between insulin and sphingolipid signaling pathways.

Table 4.1. The results of BLAST analysis.

Protein (H. Sapiens)	**Isoforms**	**E-value**	**Protein (S. Cerevisiae)**
PDK 1/2		1E-77	PKH1
Akt	Akt3	6E-87	SCH9
	Akt1	2E-84	
	Akt2	9E-86	
JNK	MAPK8	4E-69	HOG1
	MAPK9	3E-53	
	MAPK10	1E-70	
aPKC	PRKCI	3E-80	PKC1
	PRKCZ	2E-73	
AMPK	PRKAG2	4E-50	*SNF1*
	PRKAA1	2E-111	
	PRKAA2	4E-116	
ACC	ACACA	0	*ACC1*
	ACACB	0	

Table 4.1. The results of BLAST analysis (Continued).

Protein (H. Sapiens)	Isoforms	E-value	Protein (S. Cerevisiae)
	PFKM	7E-138	
	PFKP	1E-139	
PYK	PKLR	7E-138	*PYK2*
	PKM2	1E-139	
FBP	FBP1	5E-83	*FBP1*
	FBP2	2E-81	
TC10		8E-68	*CDC42*
GSK-3b		8E-103	*RIM11*
GYS	GYS1	0	*GSY2*
	GYS2	0	
PP1	PPP1CA	1E-152	*GLC7*
	PPP1CB	2E-152	
	PPP1CC	6E-157	
PYGB	PYGB	0	*GPH1*
	PYGBL	0	
	PYGLM	0	
PKA	PRKACA	1E-97	*TPK2*
	PRKACB	3E-98	
	PRKACG	3E-93	
	PRKAR1A	4E-54	
	PRKAR1B	2E-53	
	PRKAR2A	4E-57	
	PRKAR2B	5E-55	
	PRKX	1E-95	
	PRKY	2E-72	
Raptor		5E-119	*KOG*
p70s6k	RPS6KB1	5E-88	*YPK1/2*
	RPS6KB2	7E-86	
S6		5E-50	*RPS6B*
Ras	HRAS	7E-51	*RAS2*
	KRAS	5E-51	
	NRAS	7E-51	
MEK1/2	MAP2K1	2E-67	*PBS2*
	MAP2K2	2E-69	
ERK1/2	MAPK1	4E-93	*FUS3*
	MAPK3	8E-95	

Table 4.2. The sphingolipid pathway proteins in *S. cerevisiae.*

Role in Sphingolipid Pathway	Proteins (H. Sapiens)	Proteins (S. Cerevisiae)
Core Proteins	PDK1/2	*PKH1*
	Akt	*SCH9*
	aPKC	*PKC1*
	p70s6k	*YPK1/2*
Primary Neighbors	JNK	*HOG1*
	AMPK	*SNF1*
	mTOR	*TOR2*
Secondary Neighbors	PP1	*GLC7*
	PKA	*TPK2*
	ERK1/2	*FUS3*
Tertiary Neighbors	GSK-3b	*RIM11*
	Raptor	*KOG*

4.2. Batch Experiments with Yeast Cells (Wild Type and Deletion Mutants)

The wild type and three homozygous deletion mutant strains , and were used in the experiments, and these experiments were repeated for two or three times. The growth curve of yeast cells were obtained by optical density measurements at different glucose concentrations and given in Figures 4.2-4.4. Moreover, samples were taken for glucose and lipid analysis at different phases of growth, i.e. exponential and stationary phases.

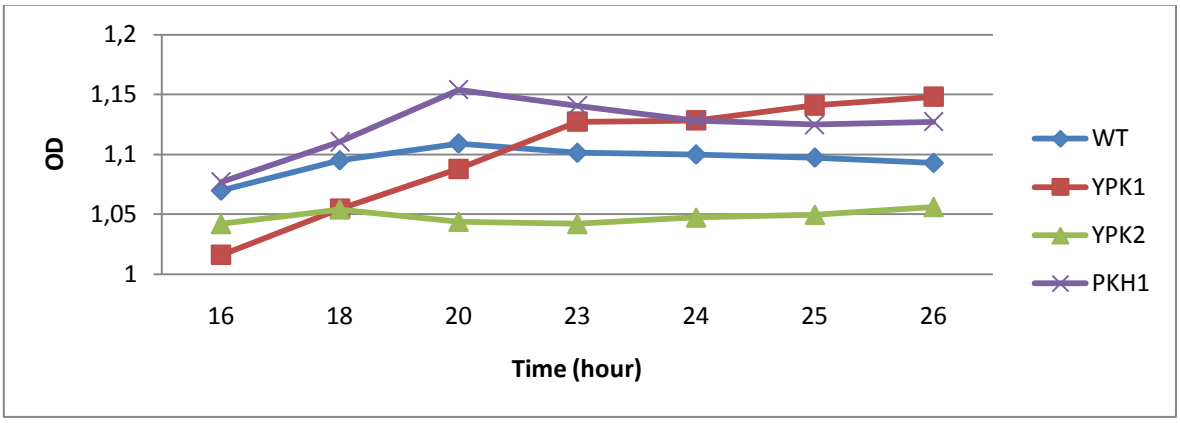

Figure 4.2. Growth profile of wild type and deletion mutants (20g/l initial glucose concentration).

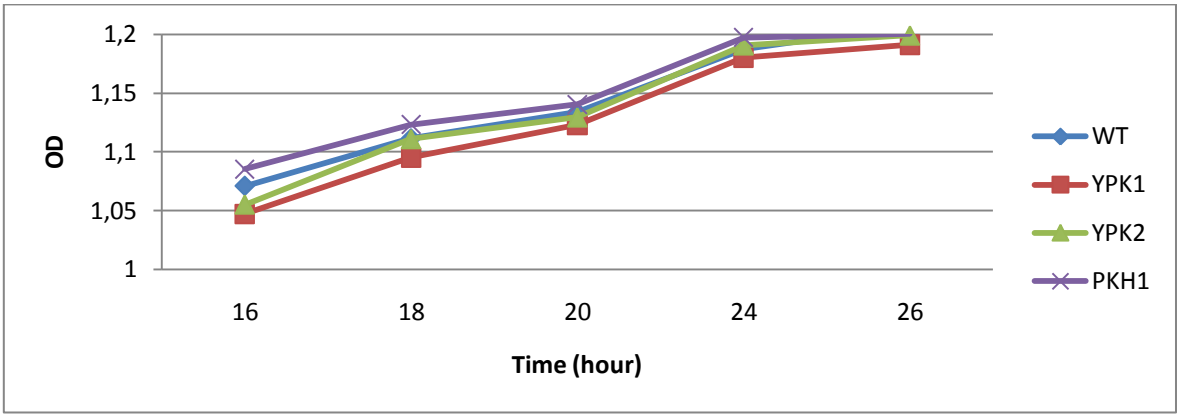

Figure 4.3. Growth profile of wild type and deletion mutants (30g/l initial glucose concentration).

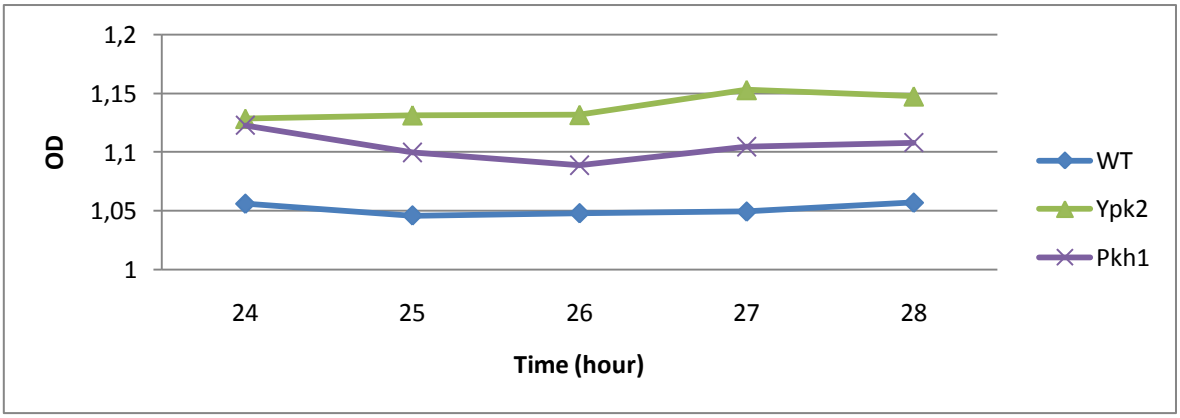

Figure 4.4. Growth profile of wild type and deletion mutants (40g/l initial glucose concentration).

The initial concentration of the glucose in F1 medium was changed (20g/l, 30g/l and 40g/l) and the effects of the glucose concentration on glucose uptake by the cells were investigated. The wild type yeast cells consume more glucose than the deletion mutant strains at different initial glucose concentrations. Moreover, the remaining glucose concentrations in the medium are highest for the deletion mutant of and lowest for the deletion mutant of (Figures 4.5-4.7).

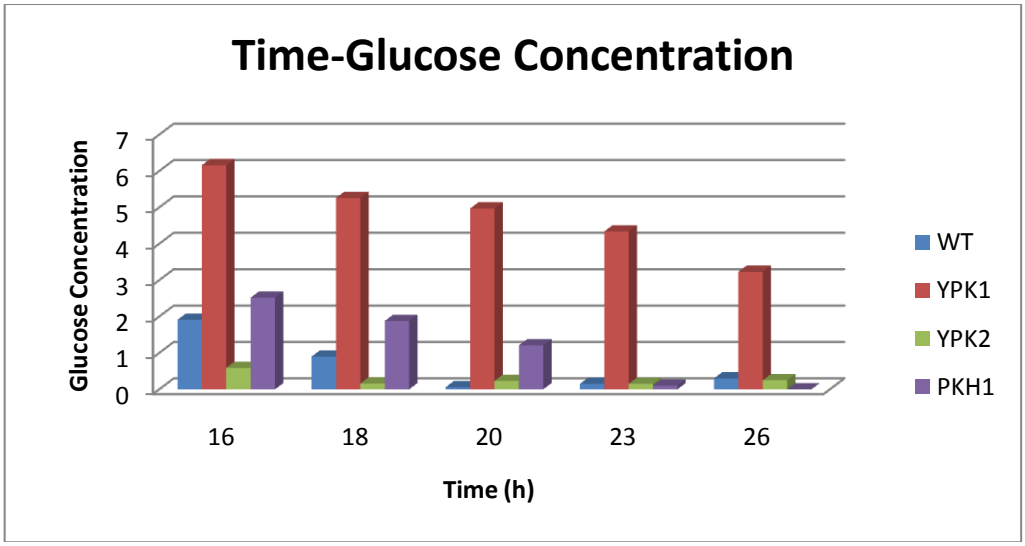

Figure 4.5. Time course of glucose remaining in the medium (for 20 g/l initial glucose concentration).

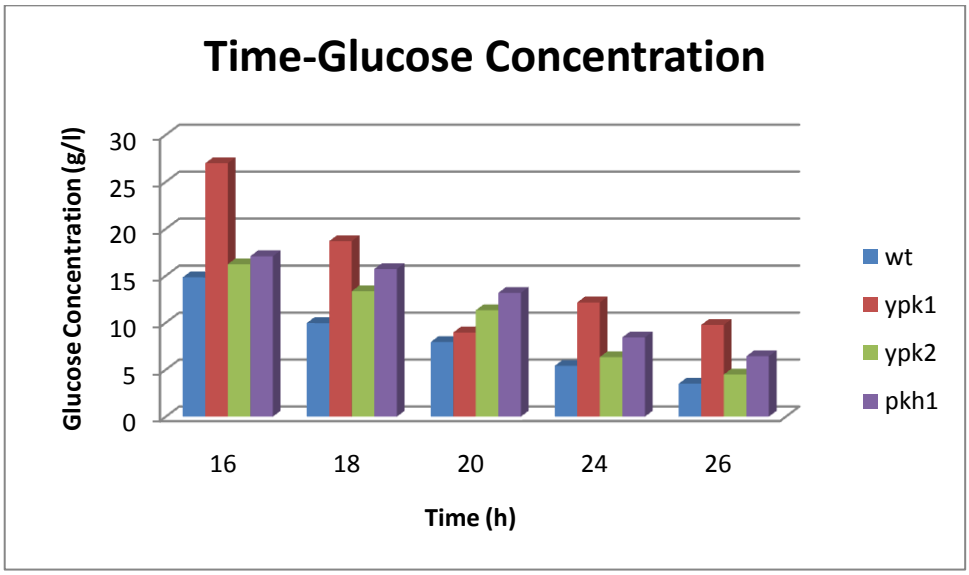

Figure 4.6. Time course of glucose remaining in the medium (for 30 g/l initial glucose concentration).

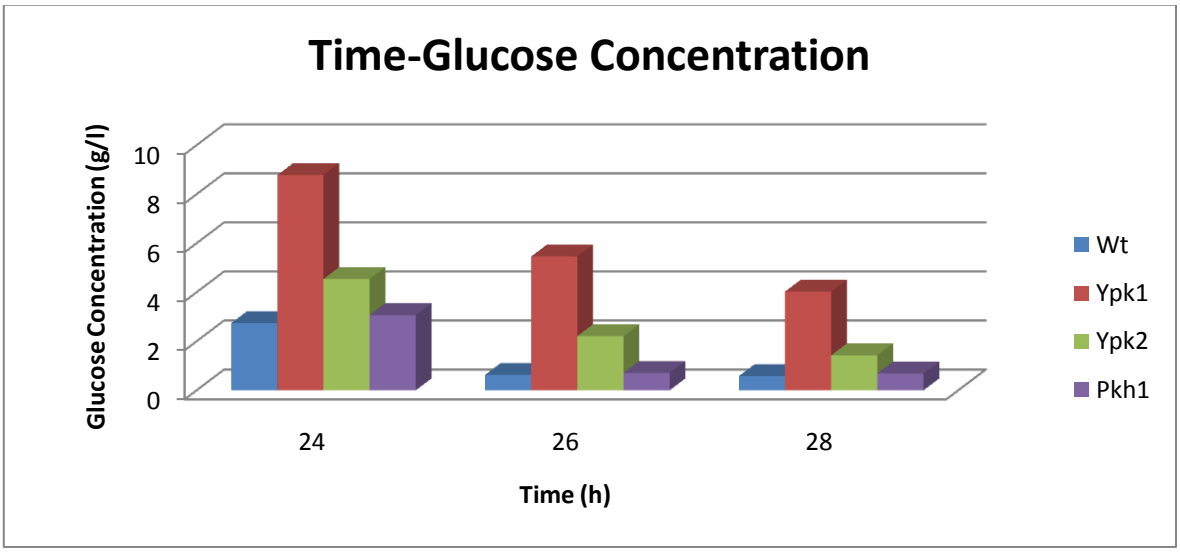

Figure 4.7. Time course of glucose remaining in the medium (for 40 g/l initial glucose concentration).

The results of lipid analysis by HPLC are given in Tables 4.3 and 4.4 for 30 g/l and 40 g/l initial glucose concentrations, respectively. The retention times of complex sphingolipids in yeast, IPC, MIPC and M $(IP)_2$ C, are 4.3, 4.0 and 3.8 minutes, respectively (Figures 4.8-4.15). The amount of IPC is highest in wild type strain. The deletion mutants of , and have 87.75, 88.04 and 90.62% IPC at 30g/l initial glucose concentration and 92.23, 87.93 and 85.65 % IPC at 40g/l initial glucose concentration, respectively.

Table 4.3. The amounts of lipids measured by HPLC for 30g/l initial glucose concentration.

	IPC (%)	**MIPC (%)**	**M$(IP)_2$C (%)**
Wild Type	92.46	6.21	1.33
YPK1	87.75	6.54	0.86
YPK2	88.04	5.38	6.58
PKH1	90.62	7.90	1.48

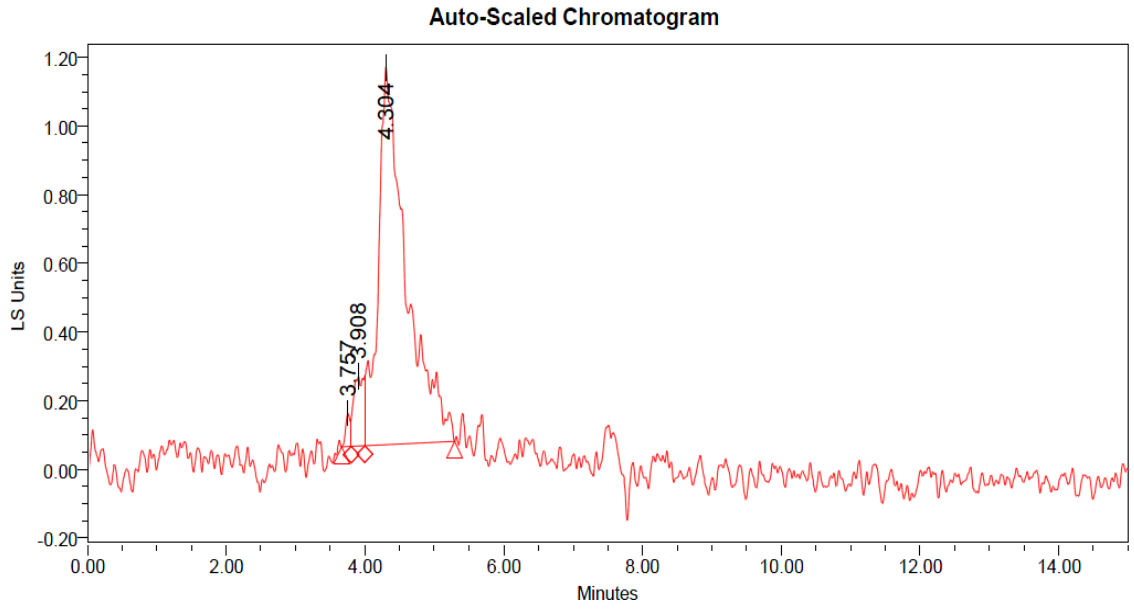

Figure 4.8. Lipid analysis of wild type strain by HPLC (30 g/l initial glucose concentration).

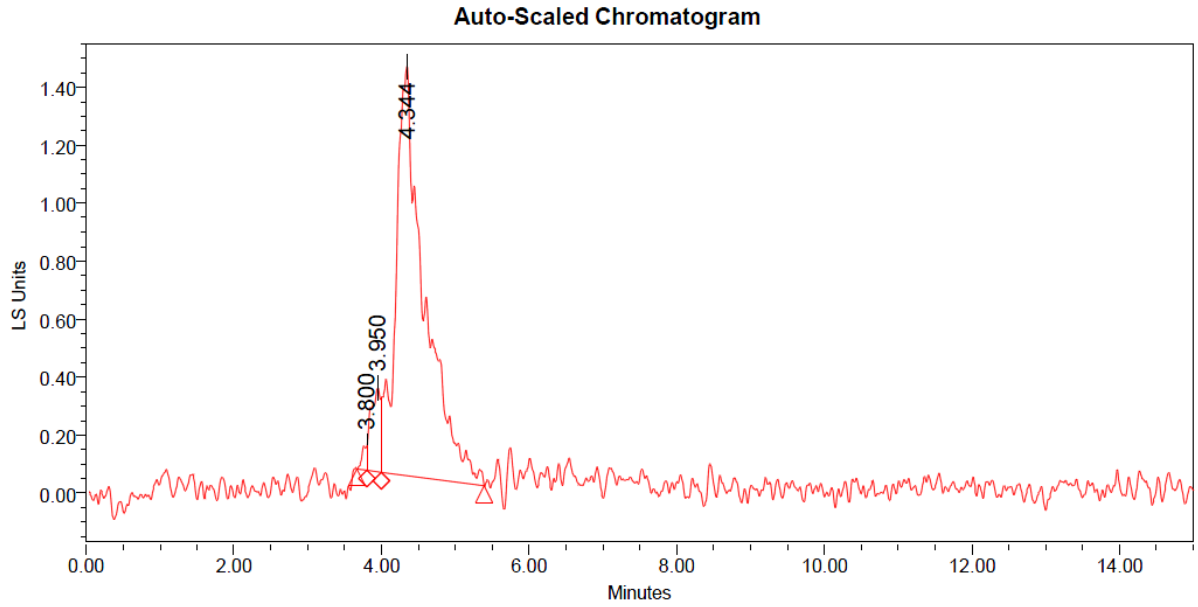

Figure 4.9. Lipid analysis of the deletion mutant of by HPLC (30 g/l initial glucose concentration).

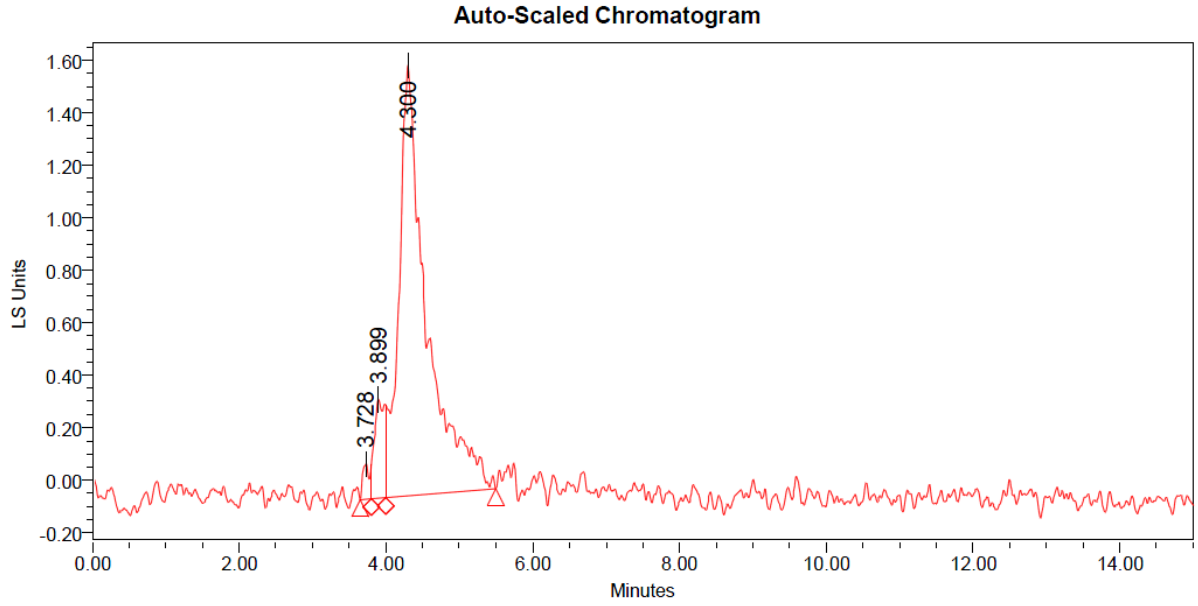

Figure 4.10. Lipid analysis of the deletion mutant of by HPLC (30 g/l initial glucose concentration).

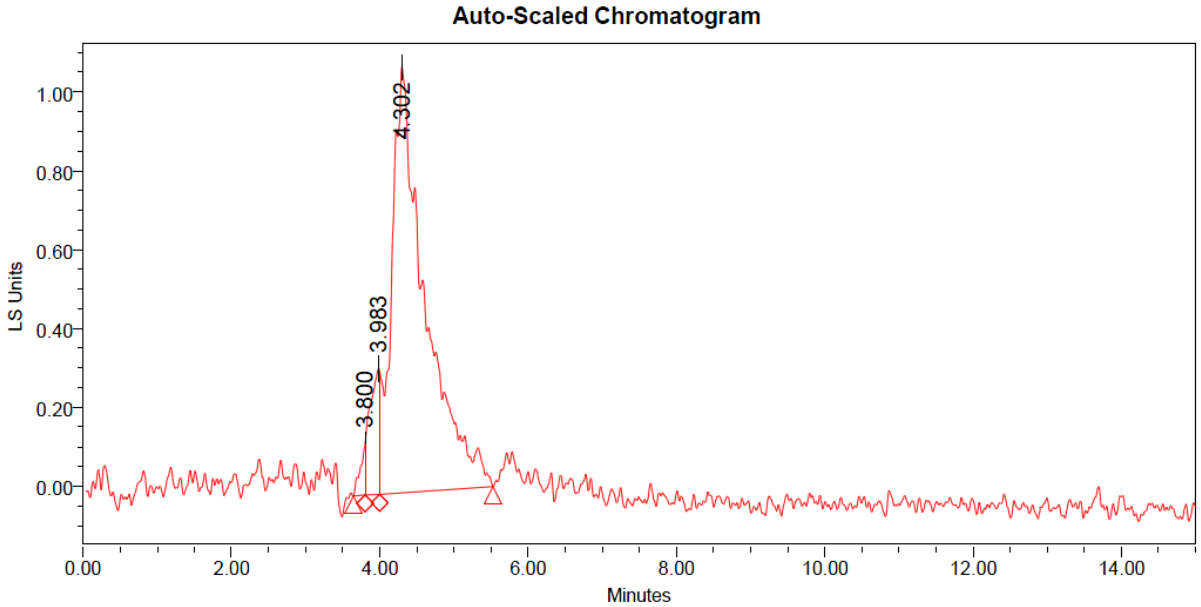

Figure 4.11. Lipid analysis of the deletion mutant of . By HPLC (30 g/l initial glucose concentration).

Table 4.4. The amounts of lipids measured by HPLC for 40g/l initial glucose concentration.

	IPC (%)	MIPC (%)	$M(IP)_2C$ (%)
Wild Type	85.45	12.40	2.15
Ypk1	92.23	3.48	4.28
Ypk2	87.93	7.20	4.86
Pkh1	85.65	11.64	2.71

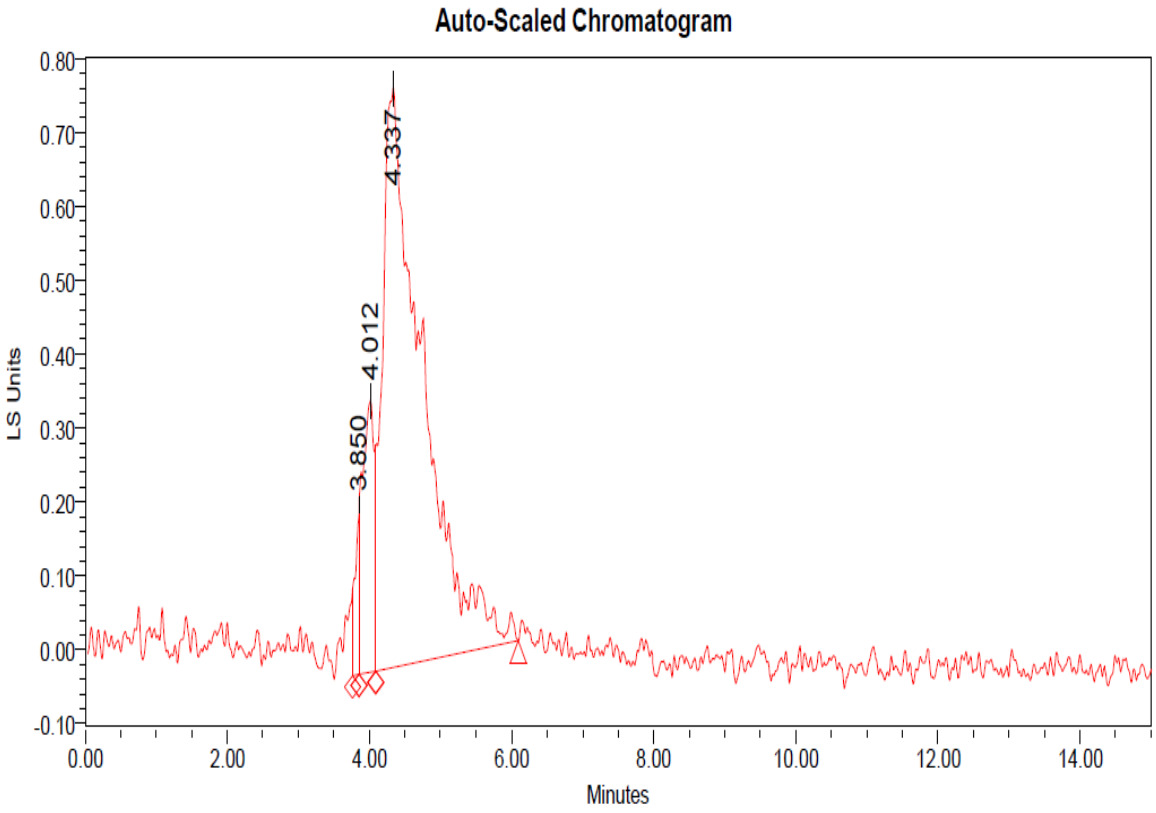

Figure 4.12. Lipid analysis of wild type strain by HPLC (40 g/l initial glucose concentration).

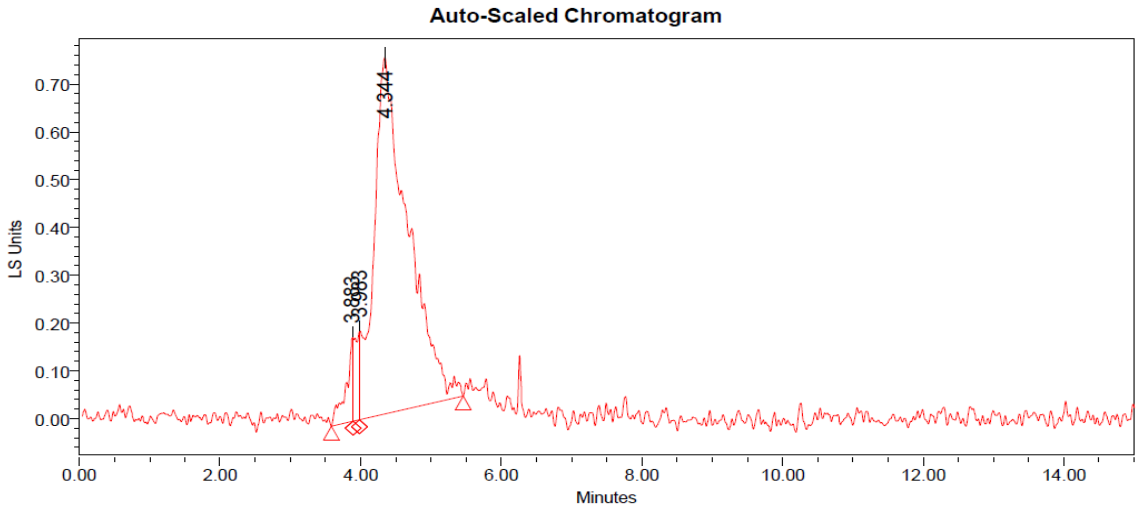

Figure 4.13**.** Lipid analysis of the deletion mutant of by HPLC (40 g/l initial glucose concentration).

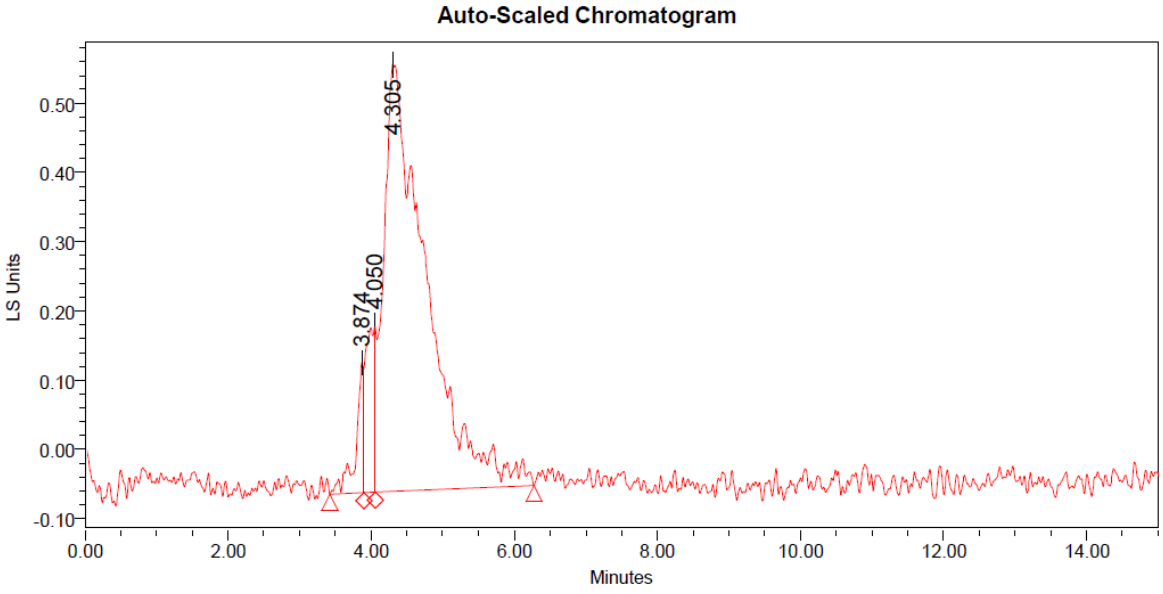

Figure 4.14. Lipid analysis of the deletion mutant of by HPLC (40 g/l initial glucose concentration).

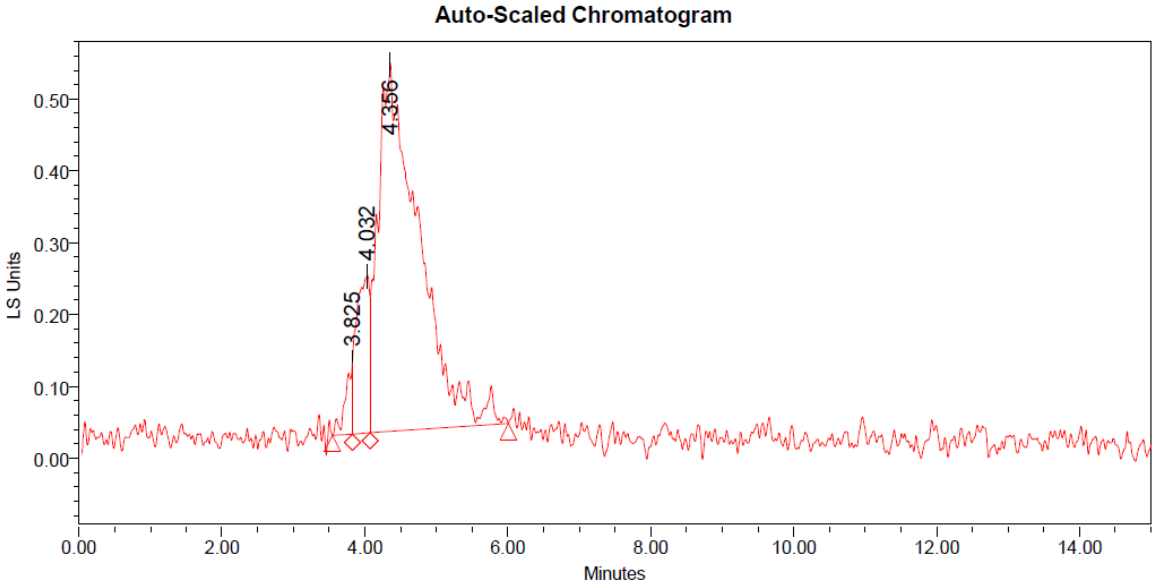

Figure 4.15. Lipid analysis of the deletion mutant of . by HPLC (40 g/l initial glucose concentration).

4.3. Crosstalk between Sphingolipid and Insulin Signaling Networks

4.3.1. Regulation of Akt/Protein Kinase B by Sphingolipid Pathway Metabolites

Sphingolipid ceramide regulates many cellular processes such as apoptosis, differentiation and proliferation (Stratford et al., 2004). Ceramide affects both protein kinases and phosphatases so ceramide signaling is associated with the activation of the important signaling pathway, insulin signaling pathway (Schubert et al., 2000). Akt/PKB is a central mediator of insulin signaling pathway and it plays significant roles on glucose uptake and anabolic metabolism (Stratford et al., 2004). The maximal PKB activation requires the phosphorylation of both Threonine-308 and Serine-473.

The relation between ceramide and Akt/PKB is explained by two independent mechanisms (Figure 4.16). In these mechanisms, the activation and phosphorylation of Akt/PKB are inhibited by ceramide. In the first mechanism, protein phosphatase 2A (PP2A) is directly activated by ceramide and then PP2A dephosphorylates Ser473 residue of Akt/PKB. On the other hand, PKC is also activated by ceramide, then it phosphorylates

the residue of Thr34 on PH domain of Akt thus Akt/PKB translocation from cytoplasmic store to the plasma membrane is blocked (Summers, 2006).

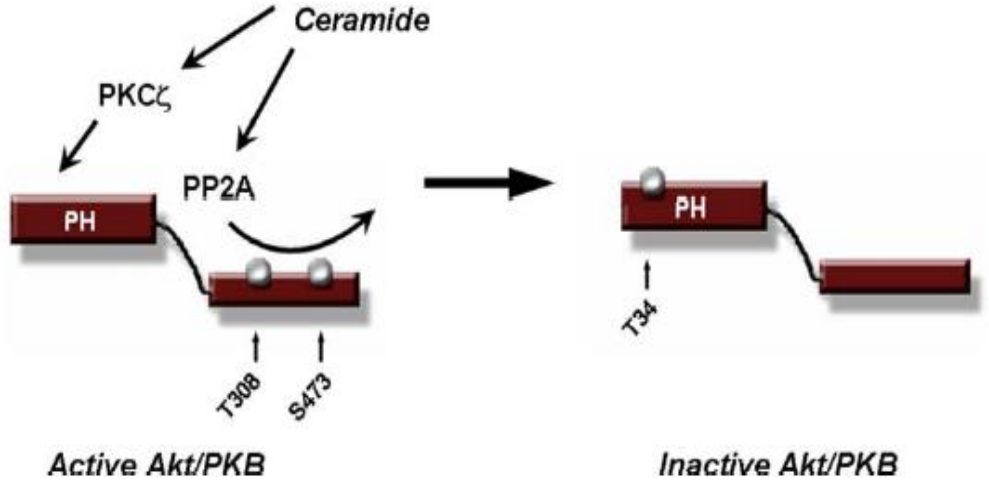

Figure 4.16. The regulation of insulin action by ceramide (Summers, 2006).

Phytosphingosine (PHS) is a signaling molecule taking part in sphingolipid pathway. PHS activates Pkh1p in yeast and Pkh1p activates the downstream protein kinases Ypk1p, Ypk2p, Pkc1p and Sch9 (Figure 4.17). The mammalian 3-phosphoinositide-dependent protein kinase (PDK1) is the homolog of Pkh1 in yeast. In mammals, PDK1 is activated by various survival and growth factors. Moreover, many protein kinases, especially protein kinase A, protein kinase G and protein kinase C (AGC kinase family) are phosphorylated and activated by activated PDK1. The importance of AGC family is due to its function of controlling multiple cellular processes (Liu et al., 2005).

The loss of Pkh1p or Pkh2p has little impact on cell growth but the loss of both proteins is lethal (Liu et al., 2005). Pkh1p and Pkh2p are necessary for actin cytoskeleton organization and endocytosis. Endocytosis is one of the cell processes where cell absorbs the molecule from outside. Endocytosis requires sphingoid base mediated signaling pathway and Pkh1/2p kinases are sphingoid base activated kinases which start the cascades for endocytosis (Friant et al., 2001).

Ypk1p and Ypk2p are also phosphorylated and activated by PHS stimulation. Ypk1p is a substrate for Pkh1p both in vivo and in vitro. Furthermore, maximal Ypk1p phosphorylation requires Pkh kinase activity. Ypk1p and Ypk2p are also phosphorylated by Pkh1p and Pkh2p, respectively.

The deletion of Ypk1p decreases the growth rate of yeast but the loss of both Ypk1p and Ypk2p is lethal. Eisosomes are dynamic structures, and Ypk kinases control the stability and disassembly of eisosomes. The organization and formation of eisosomes are also regulated by the sphingolipid Pkh1/2-Ypk1/2 signaling pathway (Luo et al., 2008). Ypk1p and Ypk2p also play role in maintaining and remodeling of cell wall (Roelants et al., 2002). Additionally, the conserved kinase cascade of Pkh-Ypk is necessary for endocytosis in *S. cerevisiae*.

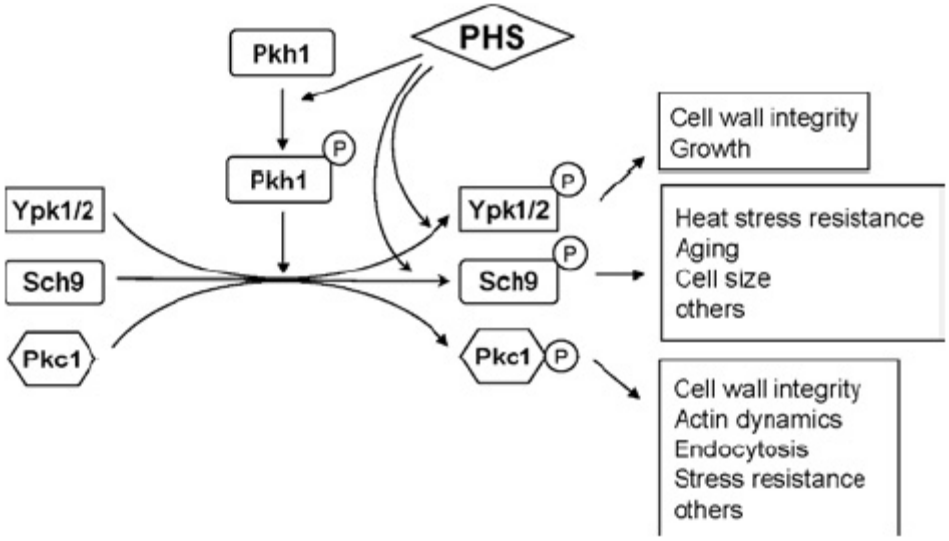

Figure 4.17. PHS activates AGC protein kinases (Liu et al., 2005).

Torc2 protein adjusts the biosynthesis of ceramide by Ypk2p which is activated by Pkh1 and Pkh2 proteins (Figure 4.18). Pkh1p and Ypk2p are also activated by PHS as mentioned before (Aronova et al., 2008).

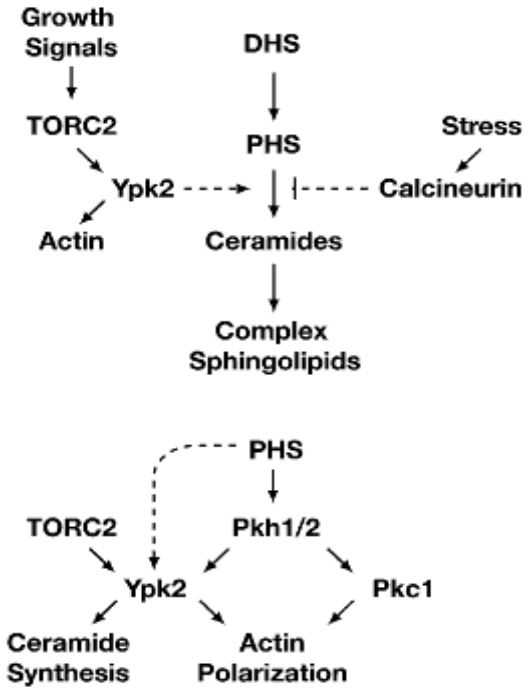

Figure 4.18. Torc2p and PHS activate Ypk2p for ceramide synthesis (Aronova et al., 2008).

In the light of the above mentioned literature information, one can conclude that phytosphingosine (PHS) activates Pkh1p which in turn activates the kinases Ypk1p, Ypk2p, Pkc1p and Sch9p (Akt/Protein Kinase B). Ypk2p further leads to ceramide synthesis, and ceramide synthesized can inhibit Akt/Protein kinase B translocation from cytoplasmic store to plasma membrane through protein kinase C (PKCζ) and protein phosphatase 2A (PP2A). Hence, in the absence of any following protein, Ypk1p, Ypk2p and Pkh1p, ceramide synthesis is expected to decrease and glucose intake to the cell to increase. If Table 4.3 is investigated, one can note that the deletion mutants at 30g/l initial glucose concentration have reduced IPC percentages compared to wild type strain in agreement with literature information. However, at 40 g/l initial glucose concentration, the deletion mutants result in higher percentages of lipid composition (see Appendix B) compared to wild type strains as well as higher amounts of remaining glucose in the medium (Figure 4.7) as expected. When the initial glucose concentration in the medium is increased, the effect of other proteins having roles in glucose signal reception and transduction might be dominant. Nevertheless, the experimental results on the relation between glucose consumption and complex sphingolipid production are found to be in agreement with the literature.

4.3.2. The Physical and Genetic Interactions of PKH1, *YPK1* and *YPK2*

In order to get further insight about the crosstalk between the sphingolipid and insulin signaling networks, the individual physical and genetic interactions of Pkh1, Ypk1 and Ypk2 are investigated through databases and by OSPREY. The lists of interactions are given in Tables 4.5 and 4.6. Pkh1, Ypk1 and Ypk2 interact physically with 15, 18 and 13 proteins, respectively and genetically with 18, 30 and 5 proteins, respectively. Moreover, Pkh1, Ypk1 and Ypk2 interact with each other physically but not genetically. Figures and 4.19-4.21 display the interaction networks of Pkh1, Ypk1 and Ypk2.

Table 4.5. Physical interactions of Pkh1, Ypk1 and Ypk2.

Pkh1		**Ypk1**		**Ypk2**	
Ypk1	Hsp82	Tor1	Leu9	Tor2	Cdc33
Ypk2	Bmh2	Tor2	Avo2	Ypk1	Snf1
Sch9	Reb1	Ypk2	Ubi4	Pkh1	Yel023c
Myo5	Aep3	Pkh1	Crn1	Arg81	Ygr016w
Yrf1-4	Tpk3	Pkh2	Rpn3	Pet112	
Lsp1	Yir044c	Hsp82	Inp52	Myo5	
Pil1		Bmh2	Ncs2	Prb1	
Ssb1		Hsc82	Sac6	Ubi4	
Set5		Tec1	Slm1	Tfp1	

Table 4.6. Genetic interactions of Pkh1, Ypk1 and Ypk2

Pkh1		**Ypk1**			**Ypk2**
Ypk1	Slm1	Ypk2	Exg1	Clb6	Tor2
Ypk2	Ypt6	Pkh1	Cts2	Avo2	Ypk1
Sch9	Cdc8	Pkh2	Rps6b	Tsc11	Avo2
Tos3	Mck1	Tor1	Srb4	Hlj1	Tsc11
Sgv1	Ncs2	Pkc1	Smp1	Hsc82	Myo5
Sip1	Hsc82	Hsp82	Plb1	Sac7	
Mnn11	Myo5	Bmh2	Ypc1	Jnm1	
Sw15	Ras2	Bmh1	Ybl103l-a	Got1	
Cup2		Knh1	Frq1	Vrs74	
Hsp82		Skt5	Sli1	Ymr291w	

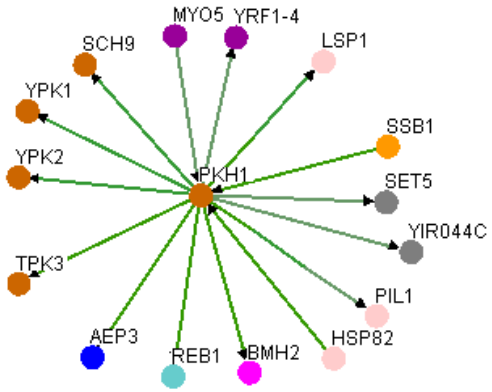

Figure 4.19.a. Physical interaction of Pkh1p.

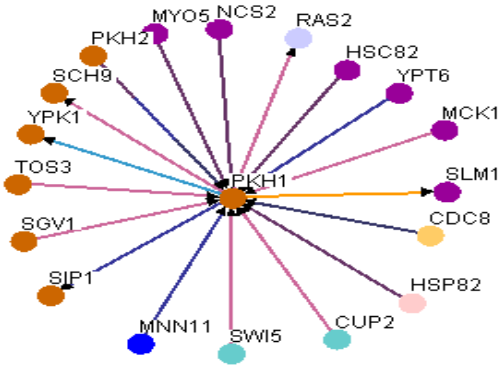

Figure 4.19.b. Genetic interaction of Pkh1p.

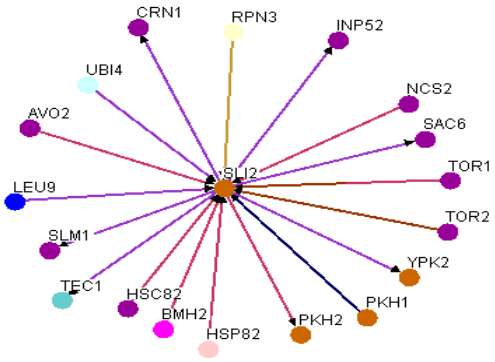

Figure 4.20.a. Physical interaction of Ypk1p.

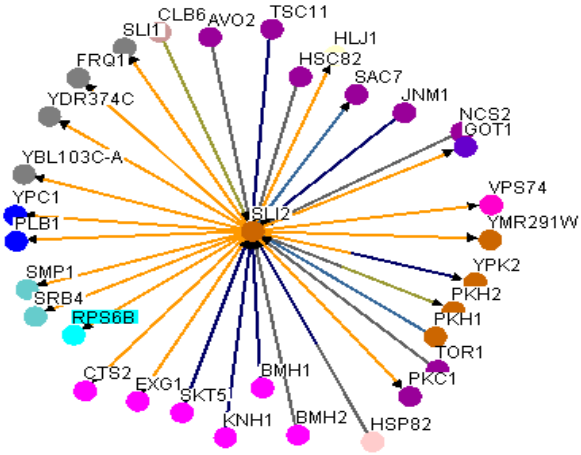

Figure 4.20.b. Genetic interaction of Ypk1p.

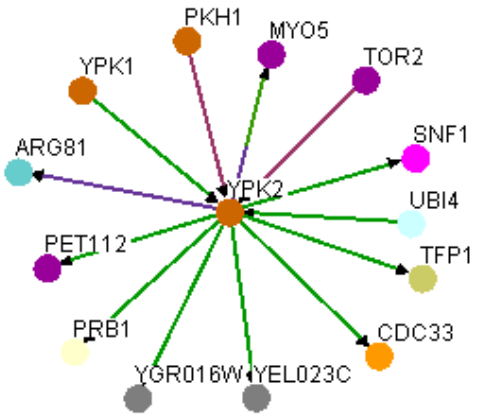

Figure 4.21.a. Physical interactions of Ypk2p.

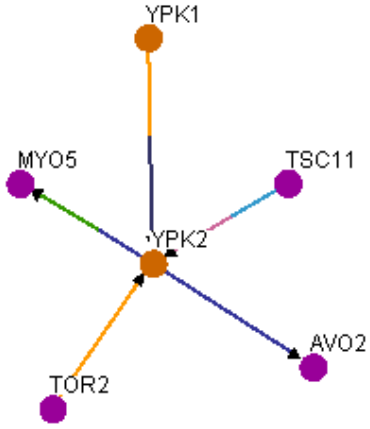

Figure 4.21.b. Genetic interactions of Ypk2p.

The physical interactions between Pkh1, Ypk1, Ypk2 and Sch9 are further analyzed. Pkh1 interacts with Ypk1,Ypk2 and Sch9 directly. Another relation between Ypk2 and Pkh1 is provided by Myo5 which is a mediator protein. Moreover, *Ypk1* interact with Ypk2 directly, and Ypk2 connects with Sch9 via Snf1. The homolog of PP2A and PKC in *H. Sapiens* are identified as Pph22 and Pkc1, respectively, in yeast. Pph22 is catalytic subunit of PP2A. Thus, the physical interactions of Pph22 and Pkc1 are also examined carefully since they are the key components between the sphingolipid and insulin signaling pathways. Pph22 interacts with Myo5 via Cdc55. Cdc55 is the nonessential regulatory subunit B **of** protein phosphatase PP2A and it plays roles in cell cycle, signal transduction and protein amino acid dephosphorylation. Ubi4 interacts with Ypk1, Ypk2 and Pph22. Ubi4 has roles in DNA repair, translation and ribosome biogenesis. As a result of this interaction network, Pkh1, Ypk1 and Ypk2 do not directly interact with Pph22 and Cdc55(Figure 4.22). However, Ypk1/2 and Pkh1 have roles in ceramide synthesis, and the deletion of the Ypk1/2 and Pkh1 cause decreases in ceramide synthesis as it was here found in batch experiments; thus, the deletion of the Ypk1/2 and Pkh1 may indirectly affect the activation of Pph22.

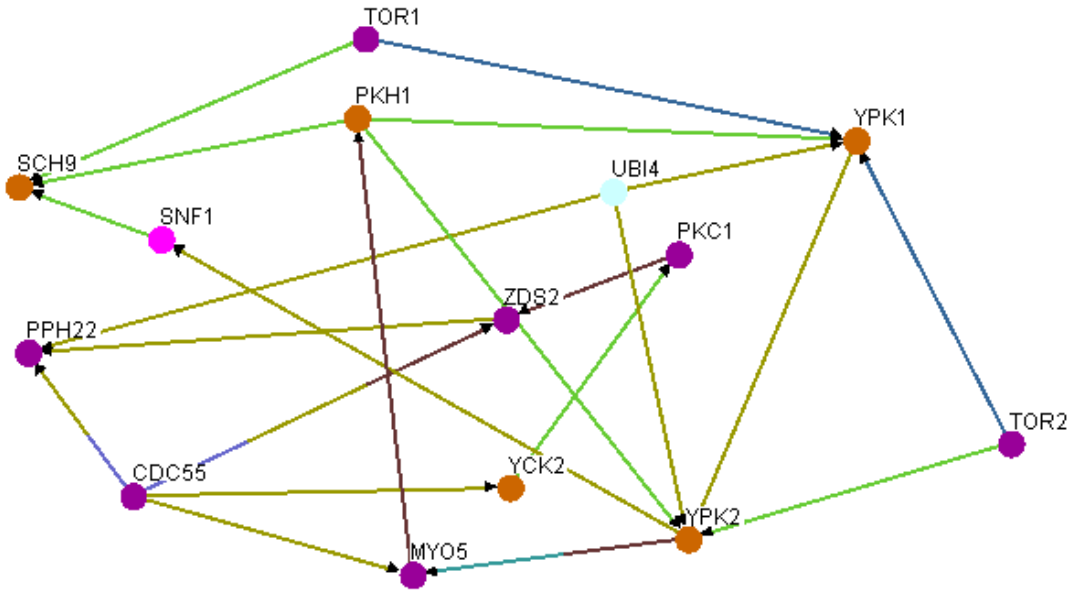

Figure 4.22. Pyhsical interaction network of *PKH1*, *YPK1*, *YPK2*, *SCH9*, *PPH22* and *PKC1*.

Lcb1, Lcb2, Tsc3, Tsc10, Lag1, Lac1 and Lip1 are other important genes to synthesize ceramide. Thus, the physical interactions of these proteins with Pkh1, Ypk1, Ypk2 and Sch9 are figured out by using OSPREY again. The interactions most related to this work are that Pkh1 interacts with Bmh2 which in turn interacts with Lcb2. Bmh2 has roles in glycogen metabolic process and Ras/MAPK protein signal transduction. Lcb2 takes part in the initial step of sphingolipid metabolism. Therefore, the loss of Pkh1 may also affect Lcb2 and ceramide synthesis. On the other hand, Lcb1 interacts with Ubi4 which interacts with Ypk2. Furthermore, Ubi4 interacts with Pph22 as shown in Figure 4.23.

Pkh1 interacts with Sch9 (Akt/Protein Kinase B) directly whereas Ypk2 interacts with Sch9 via Snf1, and Ypk1 interacts with Sch9 through Ypk2 and Snf1. It is here important to note that Snf1p has a primary role in glucose sensing and transduction where it is active at low glucose concentrations. Snf1 kinase is known to inhibit lipid biosynthesis. The results from glucose analysis also indicate that the glucose uptake is lowest in the deletion mutant of Ypk1. On the other hand, the amounts of complex sphingolipids are lowest for the deletion mutant of Pkh1 at 40 g/l initial glucose concentration. This stiuation can be explained by the interaction of Pkh1 with Lcb1 via Bmh2. Furthermore, Ypk2 interacts with Lac1 via Snf1. Lac1p is a ceramide synthase

component, and it is involved in synthesis of ceramide from C26 (acyl) coenzyme A and dihydrosphingosine or phytosphingosine. That explains lower IPC level in the deletion mutant of Ypk2 compared to the deletion mutant of Ypk1 at 40 g/l initial glucose concentration.

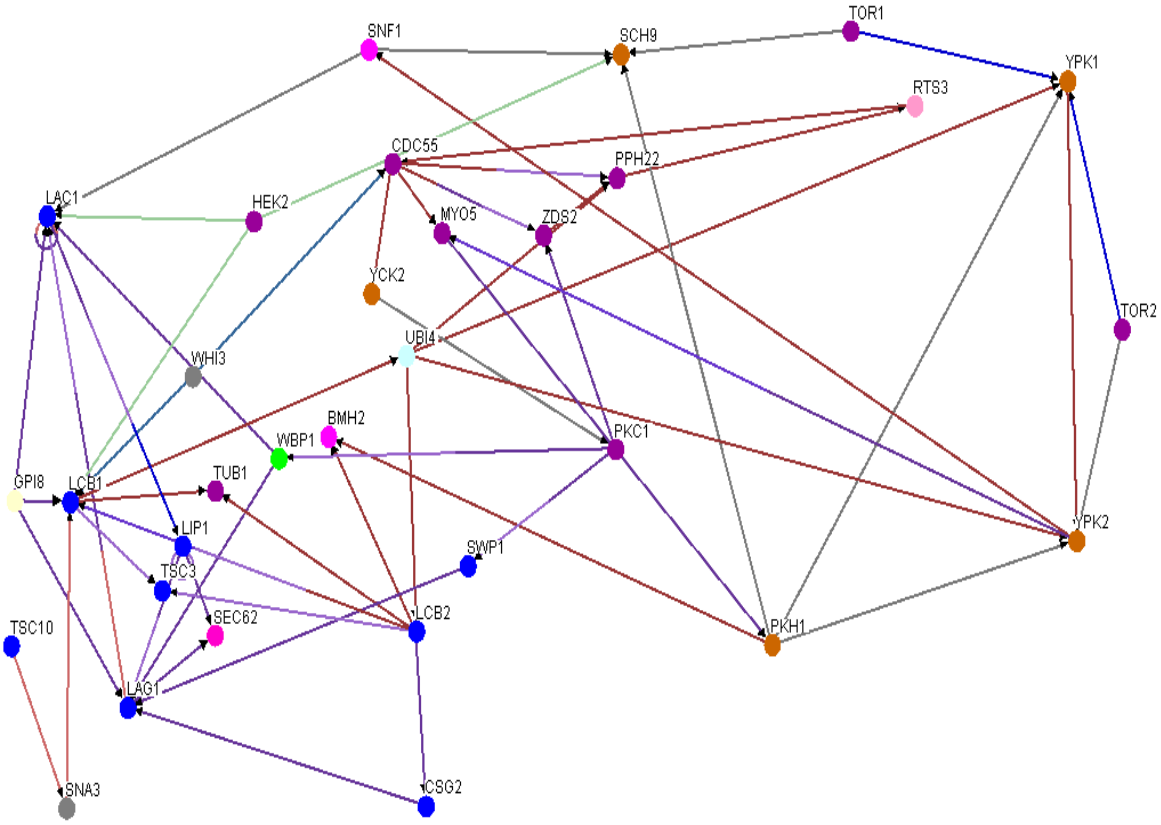

Figure 4.23. Pyhsical interaction network of Pkh1, Ypk1, Ypk2, Sch9, Pph22, Pkc1, Lcb1, Lcb2, Tsc3, Tsc10, Lag1, Lac1 and Lip1.

Akt/PKB (Sch9p in yeast) is the most significant protein that affects GLUT4 translocation, and Akt is also defined as a critical target protein for anticancer drug discovery (Lawlor and Alessi, 2001; Cheng *et al.*, 2005). In the next section, Akt2 protein is further investigated from the aspect of drug discovery.

5. AKT2 POCKET IDENTIFICATION FOR DRUG DEVELOPMENT

5.1. Structure of Akt2

Three isoforms of Akt (Akt1, Akt2 and Akt3) are highly conserved in humans and they share the same regulatory phosphorylation sites. Protein kinase B is the alternative name of Akt, which is a member of the AGC family of protein kinases (Yang et al., 2002). In this study, Akt2 is chosen as a drug target and its ligand binding sites are investigated by using geometry-based and energy-based methods.

Information about Akt2 is accessed through the UniProt web site (http://www.uniprot.org/uniprot/P31751). Akt2 contains 481 amino acids and is composed of three domains, protein kinase domain, pleckstrin homology (PH) domain and AGC-kinase C-terminal domain. Protein kinase, PH and AGC-kinase C-terminal domains are formed by 258, 104 and 72 amino acids, respectively. Akt2 includes two significant sites which are the active site (ASP-275) and the binding site (LYS-181).

Ligand binding site prediction methods are applied to three different structures of Akt2 protein: protein kinase domain (PDB 1gzn), PH domain (PDB 1p6s) and protein kinase domain complexed with inhibitor A-443654 (PDB 2jdr). Figure 5.1 demonstrates the structure of protein kinase domain (PDB 1gzn) which has only one chain, A and contains 335 residues. Moreover, the structure of PH domain is shown in Figure 5.2 and it also has one chain, A and is composed of 111 residues. The complex of protein kinase domain with inhibitor A-443654 has two chains, A and C which are composed of 342 and 10 residues respectively (Figure 5.3).

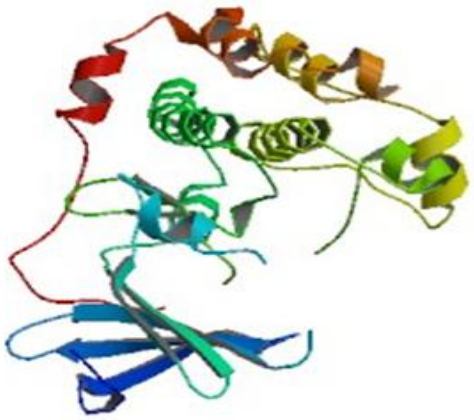

Figure 5.1. The structure of the protein kinase domain of Akt2 protein (PDB 1gzn).

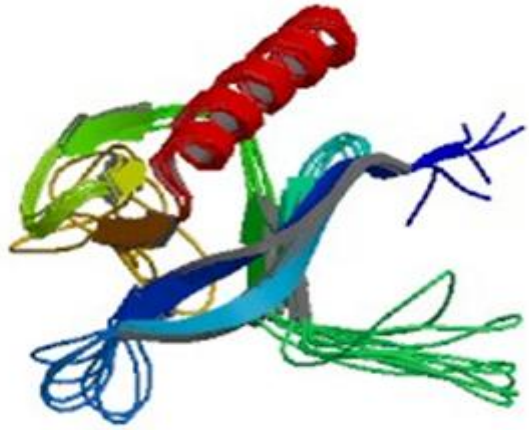

Figure 5.2. The structure of PH domain of Akt2 protein (PDB 1p6s).

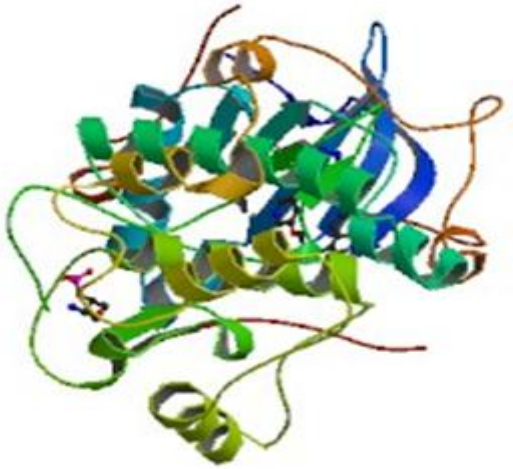

Figure 5.3**.** The structure of protein kinase domain complex with inhibitor A-443654 (PDB 2jdr).

In literature, many inhibitors of Akt2 can be encountered since the inhibition of Akt protein is related to the oncology therapy. Rouse et al., (2009) described the residues of Phe163, Glu200, Ala232, Asn280, Asp293 and Phe294 as a pocket for Aminofurazans, the potent inhibitors of Akt kinase (Rouse et al., 2009). Moreover, Val166, Met229, Glu230, Ala232 and Glu236 formed another interaction site for different inhibitors of Akt2 protein (Saxty et al., 2007). McHardy and her colleagues (2009) discovered orally active inhibitors of protein kinase B (Akt) and Glu236, Glu279, Met282 and Asp293 were the residues that formed a pocket for these inhibitors (McHardy et al, 2009). Glu200, Leu204, Met229, Ala232, Glu236 and Phe294 were other discovered residues for different novel inhibitors of Akt2 (Heerding et al., 2008). 11 residues of the protein kinase domain (Gly159, Phe163, Val166, Lys181, Glu230, Ala232, Glu236, Asn280, Met282, Asp293 and Phe439) formed a pocket for the inhibitor A-443654 (Davies et al., 2007). The residues of the pockets interacting with different inhibitors are given in Table 5.1.

Table 5.1. The residues of the pocket that interacts with inhibitors.

Davies et al. (2007)	**Rouse et al. (2009)**	**Saxty et al. (2007)**	**Mchardy et al. (2009)**	**Heerding et al. (2008)**
Gly159	Phe163	Val166	Glu236	Glu200
Phe163	Glu200	Met229	Glu279	Leu204
Val166	Ala232	Glu230	Met282	Met229
Lys181	Asn280	Ala232	Asp293	Ala232
Glu230	Asp293	Glu236		Glu236
Ala232	Phe294			Phe294
Glu236				
Asn280				
Met282				
Asp293				
Phe439				

5.2. Ligand binding site identification by geometric approaches

The binding sites of small molecules are generally pockets on the protein surface. The identification of pockets provides information for protein function annotation, protein-ligand docking, and protein structure-based drug design. Geometric approaches are relatively straightforward and define the size, shape, surface and atoms lining the concavity of the pockets.

5.2.1. CAST/CASTp

CASTp finds 46 pockets for the structure of Akt2 kinase domain (PDB 1gzn). The output of CASTp web server for Akt2 is shown in Figure 5.4. CASTp requires only PDB code for the detection of the pockets. A corresponding sequence map, where residues in highlighted pocket are also highlighted in the same color, is represented below in Figure 5.4.

CASTp also gives information about the volume and the area of the identified pockets and sorts them by their areas. Figure 5.5 displays the last 10 pockets of Akt2 protein kinase domain and their volume and area relations. The largest pocket (pocket 46) includes 51 residues and its area and volume are 1302.4 $Å^2$ and 1693.3 $Å^3$ respectively. Thus, the volume percentage of the largest pocket is 6.5. Furthermore, the second largest pocket's area is 220.3 $Å^2$ and the volume is 261.6 $Å^3$. The volume percentage of 45^{th} pocket is only 1.00.

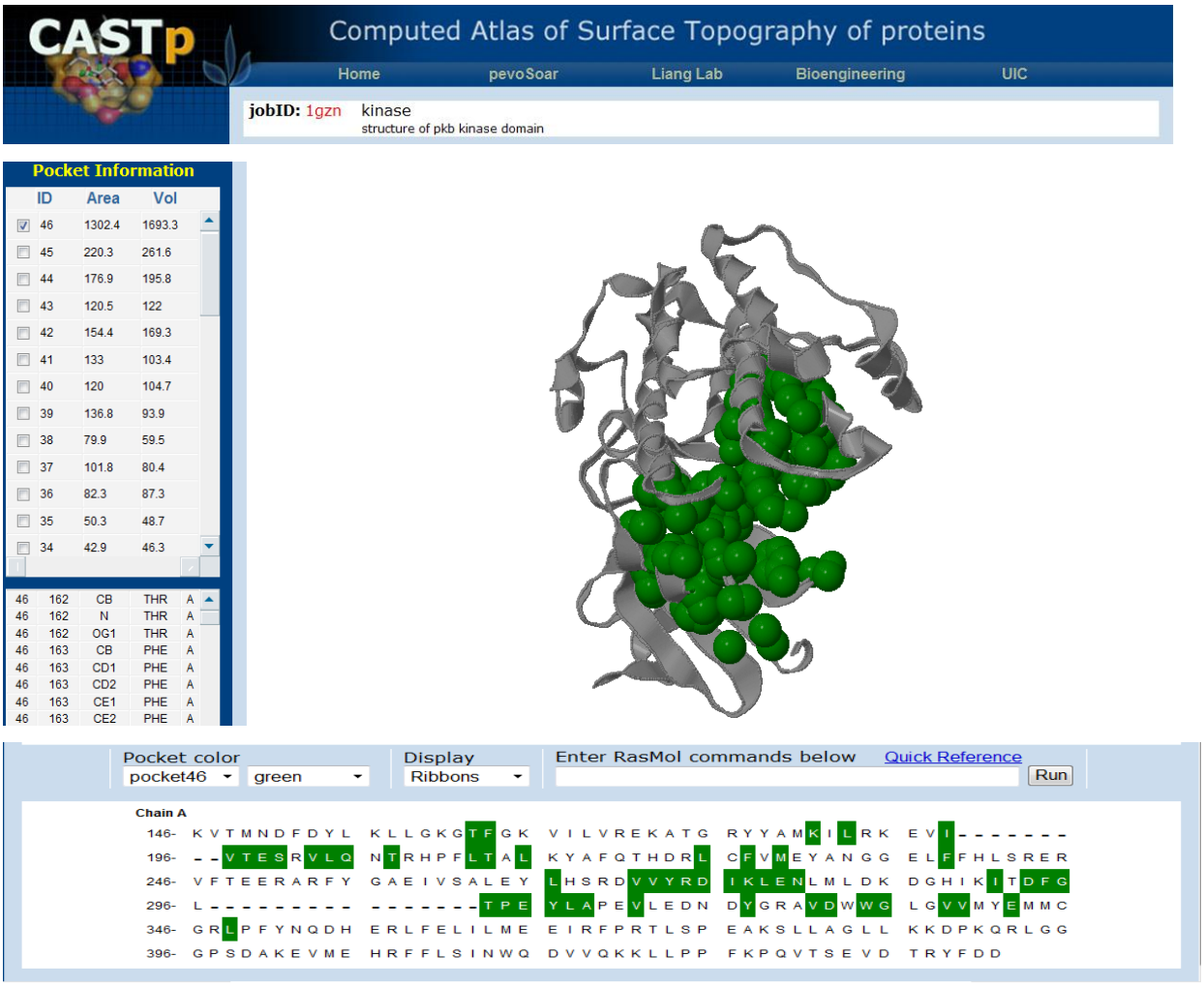

Figure 5.4. Jmol visualization of Akt2 (PDB 1gzn) by using CASTp.

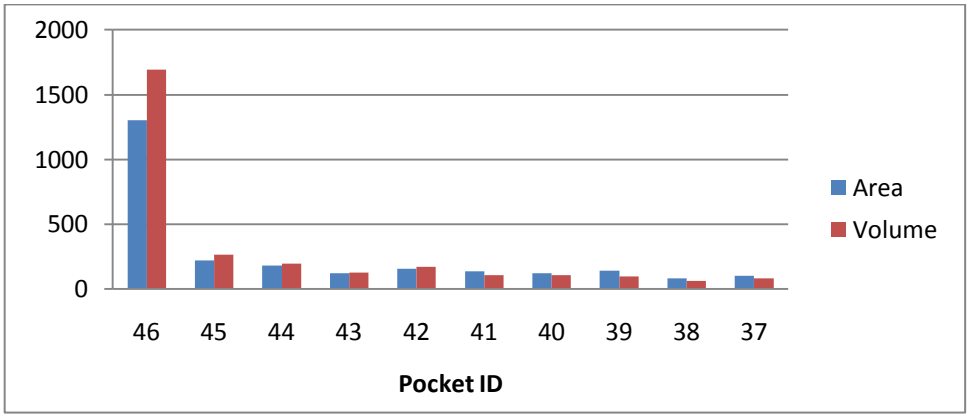

Figure 5.5. The areas and volumes of the protein kinase domain of Akt2 pockets as a result of CASTp quest.

Over 100 proteins were analyzed by CAST including both small and large proteins and the results of CAST showed that medium size proteins have 10-20 pockets which have 1-2 mouth openings. Moreover, ligand binding pockets differ by size, within the range of 10^2-10^3 $Å^3$. For instance, glycogen phosphorylase binds pyridoxal 5"phosphate; the binding site has a volume of 1398 $Å^3$ and a surface area of 1300 $Å^2$. The importance of the size of the pocket is that small ligands are known to bind to the largest cavity on the surface of the protein (Liang et al., 1998).

Pocket 46 contains both active site residue ASP and binding site residue LYS although the second largest pocket (pocket 45) which has 13 residues does not include any of these sites. Additionally, there are not any common residues between pocket 46 and 45. Figure 5.6 shows amino acid composition of the largest pocket (pocket 46) and it contains 17.6 % Leucine and 15.7% Valine and both of them are nonpolar and hydrophobic.

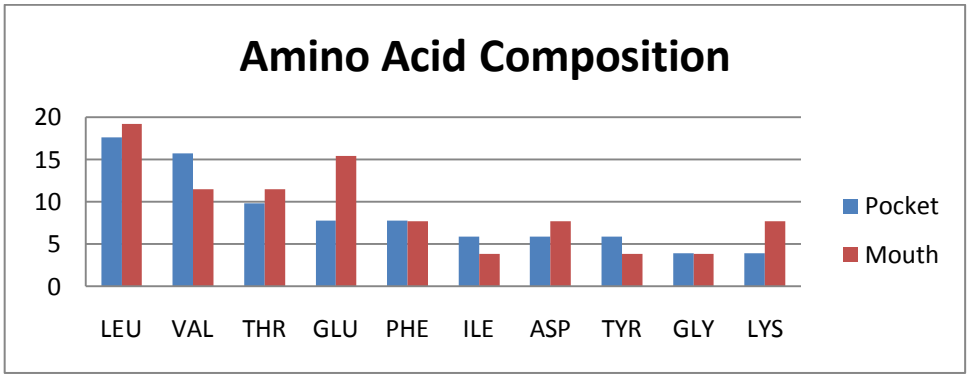

Figure 5.6. Amino acid composition of the largest pocket and its mouth (PDB 1gzn).

Phe163, Lys181, Asn280 and Asp293 which are included by the pocket of the protein kinase domain complex with inhibitor A-443654 (PDB 2jdr) are also predicted by 46^{th} pocket of the CASTp.

CASTp computes the number of mouths and the areas of the mouth openings for each pocket. The "rim" atoms are also identified by CASTp. Furthermore, the features of the mouth openings indicate ligand accessibility to the pocket interior. The volume of the protein is not related with the number of mouth openings. However, larger pockets have larger mouth opening area. In general, if the volume of ligand binding site is >1800 $Å^3$, the binding site has more than two mouths (Liang et al., 1998). 46^{th} pocket has 7 mouth

openings and the solvent accessible and molecular surface area of the mouth openings are 196.5Å^2 and 437.2Å^2 respectively. The mouth openings of pocket 46 include both active and binding sites and are formed totally of 26 residues. The mouth of pocket 46 contains 23% Leucine, 15.4% Glutamic Acid, 11.5 % Valine and Threonine (Figure 5.6). Both the largest pocket and its mouths are mainly composed of Leucine, Valine, Threonine and Glutamic Acid. Additionally, 45th pocket has only one mouth opening and is formed by 7 residues. The solvent accessible and molecular surface areas of 45th pocket are 15.2 Å^2 and 52.9 Å^2, respectively. The mouth of pocket 45 includes 28.5% Glutamic acid and Lysine.

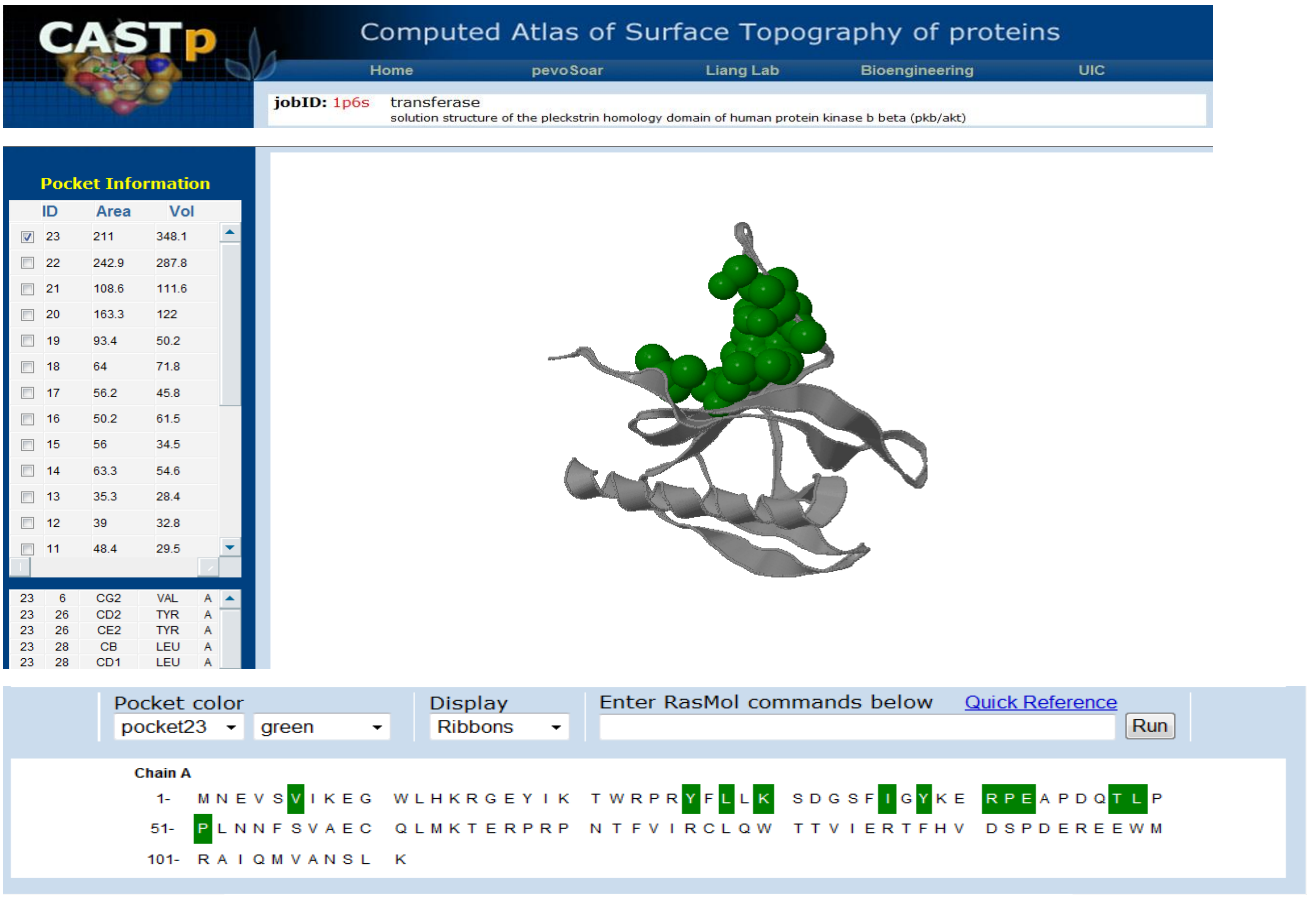

Figure 5.7. Jmol visualization of Akt2 (PDB 1p6s) by using CASTp.

The pockets of the pleckstrin homology (PH) domain of human protein kinase B are also identified by CASTp (Figure 5.7). 23 pockets are characterized and the area of the largest pocket is 211 Å^2 and the volume is 348.1 Å^3.The volume comparison of pockets are important since ligands generally prefer the largest pocket of the protein for binding (Figure 5.8). Thus the largest pocket features are necessary for analysis. The largest pocket

(23th pocket) volume is about 3.2 percent of the PH domain and it has 12 residues. It is composed of 16.7 % Leucine, 16.7 % Proline, and 16.7 % Tyrosine (Figure 5.9).

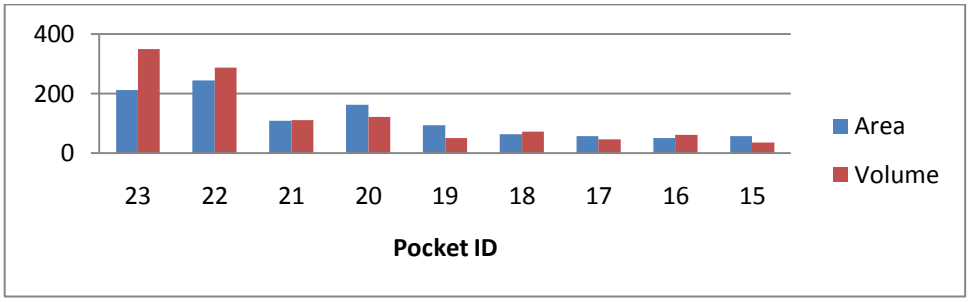

Figure 5.8. The areas and volumes of the PH domain pockets' as a result of CASTp quest.

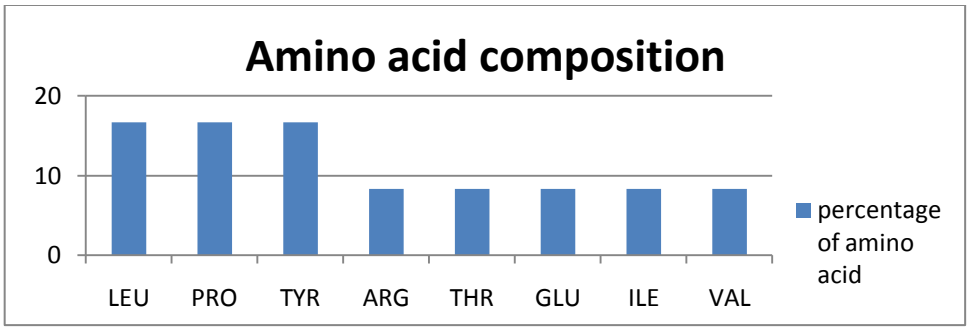

Figure 5.9. Amino acid composition of PH domain of Akt2 by using CASTp results.

In summary, CASTp finds 46 pockets for protein kinase domain whereas it finds 23 pockets for PH domain of Akt2 (Table 5.2). Leucine is the main common amino acid in the pockets of both kinase domain and PH domain. The volume of protein kinase domain is larger than that of PH domain and both the volume and area of the largest pocket of kinase domain are also larger than those of the largest pocket of PH domain (Table 5.3).

Table 5.2. The comparison of the domains of Akt2.

	Protein Volume ($Å^3$)	Number of Pockets
Protein Kinase Domain	26068	46
Pleckstrin Homology Domain	10907	23

Table 5.3. The analysis of the largest pocket of protein kinase domain and pleckstrin homology domain of Akt2.

Domain	Number of Residues	Area ($Å^2$)	Pocket Volume ($Å^3$)	Site Volume/Domain Volume	Highly Encountered A. Acids
Protein Kinase	51	1302.4	1693.3	6.5	LEU VAL THR
Pleckstrin Homology	12	211	348.1	3.2	LEU PRO TYR

5.2.2. SCREEN

SCREEN is accessed through Function Annotation Server- MarkUs (http://luna.bioc.columbia.edu/honiglab/mark-us/cgi-bin/submit.pl). MarkUs analyzes the structure of a protein by using a file in PDB format. The PDB (1gzn) file of Akt2 is uploaded to the system and the results were explained below. Figure 5.10 demonstrates the chain A representation of Akt2 given MarkUs.

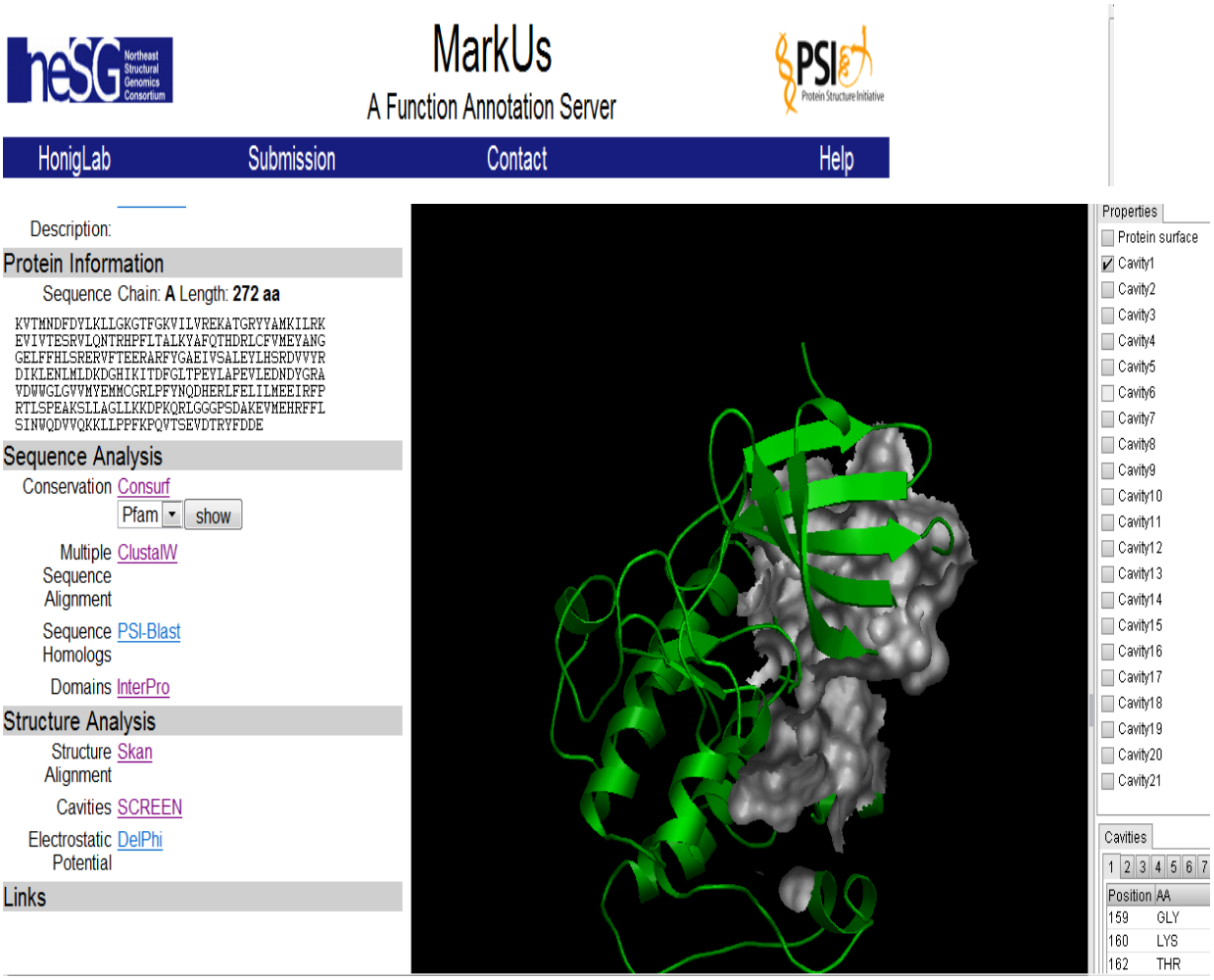

Figure 5.10. MarkUs visualization of Akt2 (PDB 1gzn).

SCREEN identifies 21 cavities on the surface of protein kinase domain of Akt2 (PDB 1gzn). The first ranked cavity consists of 37 residues and it contains both active site residue Asp and binding site residue Lys whereas the second ranked cavity which has 17 residues does not include any of these sites. The values of area, diameter and solvation energy are highest and the side chain entropy is lowest for the first ranked cavity compared to other cavities (Table 5.3). Average charge, electric potential, electric field, curvature, depth and maximum depth are also computed for each cavity (Tables 5.13 and 5.14). SCREEN also gives information about the secondary structures of the cavities. The first ranked cavity is composed of helix, sheet, turns and coils.

Figure 5.11 demonstrates the amino acid composition of the first ranked cavity and it contains 21% Valine and 10.8% Leucine that are both nonpolar and hydrophobic amino acids.

Gly159, Phe163, Lys181, Asn280 and Asp293 that were some of the inhibitor binding residues of Akt2 (PDB 2jdr) were also identified by the first ranked pocket of SCREEN.

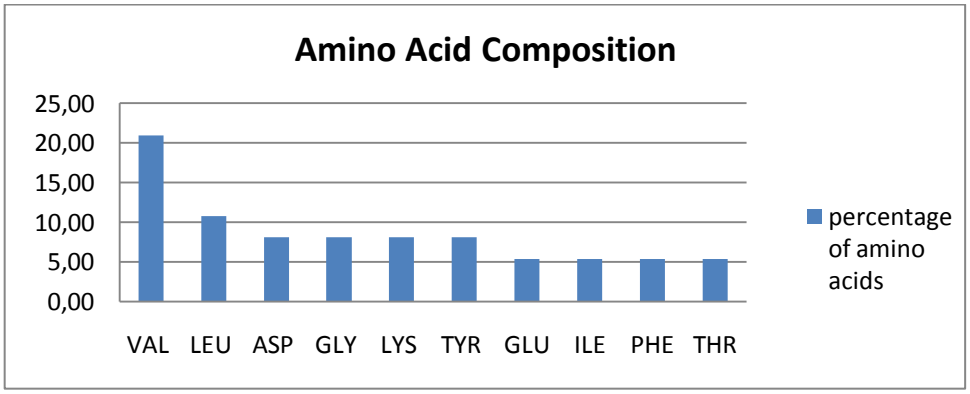

Figure 5.11. Amino acid composition of the first ranked cavity.

The ligand binding site is generally observed in the largest surface cavity. In the present study, the first ranked pocket has the largest area which is 508.5 $Å^2$ as shown in Figure 5.12 and it contains the binding site residue Lys and also active site residue Asp as mentioned above. In another work reported in literature, SCREEN identifies the largest cavity for Protein-tyrosine phosphatase 1B with an area of 184 $Å^2$ (Nayal and Honig, 2006).

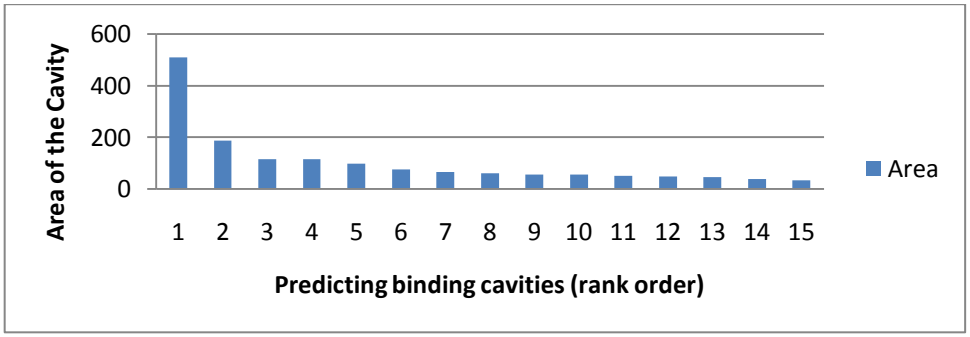

Figure 5.12. Analysis of the role of cavity area on the predicting binding sites.

10 cavities are identified on the surface of PH domain of Akt2 protein by SCREEN (Figure 5.13). The first ranked cavity (145.7 $Å^2$) has 12 residues and it is formed by 16.7% Leucine, Proline and Tyrosine, and 8.3% Glutamic Acid, Alanine, Lysine, Valine, Isoleucine and Threonine (Figure 5.14).

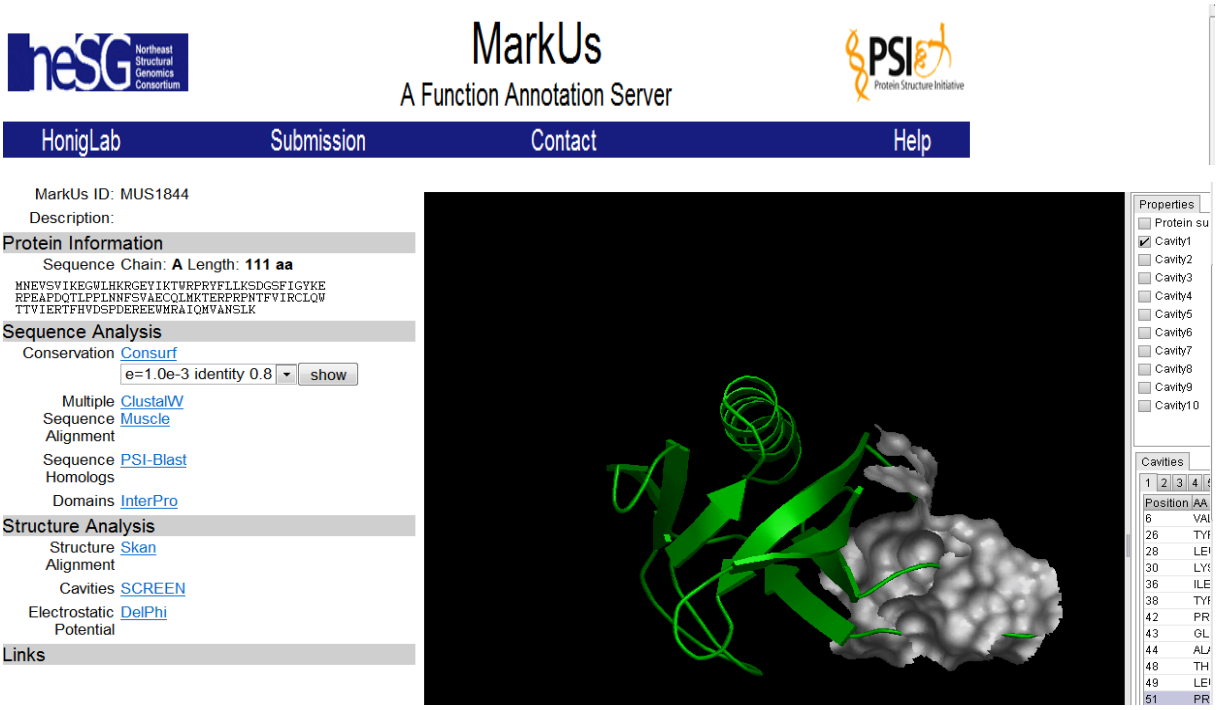

Figure 5.13. MarkUs visualization of Akt2 (PDB 1p6s).

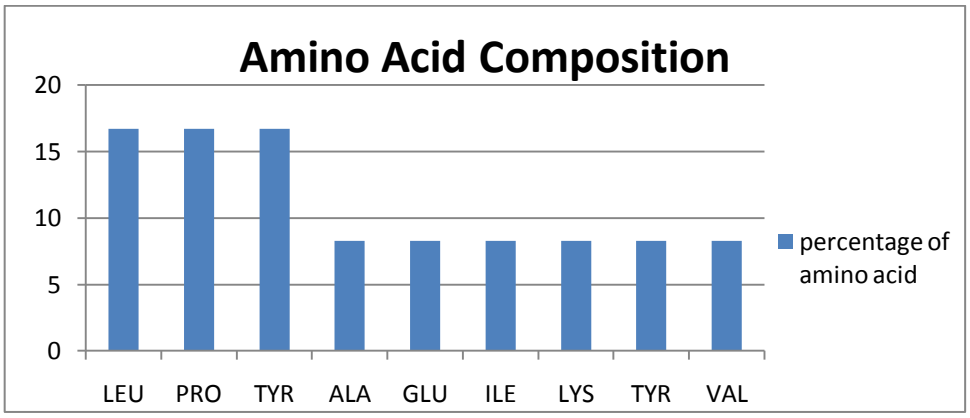

Figure 5.14. Amino acid composition of PH domain as a result of SCREEN.

The detection of the largest cavity plays a significant role in predicting the ligand binding sites. The ranking of SCREEN is associated with the areas of the cavities so the largest cavity is ranked as number 1 and the relation of rank order and area of each cavity is given in figure 5.15.

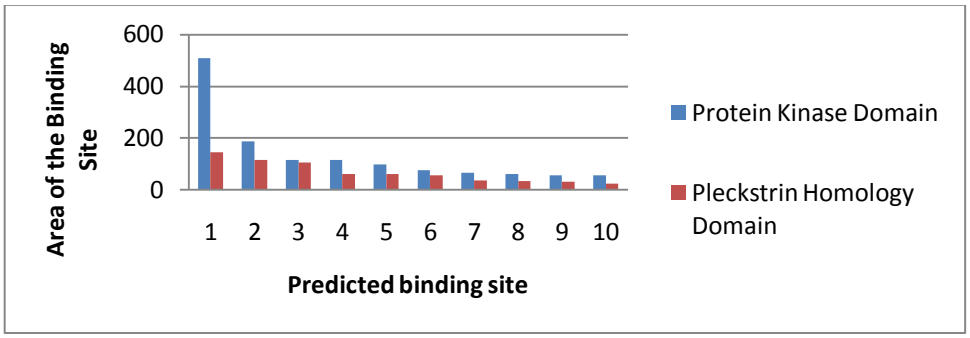

Figure 5.15. The connection between the area and the rank order of the pockets.

Kinase domain has larger cavities than PH domain. Moreover, the solvation energy is higher and the side chain entropy is lower for protein kinase domain. On the other hand, there is not a big gap between the values of the average charge and electric field of both domains (Table 5.4).

Table 5.4. The features of Kinase domain and PH domain of Akt2.

	Kinase Domain	**PH Domain**
Number of Residues	37	12
Area (Å^2)	508.5	145.7
Diameter (Å)	24.6	13.0
Solvation Energy (kcal/mol)	1.688	0.982
Side Chain Entropy (kcal)	-4.271	-1.049
NonPolar %	0.6	0.7
Polar %	0.4	0.3
Average Charge	-0.07	-0.062
Average Electric Field (mV/nm)	11.63	11.51

5.2.3. SplitPocket

The geometric measurements of a protein's pre-computed functional surfaces are provided by SplitPocket. This web server gives residue composition (spatial patterns), solvent-accessible area and molecular volume of the pockets and mouths. Figure 5.16 shows a standard output page belonging to SplitPocket server.

SplitPocket concept is designed to distinguish the functional surfaces of a bound structure; therefore the structure of PKB-beta (Akt2) complexed with the inhibitor A-443654 is used to predict ligand binding pockets. It is significant to note that a predicted pocket is a putative binding site and may not necessarily be a functional surface. SplitPocket finds 22 patches for Akt2 (PDB 2jdr).

The 22^{nd} pocket is placed on the functional surface and it is the largest pocket (Figure 5.17). This pocket has 39 amino acids, its solvent accessible area is 870.98 $Å^2$ and the molecular volume is 1080.19 $Å^3$. Tseng and their colleagues analyzed mitogen-activated protein kinase (PDB 1ouk) by using SplitPocket, and the area and the volume of the functional surface of mitogen activated protein kinase are 416.37 $Å^2$ and 711.51 $Å^3$, respectively. Surface conservation index is computed as 0.717 for Akt2 protein complexed with an inhibitor. The conservation index is a useful evolutionary feature to distinguish a protein's functional surface (binding site) from other regions. The 22^{th} pocket is formed by 15.4% Phenylalanine, 12.8% Threonine, 12.8% Glutamic Acid, 10.3% Leucine, 7.7% Aspartic Acid, 7.7% Lysine, 7.7% Glycine, 5.1% Valine, 5.1% Alanine and 5.1% Methionine (Figure 5.18).

The inhibitor binding residues of Akt2 are Gly159, Phe163, Val166, Lys181, Glu230, Ala232, Glu236, Asn280, Met282, Asp293, Phe439 (Davies et al., 2007) and all of these residues are identified by the split pocket (22^{nd}) on the functional surface.

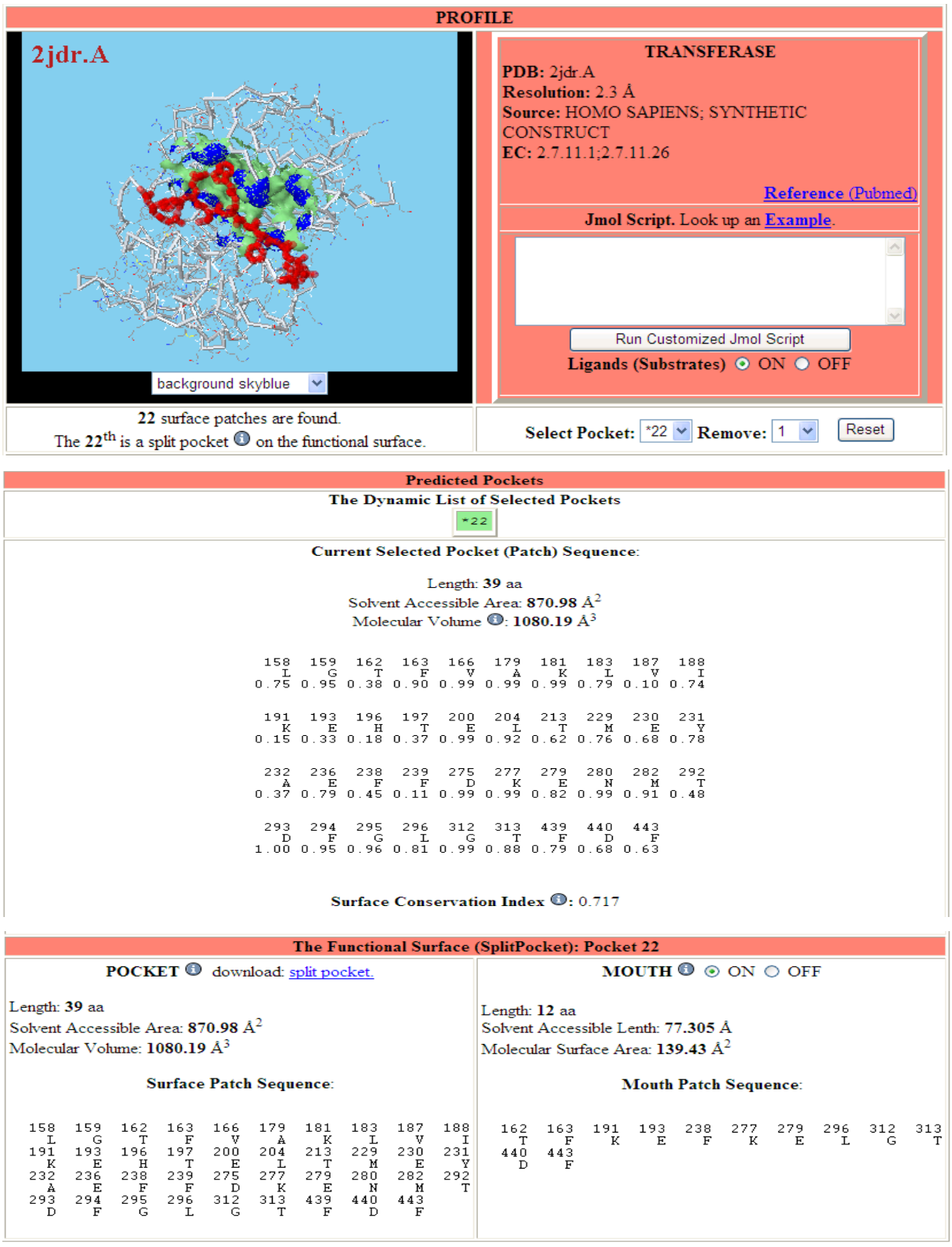

Figure 5.16. SplitPocket output window for Akt2.

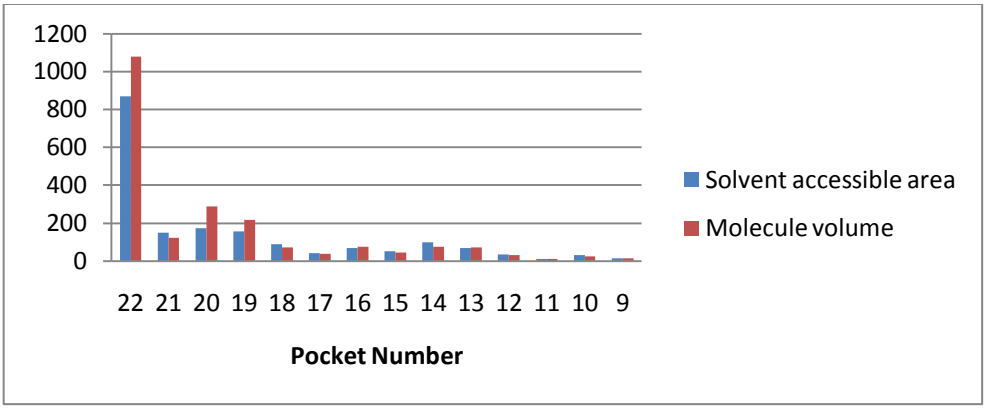

Figure 5.17. Analysis of volume and area relation with pocket number (SplitPocket-protein kinase domain).

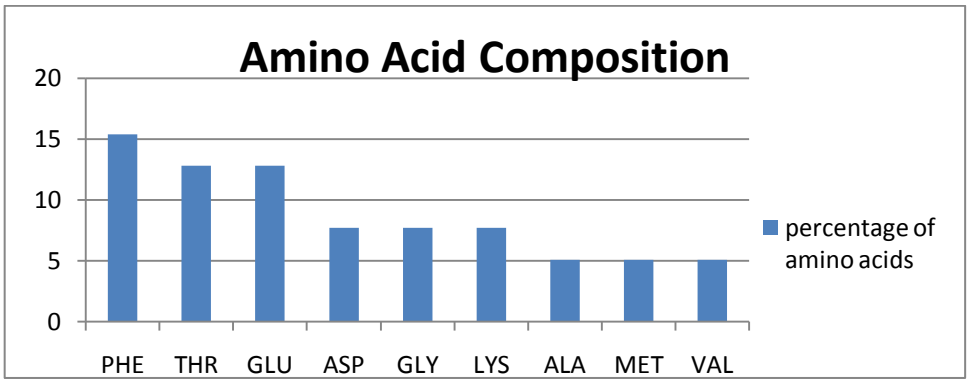

Figure 5.18. Amino acid composition of functional surface of Akt2 protein kinase domain (PDB 2jdr).

SplitPocket also characterizes the mouth opening of the functional surface. It includes 12 residues and 6 of them are same as the mouth opening residues found by CASTp. The mouth of the functional surface is made up of 23% Phenylalanine, 16.7% Glutamic Acid, Lysine and Threonine (Figure 5.19).

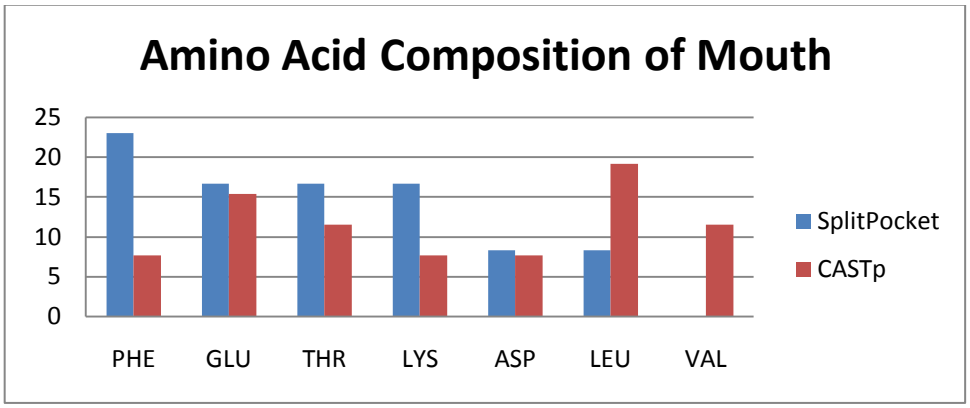

Figure 5.19. The comparison of amino acid composition of mouth opening.

5.2.4. Comparison of Geometry Based Web Servers

The pockets detected by CASTp and SCREEN coincide well for kinase domain of Akt2 protein. However, the extent and size of the corresponding cavities differ. A cavity defined by SCREEN is usually broken up into two or more cavities by CASTp. As a result, CASTp finds 46 pockets for kinase domain of Akt2 compared to 21 cavities found by SCREEN for the same domain. Furthermore, SplitPocket predicts 22 pockets. The comparison of web server results are given in Table 5.5 and 5.6. CASTp and SCREEN detects 23 and 10 pockets, respectively, for PH domain. SplitPocket detects pockets of only bound proteins and there is not any ligand bound structure of pleckstrin homology domain.

Table 5.5. Comparison of the number of pockets detected by CASTp, SCREEN and SplitPocket.

Ligand Binding Prediction Methods	**Number of Predicted Pockets**	
	Protein Kinase Domain	**PH Domain**
CASTp	46	23
SCREEN	21	10
SplitPocket	22	N.A

The first ranked pockets of protein kinase domain have larger volume and area than those of PH domain and the first ranked pocket of CASTp has the largest volume and area. Leucine is the common residue of both kinase and PH domains as determined by all methods, although Glutamic acid and Phenylalanine are the most common residues that compose ligand binding pockets reported in literature. CASTp and SplitPocket give information about mouth openings whereas SCREEN does not include any data concerned with mouth openings. Threonine and Glutamic Acid are main shared residues of mouth openings found by CASTp and SplitPocket (Table 5.6).

Table 5.6. The first ranked pocket comparison predicted by CASTp, SCREEN and SplitPocket.

	CASTp		**SCREEN**		**SplitPocket**	
Information on Pockets	**Kinase Domain**	**PH Domain**	**Kinase Domain**	**PH Domain**	**Kinase Domain**	**PH Domain**
Number of Residues	51	12	37	12	39	N. A.
Area ($Å^2$)	1302.4	211	5085	145.7	870.98	N. A.
Volume ($Å^3$)	1693.3	348.1	N. A.	N. A.	1080.19	N. A.
Highly encountered A.A.(top 3)	LEU VAL THR	LEU PRO TYR	VAL LEU ASP GLY LYS TYR	LEU PRO TYR	PHE THR GLU LEU	N. A.
Highly encountered A.A on mouth opening	LEU GLU VAL THR	N. A.	N. A.	N. A.	PHE GLU LYS THR	N. A.

Figure 5.20 displays the overlap of residues in the first predicted site of CASTp and SCREEN for protein kinase domain. CASTp predicts 17 residues that are not predicted by SCREEN and SCREEN predicts only 3 residues that are not predicted by CASTp and 34 residues are predicted by both methods.

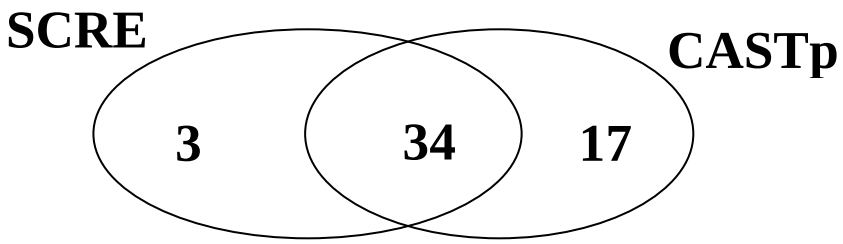

Figure 5.20. Overlap in ligand binding residues in the first predicted site of protein kinase domain.

13 residues are predicted by CASTp, SCREEN and SplitPocket in common. CASTp predicts 15 residues that are not predicted by other methods and SCREEN finds 3 residues which are not predicted by other methods. Moreover, SplitPocket finds 20 residues which are not detected by others (Figure 5.21).

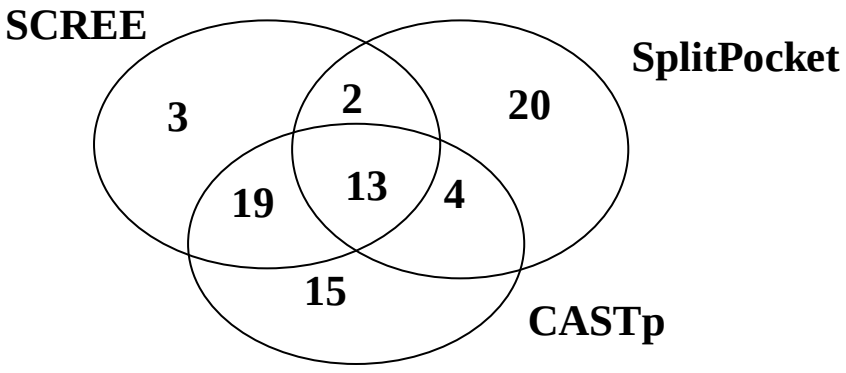

Figure 5.21. Overlap in ligand binding residues in the first predicted site of protein kinase domain (all geometry based methods).

Additionally, CASTp and SCREEN detect 12 residues in the first predicted site of PH domain and 11 residues are predicted by both methods (Figure 5.22). Hence same pocket is found for PH domain of Akt2 protein by both CASTp and SCREEN servers.

SplitPocket detects pockets of only bound proteins and there is not any ligand bound structure of pleckstrin homology domain.

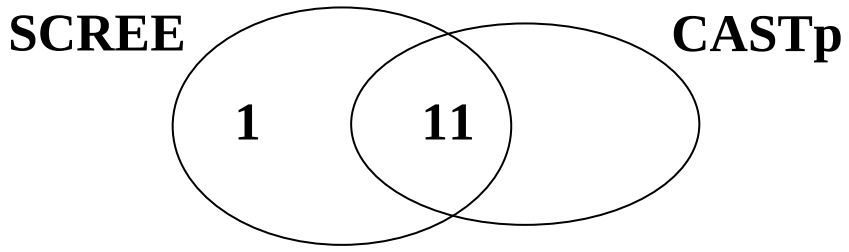

Figure 5.22. Overlap in ligand binding residues in the first predicted site of pleckstrin homology domain.

In the literature, totally 13 residues of Akt2 protein are identified to interact with inhibitors (Rouse et al., 2009, Saxty et al., 2007, McHardy et al., 2009 and Heerding et al., 2008). These are Phe163, Val166, Glu200, Leu204, Met229, Glu230, Ala232, Glu236, Glu279, Asn280, Met282, Asp293 and Phe294. The 46th pocket of CASTp includes 8 of these 13 residues which are Phe163, Glu200, Leu204, Met229, Glu279, Asn280, Asp293 and Phe294. The first ranked pocket of SCREEN includes 6 of these 13 residues, Phe163, Glu200, Leu204, Asn280, Asp293, and Phe294. The split pocket (22nd) which is placed on functional surface has all 13 residues identified for inhibitor binding site in the literature.

5.3. Ligand binding site identification by energetic approaches

The energy calculations are also used to identify ligand binding sites on the protein surface. Although some energetic methods simply use van der Waals energies to describe protein shape; in generally, the interaction energy between the protein and a probe is computed by positioned probe appropriately close to protein surface atoms or at grid points surrounding the protein. Q-SiteFinder, Pocket-Finder and SITEHOUND are the web servers for the prediction of ligand binding sites by using energetic approaches (Henrich et al., 2009).

5.3.1. Q-SiteFinder

Figure 5.23 demonstrates the output of Q-SiteFinder. 10 different sites are predicted by Q-SiteFinder for Akt2 protein kinase domain (PDB 1gzn). Protein volume, site volume, binding box coordinates around selected sites and residues are given by Q-SiteFinder for each predicted site. Precision is defined as the percentage of probe sites in a single cluster within 1.6 Å of a ligand atom. Protein kinase domain of Akt2 with PDB code 1gzn does not have any ligand thus precision value cannot be computed for this case.

Predicted site 1 has the largest volume, 356 $Å^3$ and the second largest site's volume is 271 $Å^3$. Although the predicted site 1 of protein kinase domain includes 22 residues, the predicted site 2 includes only 12 residues. The predicted sites 1 and 2 constitute 1.40 and 1.04 percent by volume of protein kinase domain, respectively. The amino acid composition of the predicted site 1 is not more different than the results of SCREEN and CASTp. It contains 18.2% Valine, 13.6% Leucine and 13.6% Glutamic Acid (Figure 5.24). Though the predicted site 1 contains active site residue Asp-275, it does not include the binding site residue Lys-181.

The first ranked predicted site identified by Q-SiteFinder does not include any residues which are involved in inhibitor binding of protein kinase domain of Akt2 complexed with inhibitor A-443654 (PDB code 2jdr).

The ligand binding site is observed to be the largest pocket when the simulations are performed by SCREEN and CASTp. Predicted site 1 is also recognized as the largest one by Q-SiteFinder (Figure 5.25). Moreover, Laurie and Jackson (2005) analyzed the predicted site 1 of bilin binding protein (PDB 1bbp) by Q-SiteFinder and found the volume as 390 $Å^3$ (Laurie and Jackson, 2005). The ligand binding site volumes predicted by Q-SiteFinder are in comparable sizes for different proteins (Akt2 vs bilin binding protein).

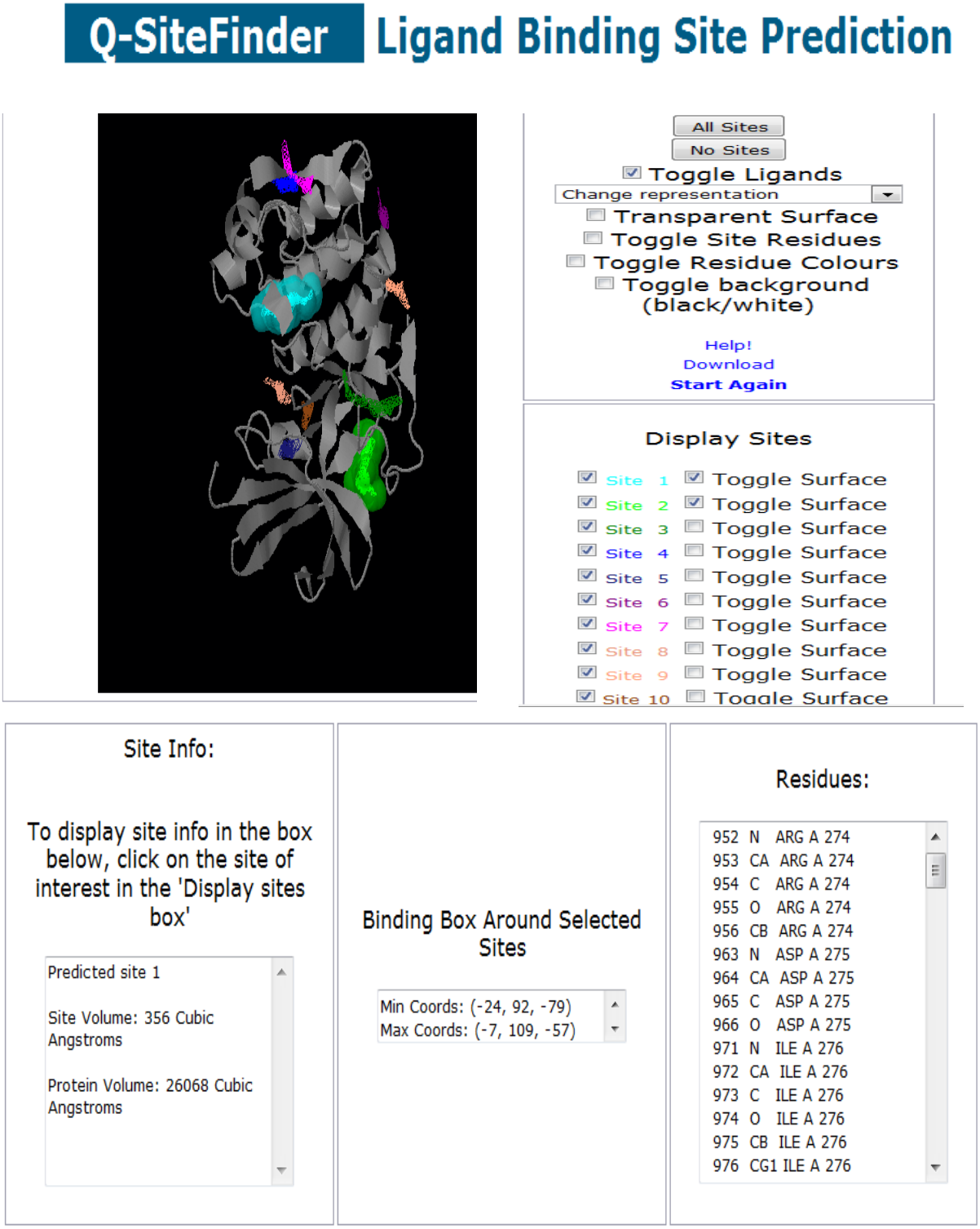

Figure 5.23. The output of Q-SiteFinder for protein kinase domain.

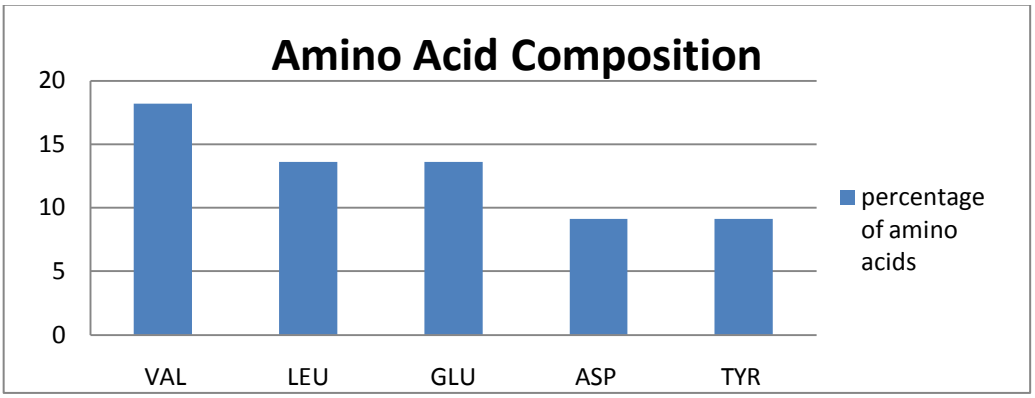

Figure 5.24. Amino acid composition of the predicted site 1 of protein kinase domain of Akt2.

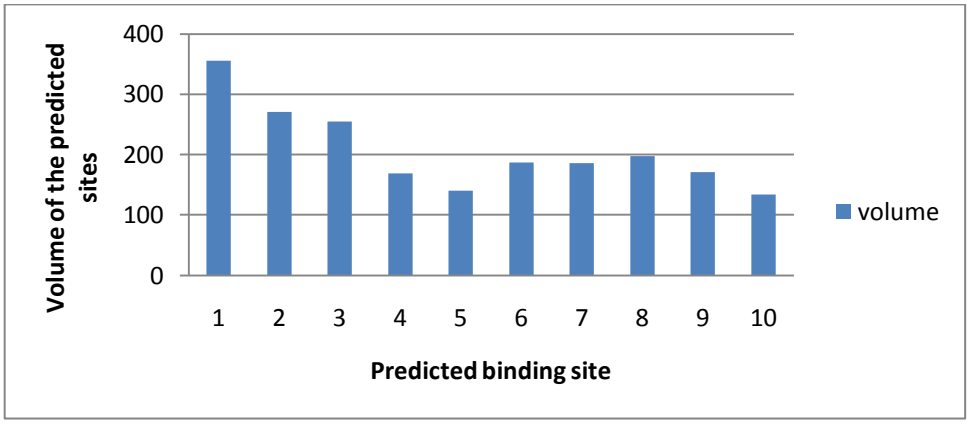

Figure 5.25. Analysis of the role of predicted site volume of protein kinase domain on the predicting binding sites.

Q-SiteFinder finds 10 different sites for pleckstrin homology domain of Akt2 (PDB 1p6s). The output window is given in Figure 5.26. The largest site volume is 374 $Å^3$ and it is 3.4 percent of the PH domain. The second largest site volume is 320 $Å^3$ and it is 2.9 percent of the domain volume. The predicted sites 1 and 2 have 22 and 28 residues, respectively. The amino acid composition is shown in Figure 5.27. 13.6% Arginine and 9.1 % Glutamic Acid, 9.1 % Valine, 9.1 % Phenylalanine, 9.1 % Histidine, 9.1 % Threonine, 9.1 % Proline form the predicted site 1.

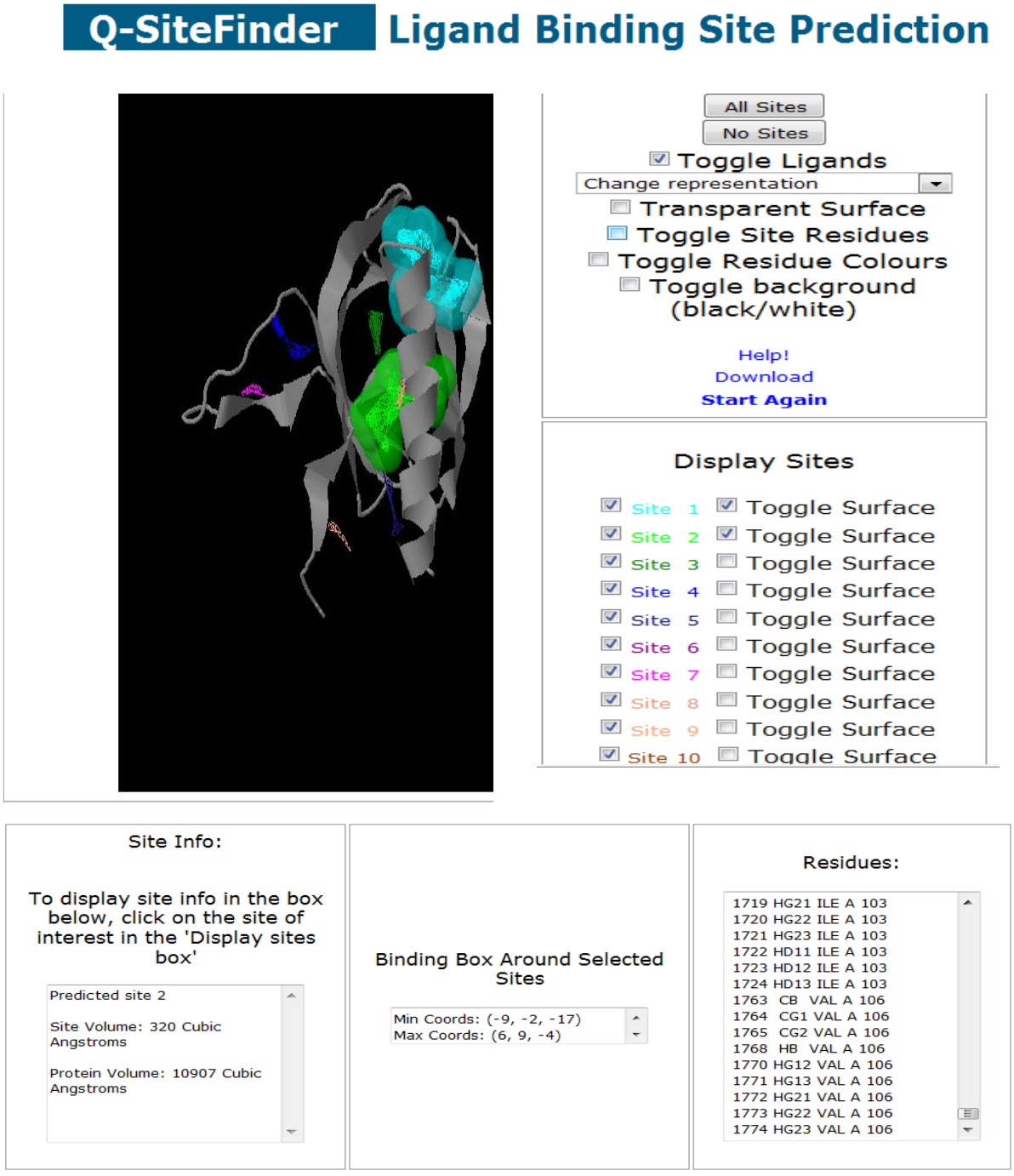

Figure 5.26. The outputs of Q-SiteFinder for pleckstrin homology domain of Akt2.

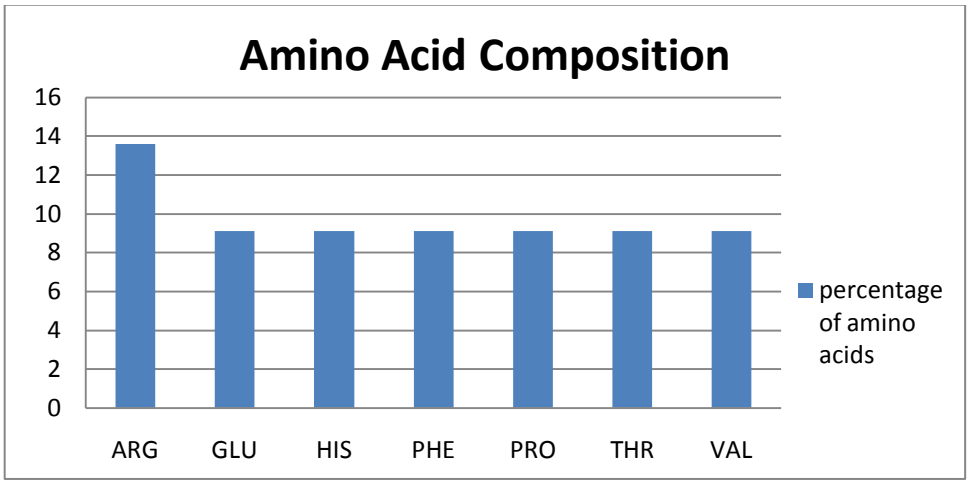

Figure 5.27. Amino acid composition of the predicted site 1 for PH domain of Akt 2.

The volumes and the ranks of the predicted sites of both protein kinase domain and pleckstrin homology domain are given in Figure 5.28.

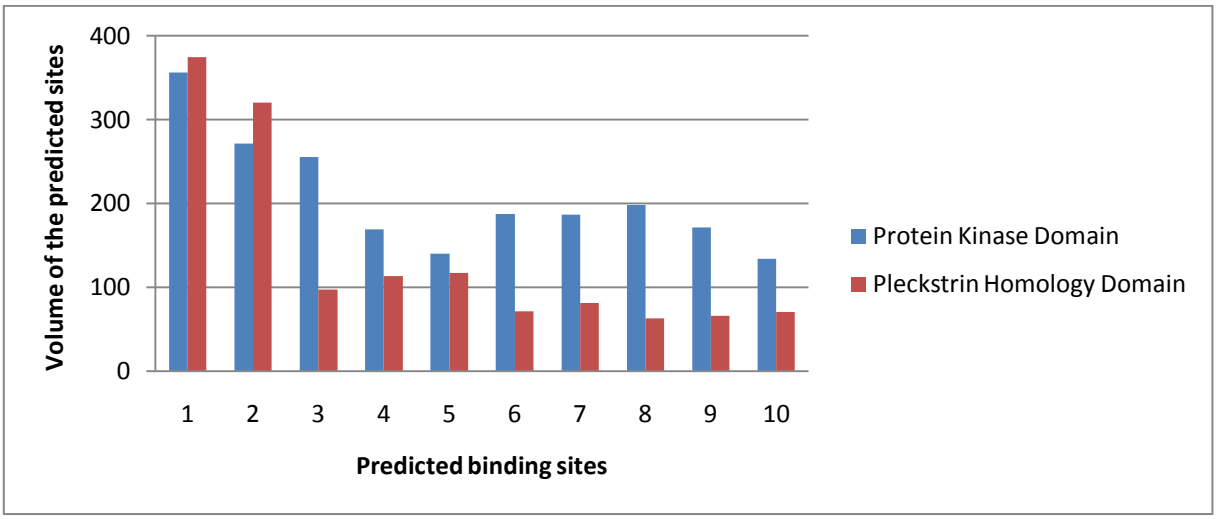

Figure 5.28. Analysis of the role of predicted site volume on the predicting binding sites.

The first predicted sites of both protein kinase and pleckstrin homology domains are composed of 22 residues. The site volume of protein kinase domain is 356 $Å^3$and the site volume of pleckstrin homology domain is 374 $Å^3$. The comparison of the Q-SiteFinder results for two domains' predicted site 1 is given in Table 5.7.

Table 5.7. The comparison of the predicted site 1 of protein kinase domain and pleckstrin homology domain of Akt2.

	Number of Residues	**Volume (Å^3)**	**Site Volume/ Domain Volume**
Protein Kinase Domain	22	356	1.4
Pleckstrin Homology Domain	22	374	3.4

5.3.2. Pocket-Finder

Pocket-Finder also employs PDB code of Akt2 protein as an input and gives the protein volume, site volume, binding box coordinates around sites and site residues as outputs. Precision value is not calculated since it is related with the ligand and the cases for Akt2 kinase and PH domain do not include any ligand. Figure 5.29 shows the output window of Pocket-Finder for protein kinase domain.

The volumes of the predicted site 1 and 2 are 591 Å^3 and 394 Å^3, respectively. In literature, the average volume of successful predictions in the first predicted site was calculated as 460 Å^3 by Pocket-Finder (Laurie and Jackson, 2005). The site 1 forms 2.3 percent of the kinase domain and it includes 27 residues. Moreover, the site 2 constitutes 1.51 percent of the domain and contains 22 residues. The active site residue of Akt2 is the only common residue between predicted binding sites 1 and 2. Figure 5.30 displays the amino acid composition of site 1 which contains 18.5% Leucine, 14.8% Threonine and 14.8% Valine and of site 2 which is formed by 18.2% Valine, 13.6% Leucine and 13.6% Glutamic acid.

Phe163, Lys181, Asn280 and Asp293 which are involved in inhibitor binding site of protein kinase domain of Akt2 (PDB 2jdr), are identified in the first ranked pocket predicted by Pocket-Finder.

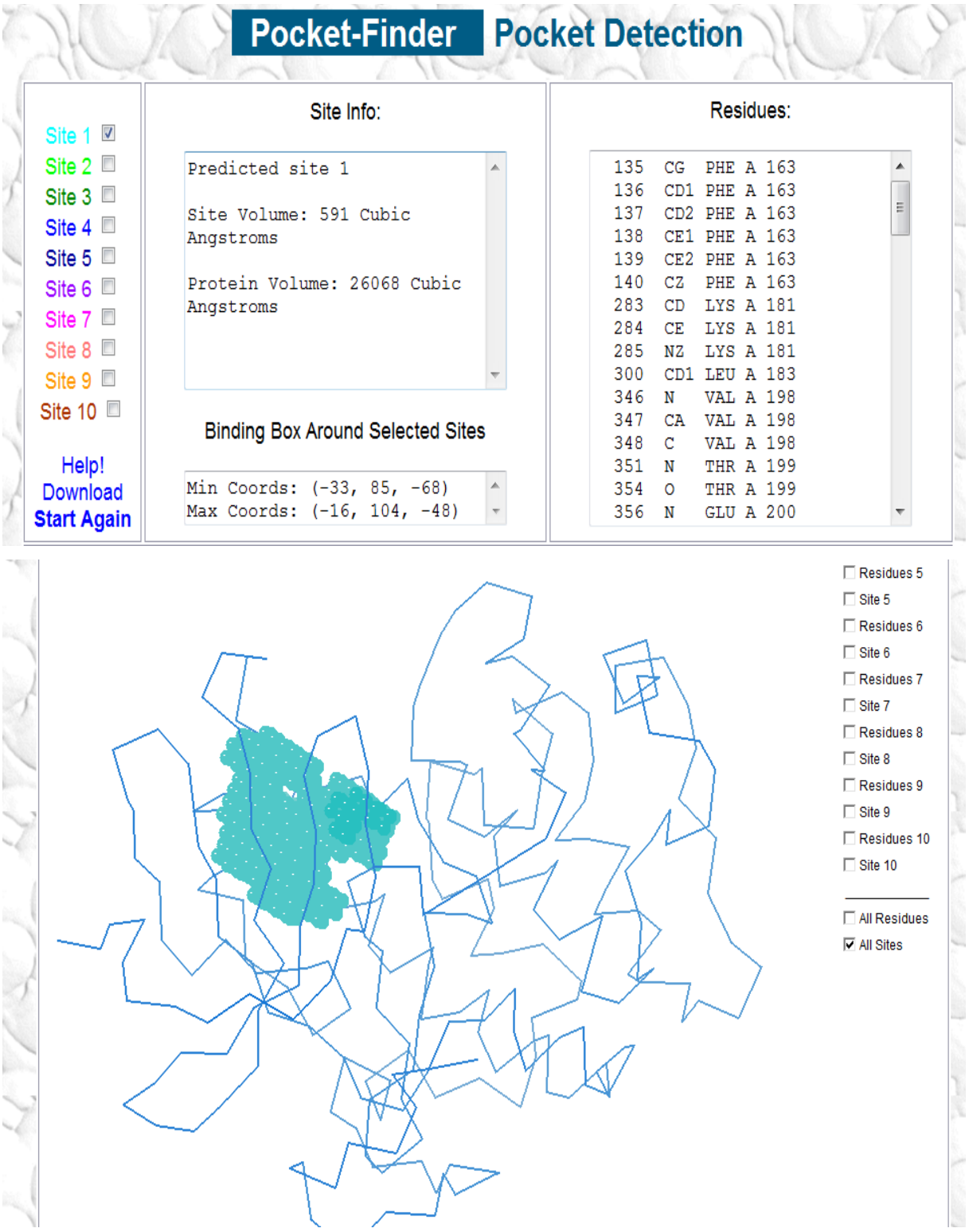

Figure 5.29. The output of Pocket-Finder for kinase domain of Akt2.

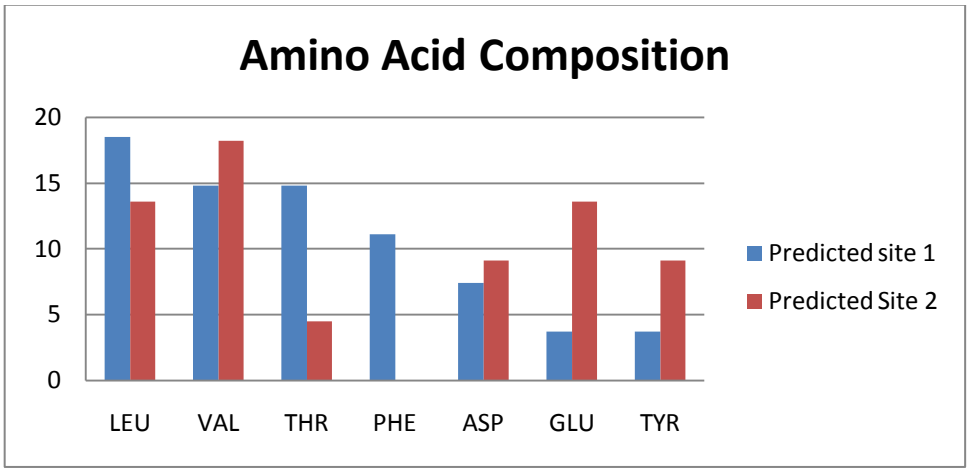

Figure 5.30. Amino acid composition of the predicted sites 1 and 2 for kinase domain of Akt2.

Pocket-Finder also gives information about 10 predicted sites for pleckstrin homology domain of Akt2 (Figure 5.31). The largest pocket is the predicted site 1 and its volume is 168 A^{o3} and the predicted site 2 has a volume of 134 $Å^3$. The site 1 and site 2 include 14 and 15 residues, respectively. Figure 5.32 demonstrates the amino acid composition of these two sites. The first site is composed of 14.3% Cysteine, 14.3% Glutamic Acid and 14.3% Valine. The second site is composed of 26.7% Leucine and 26.7% Phenylalanine. The volumes and the ranks of these sites for both protein kinase domain and pleckstrin homology domain are given in Figure 5.33.

The Pocket-finder results for both protein kinase domain and pleckstrin homology domain are compared in Table 5.8. Although 1st ranked site found by Q-SiteFinder has absolutely the same number of residues (22 residues) for both kinase domain and PH domain, Pocket-Finder predicts 27 residues for the first site of protein kinase domain and 14 residues for the 1st ranked site of PH domain. Moreover, the volume difference of the ligand binding sites is fairly high and the volume of kinase domain's site 1 is greater than that of the PH domain's.

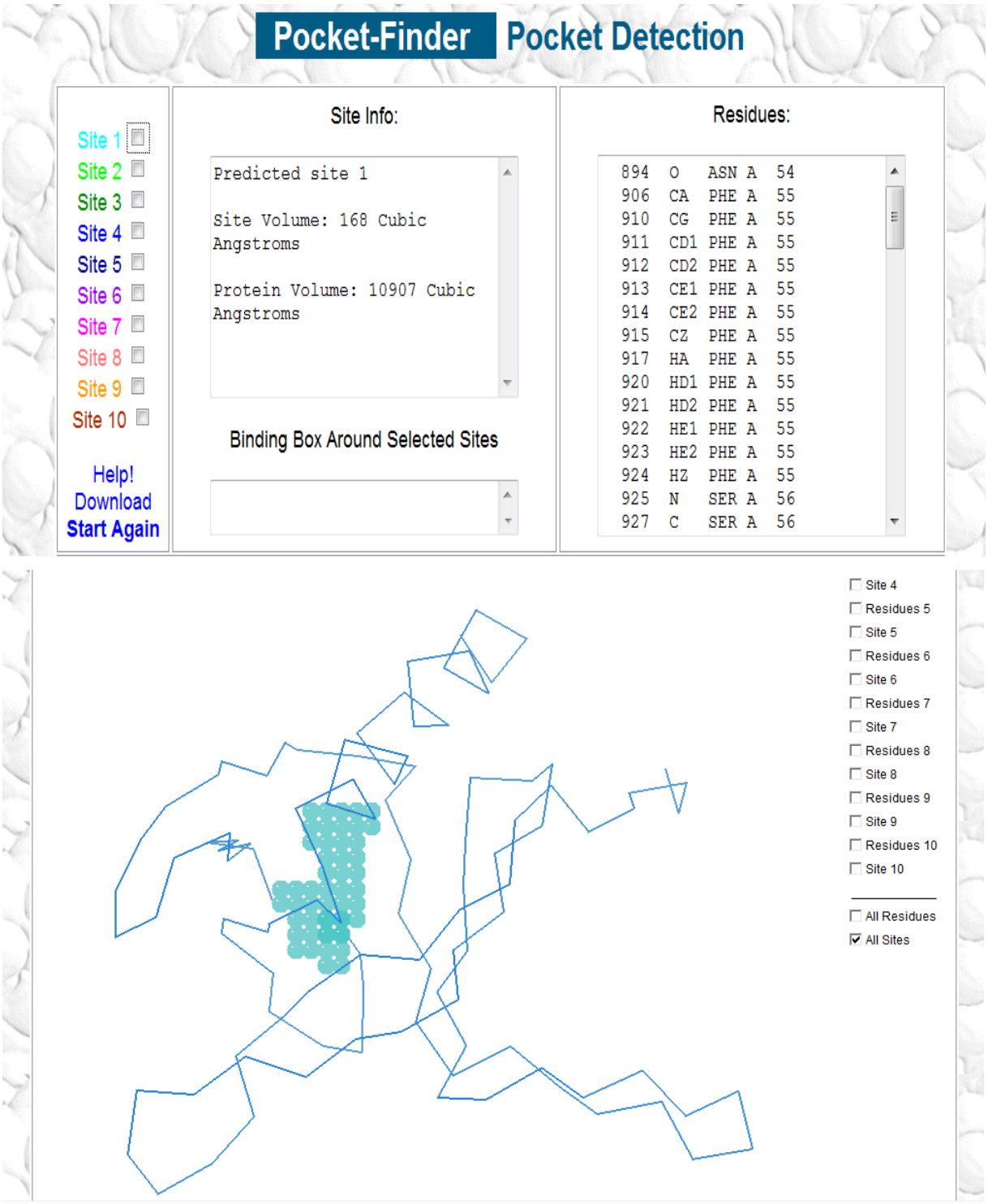

Figure 5.31. The output window of Pocket-Finder for PH domain.

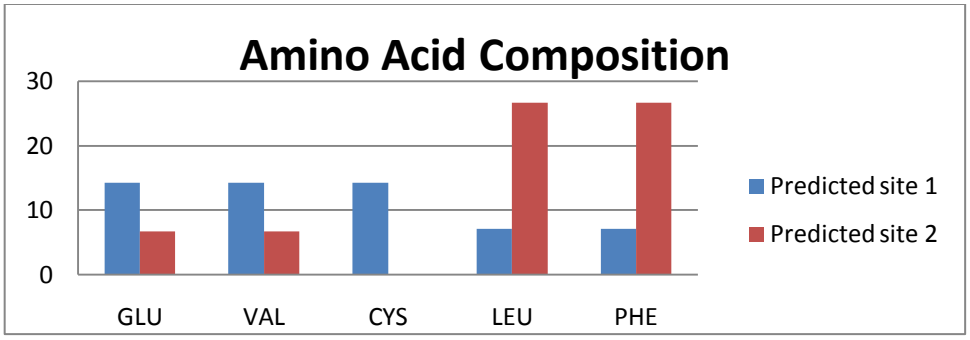

Figure 5.32. Amino acid composition of the predicted site 1 and 2 for pleckstrin homology domain of Akt2.

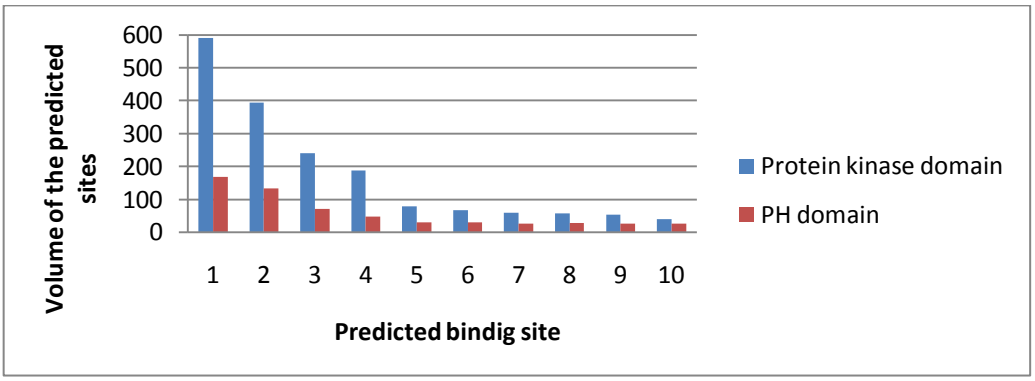

Figure 5.33. Analysis of the role of predicted site volume on the predicting binding sites.

Table 5.8. Pocket-Finder results comparison of predicted site 1 of protein kinase domain and pleckstrin homology domain of Akt2.

	Number of Residues	**Site Volume ($Å^3$)**	**Site Volume / Domain Volume**
Protein Kinase Domain	27	591	2.27
Pleckstrin Homology Domain	14	168	1.50

5.3.3. SITEHOUND

The input of the SITEHOUND is not only PDB code of the protein but the probe type and clustering algorithm should also be selected before submitting the protein. An interactive web screen and downloadable files for offline analysis are the output components of SITEHOUND (Figure 5.34).

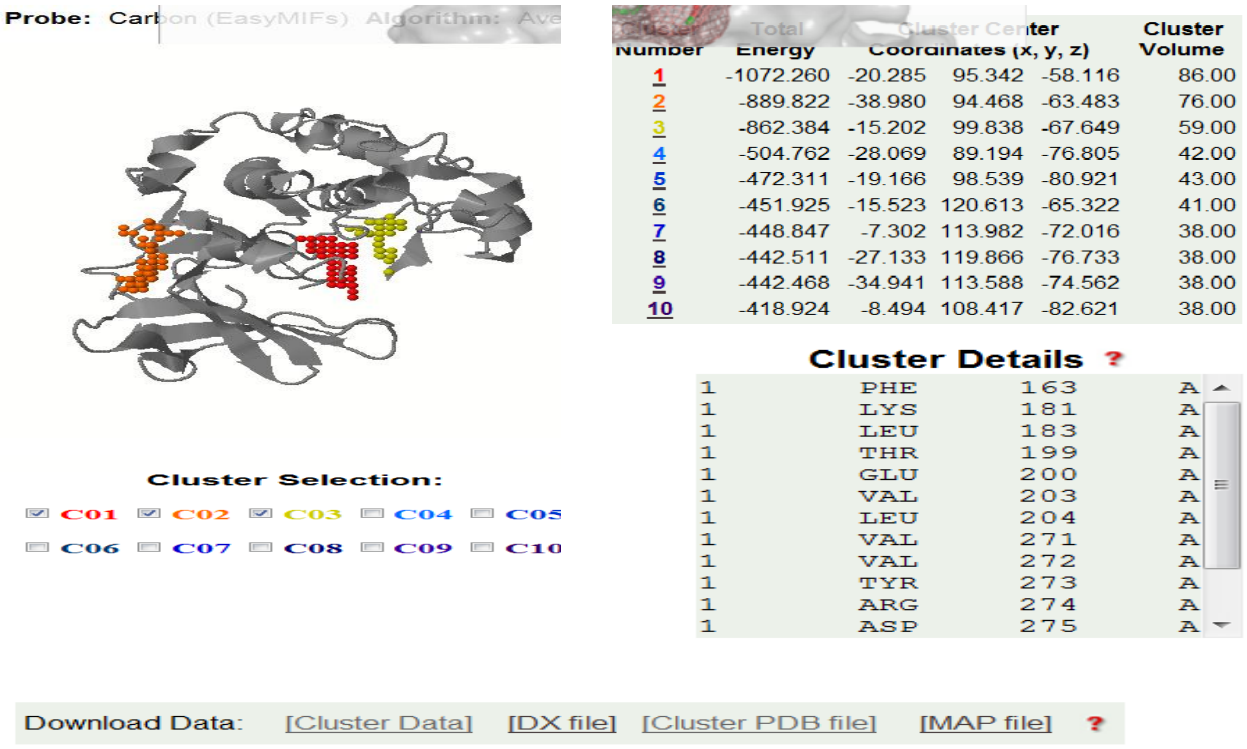

Figure 5.34. SITEHOUND-web Carbon probe, average linkage clustering algorithm output example of kinase domain.

Carbon probe is chosen since it has been employed to identify ligand binding sites for drug-like molecules. The average-linkage clustering algorithm is used to identify spherical clusters, whereas single-linkage clustering algorithm is used to identify larger elongated binding sites. Both average-linkage algorithm and single-linkage algorithm are chosen and the results are analyzed and shown in Table 5.9. The results of the different algorithms are similar for kinase domain of Akt2, eg. the volumes and the number of residues are same. The volume is 86 $Å^3$ and the energy is -1072 cal/mol for the ligand binding site of kinase domain of Akt2. Hernandes *et al. (*2009) used SITEHOUND to

identify the pockets for yeast adenylate kinase (PDB 1aky). The first ranked cluster had a volume of 127 $Å^3$ and its energy value was computed as -60.385 cal/mol by using carbon probe and average-linkage algorithm (Hernandez et al., 2009).

Table 5.9. The comparison of average-linkage and single-linkage clustering algorithm by using Carbon probe.

	Average-linkage Algorithm		**Single-linkage Algorithm**	
Cluster	1	2	1	2
Volume ($Å^3$)	86	76	85	48
Number of Residues	15	19	15	19
Energy (cal/mol)	-1072	-889	-1061	-742

Both clustering algorithms identify the active site and binding site for the kinase domain of Akt2 protein in their cluster 1 but these residues are not present in any of cluster 2. Amino acid compositions of the clusters are also obtained and the amino acid compositions of first clusters are exactly same (Figure 5.35). Cluster 1 of average-linkage and single-linkage algorithms is made up of 20% Valine, 13,3% Aspartic acid, Leucine, Phenylalanine and 6,7% Glutamic Acid, Tyrosine, Arginine and Lysine.

Phe163, Lys181 and Asp293 which are involved in inhibitor binding site of protein kinase domain of Akt2 (PDB 2jdr) are contained in the first ranked cavity of SITEHOUND.

Figure 5.36 displays the output window of SITEHOUND for PH domain of Akt2 protein. Carbon probe is again selected because the aim is to find the ligand binding sites for drug-like molecules. Both average-linkage and single-linkage algorithms are chosen and the results are analyzed and shown in Table 5.10.

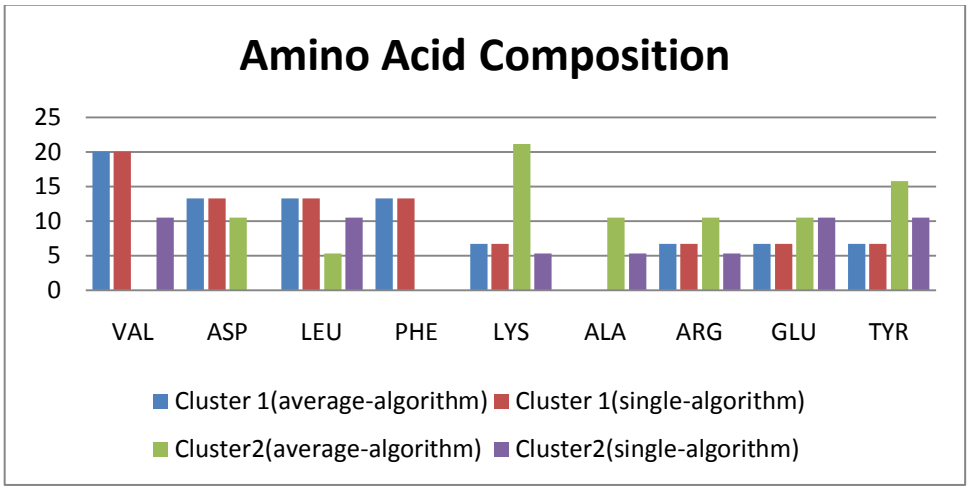

Figure 5.35. Comparison of the amino acid compositions of clustering algorithms (Protein kinase domain).

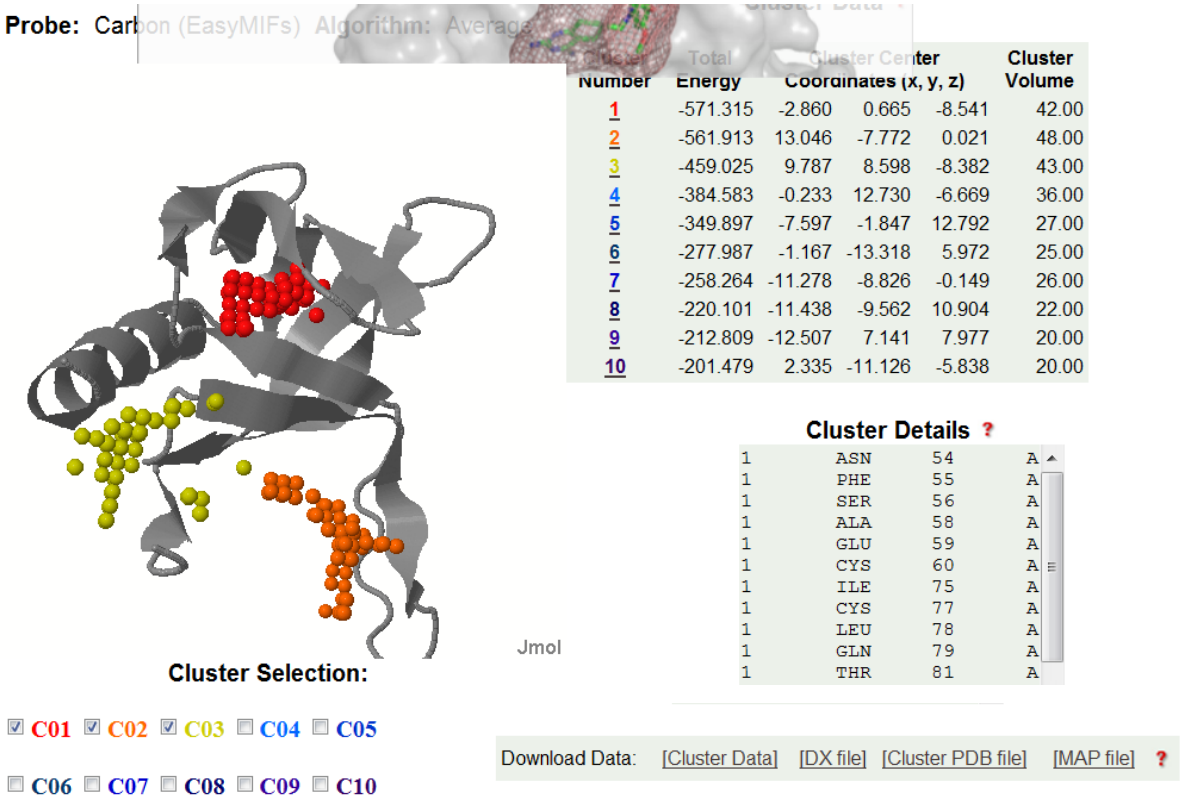

Figure 5.36. SITEHOUND-web Carbon probe, average-linkage clustering algorithm visualization of PH domain.

Table 5.10. The comparison of average-linkage and single-linkage clustering algorithms in analyzing the PH domain.

	Average-linkage Algorithm		**Single-linkage Algorithm**	
Cluster	1	2	1	2
Volume (Å^3)	42	48	38	30
Number of Residues	13	13	12	7
Energy (cal/mol)	-571.315	-561.913	-523.602	-360.819

There are not any common residues between clusters 1 and clusters 2 for PH domain. The results of both clustering algorithms do not overlap exactly but they are close to each other (Figure 5.37). According to the results of average-linkage algorithm, cluster 1 is formed by 15.4% Glutamic Acid and Cysteine but the results given by single-linkage algorithm indicate that cluster 1 is composed of 16,7% Glutamic Acid and Cysteine. Although almost all the residues are common between these clusters, cluster 1 of average-linkage algorithm includes one more residue.

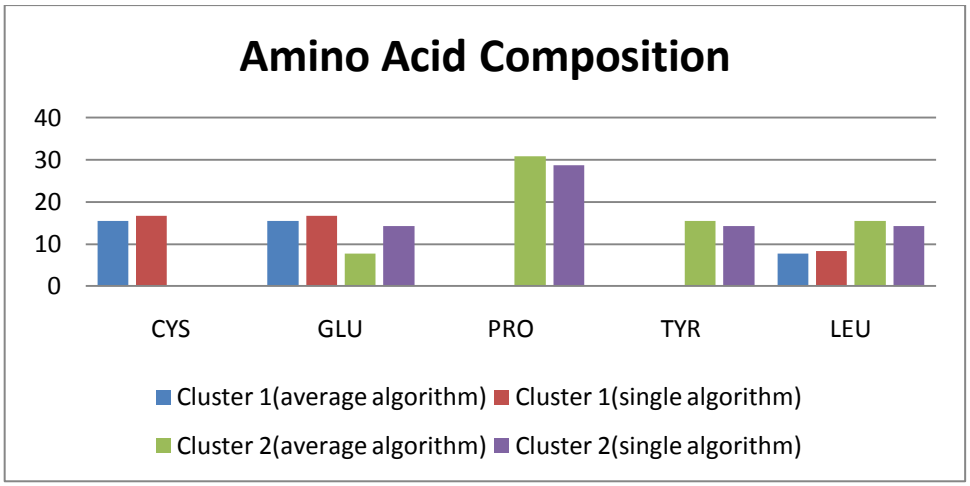

Figure 5.37. The amino acid composition comparison of clustering algorithms (PH domain).

The average–linkage clustering algorithm is the best choice for both domains since the total interaction energies are lower. Table 5.11 demonstrates the comparison of first clusters for both domains. The site of protein kinase domain has the lowest energy and the largest volume (Figure 5.38) thus it is the most suitable site for ligand binding.

Table 5.11. Comparison of first Clusters of Protein kinase domain and pleckstrin homology domain by using carbon probe and average-linkage clustering algorithm.

	Number of Residues	**Site Volume(Å^3)**	**Site Volume/Domain Volume**	**Energy (cal/mol)**
Protein Kinase Domain	15	86	0.32	-1072.260
Pleckstrin Homology Domain	13	42	0.40	-571.315

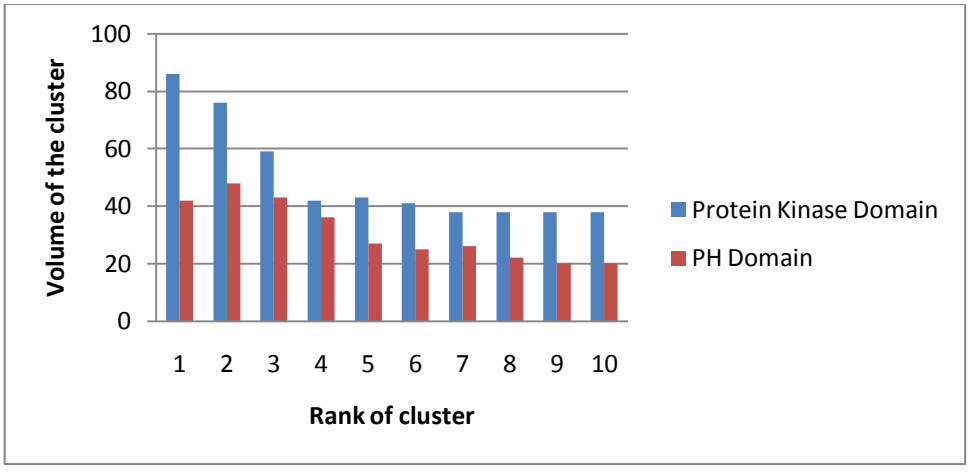

Figure 5.38. Volume and rank relation of clusters.

5.3.4. Comparison of Energy Based Web Servers

The ligand binding sites predicted by Q-SiteFinder and Pocket-Finder does not overlap for site 1 of protein kinase domain. There is only one common residue detected by Q-SiteFinder and Pocket-Finder (Figure 5.39). However, the predicted site 1 of Q-SiteFinder and predicted site 2 of Pocket-Finder exactly overlap (data not shown).

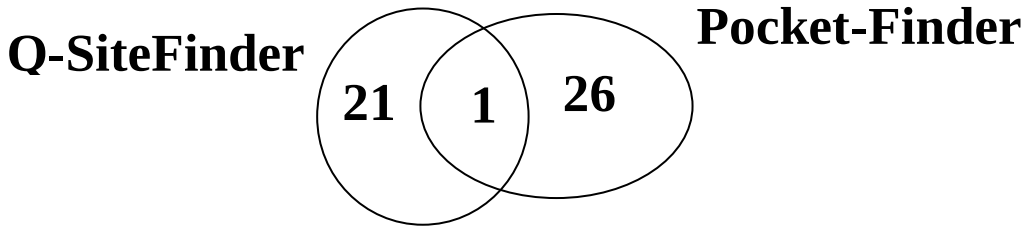

Figure 5.39. Overlap in the first ligand binding site (protein kinase domain).

Table 5.12. The correlation of the ligand binding site prediction methods, Q-SiteFinder, Pocket-Finder and SITEHOUND for protein kinase domain.

	Number of Residues		**Volume Site/ Volume Domain**	
	Pocket 1	**Pocket 2**	**Pocket 1**	**Pocket 2**
Q-SiteFinder	22	12	1.40	1.04
Pocket-Finder	27	22	2.27	1.51
SITEHOUND	15	19	0.32	0.29

The first ranked site of Pocket-Finder is the largest pocket and the first pocket of SITEHOUND is the smallest pocket (PDB 1gzn). The residues of these first pockets are compared and only one residue (Asp275) is common in all these first pockets. Q-SiteFinder predicts 20 residues that are not predicted by Pocket-finder and SITEHOUND. Moreover, Pocket-Finder predicts 13 residues that are not predicted by Q-SiteFinder and SITEHOUND. SITEHOUND predicts 15 residues and 14 of them is common with Pocket-

Finder and 2 of them is common with Q-SiteFinder when the first ranked pockets identified by 3 web servers are analyzed (Figure 5.40).

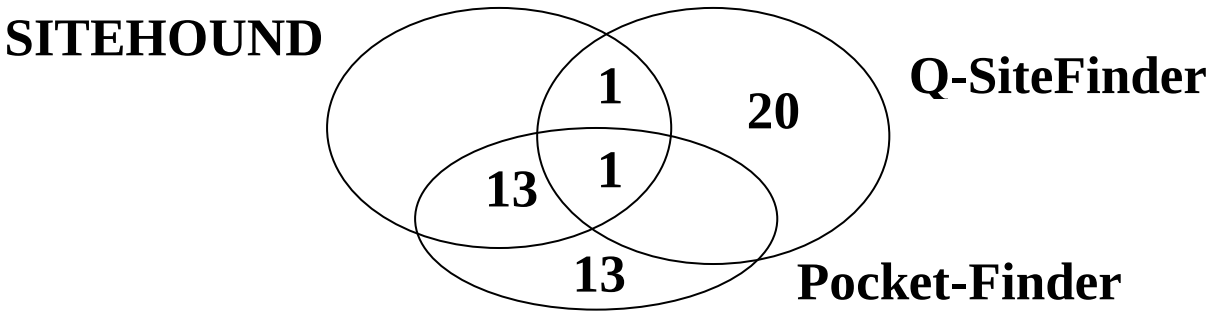

Figure 5.40. Overlap in ligand binding sites prediction in the first predicted site for protein kinase domain.

Among the second ranked pockets, Q-SiteFinder predicts only 2 residues that are not predicted by SITEHOUND, and 9 residues are predicted by only SITEHOUND. 10 residues are predicted as common by both methods for protein kinase domain of Akt2 protein (Figure 5.41).

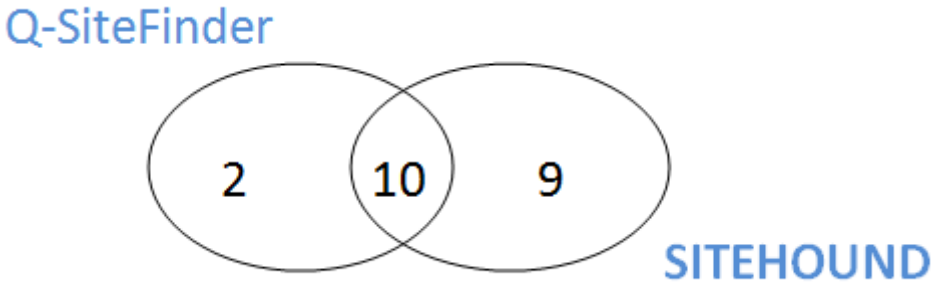

Figure 5.41. Overlap in ligand binding sites (the second ranked site) for protein kinase domain.

For PH domain of Akt protein, the predicted site 1 of Pocket-Finder includes 1 more residue than that of SITEHOUND. 13 residues are predicted as common by both methods. Furthermore, there is not any common residue between Pocket-Finder, SITEHOUND and Q-SiteFinder for PH domain (Figure 5.42).

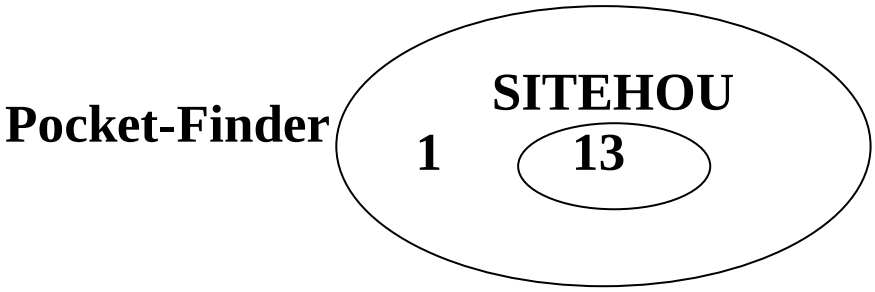

Figure 5.42. Analysis of predicted residues in the first pocket related to PH domain.

In the literature, the residues of protein kinase domain of Akt2, Phe163, Val166, Glu200, Leu204, Met229, Glu230, Ala232, Glu236, Glu279, Asn280, Met282, Asp293 and Phe294, were characterized as binding residues for inhibitors (Rouse et al., 2009, Saxty et al., 2007, McHardy et al., 2009 and Heerding et al., 2008). The first predicted site of Q-SiteFinder only contains Glu279 of these 13 residues. However, the first predicted site of Pocket-Finder includes 7 of these 13 residues which are Phe163, Glu200, Leu204, Met229, Asn280, Asp293 and Phe294. Furthermore, the first ranked pocket of SITEHOUND contains 5 residues which are Phe163, Glu200, Leu204, Asp293 and Phe294.

.

5.4. Comparison of All Pocket Detection Servers

CASTp, SCREEN, Q-SiteFinder, Pocket Finder, SITEHOUND and SplitPocket have only one common residue which is the active site residue, Asp-275 for the protein kinase domain of Akt2 protein. As only the first ranked sites are investigated, CASTp has the largest first predicted binding site which is formed by 51 residues. It has 34 common residues with SCREEN, and 23 and 18 common residues with Pocket Finder and SplitPocket, respectively (Figure 5.43). Moreover, the first ranked pocket of CASTp (geometry based method) covers all the residues identified by Q-SiteFinder and SITEHOUND (energy based methods) for protein kinase domain of Akt2 protein.

CASTp predicts 46 different pockets and the largest one is 1302.4 $Å^3$. SplitPocket detects 22 pockets and the largest one being the functional surface of kinase domain has a volume of 1080.19 $Å^3$. The first predicted cavities of energy based methods (Q-SiteFinder,

Pocket-Finder and SITEHOUND) are smaller than those identified by geometry based servers.

Although the first ranked cavities predicted by CASTp, SCREEN, Q-SiteFinder, Pocket-Finder and SITEHOUND, are composed of mainly Valine and Leucine, SplitPocket's functional surface is formed mainly by Phenylalanine, Glutamic Acid and Threonine. The features of the first ranked sites are listed in Table 5.13.

Additionally, the pockets of unphosphorylated structure of protein kinase B (Akt2) (PDB 1gzo) are also predicted by all geometry and energy-based methods. The residues of the first ranked pockets are then compared with the residues of the first ranked pockets of phosphorylated structure of protein kinase domain of Akt2. The web servers like CASTp and SCREEN that apply geometry based methods, identify exactly the same residues for the first ranked pockets of unphosphorylated kinase domain of Akt2 protein. However, the results of the energy based web servers do not exactly overlap for unphosphorylated and phosphorylated proteins. Q-SiteFinder, Pocket-Finder and SITEHOUND characterize 1, 6 and 3 more residues, respectively for unphosphorylated structure compared to phosphorylated structure of protein kinase domain of Akt2.

The ligand binding site residues of Akt2 reported in literature are compared with the residues identified by different ligand binding site prediction methods (Table 5.14). SplitPocket predicts all the residues from the literature and Q-SiteFinder finds only one residue reported in the literature. Furthermore, CAStp, SCREEN, SITEHOUND and Pocket-Finder predict 9, 8, 6 and 8 residues in their first ranked pockets in agreement with the literature.

Table 5.13. The comparison of ligand binding site identification methods for protein kinase domain of Akt2.

	CASTp	**SCREEN**	**SplitPocket**	**Q-SiteFinder**	**Pocket-Finder**	**SITEHOUND**
Number of Predicted Pockets	46	21	22	10	10	10
Number of Residues-1st site	51	37	39	22	27	15
Area-1st site(Å^2)	1302.4	508.5	870.98	N.A.	N.A.	N.A.
Volume-1st site(Å^3)	1693.3	N.A.	1080.19	356	591	86
Site Volume /Domain Volume-1st site (%)	6.5	N.A.	4.1	1.4	2.27	0.32
AA Composition 1st site	LEU VAL THR	VAL LEU ASP GLY LYS TYR GLU	PHE THR GLU ASP GLY LYS	VAL LEU GLU ASP TYR	LEU VAL THR PHE ASP	VAL LEU ASP PHE

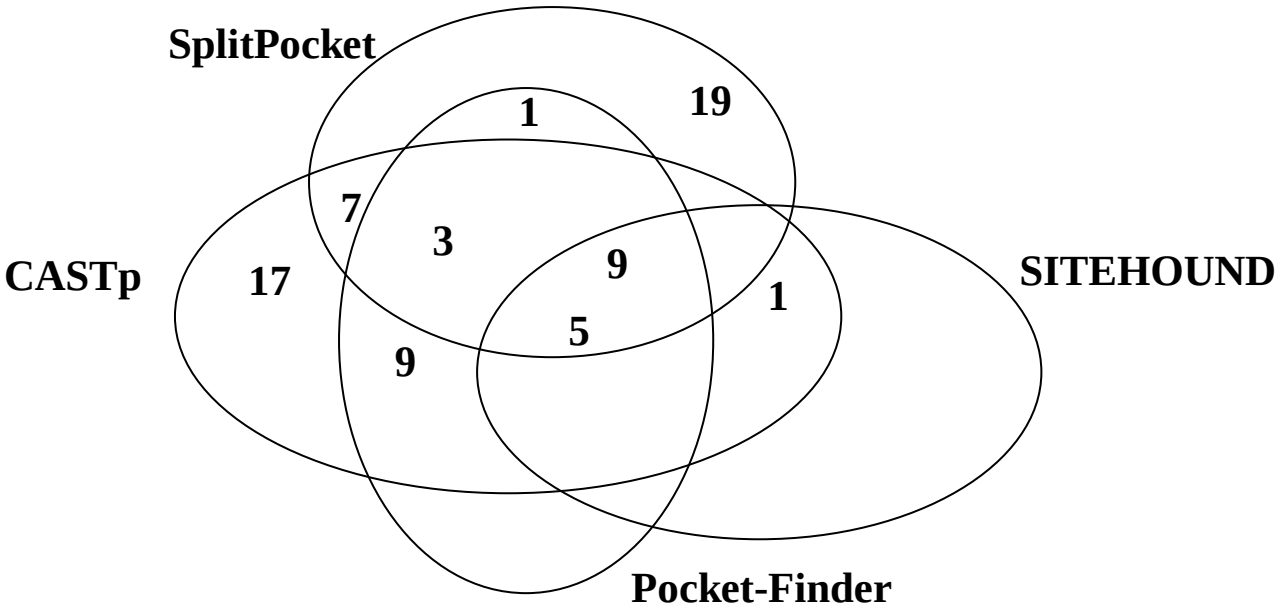

Figure 5.43. Overlap in residues in the first predicted site for protein kinase domain by using CASTp, SITEHOUND, Pocket-Finder and Split Pocket.

Table 5.14. The Ligand binding residues in literature.

Ligand Binding Residues in literature	CASTp	SCREEN	SplitPocket	Q-SiteFinder	Pocket-Finder	SITEHOUND
Gly159	-	+	+	-	-	-
Phe163	+	+	+	-	+	+
Phe166	-	-	+	-	-	-
Lys181	+	+	+	-	+	+
Glu200	+	+	+	-	+	+
Leu204	+	+	+	-	+	+
Met229	+	-	+	-	+	-
Glu230	-	-	+	-	-	-
Ala232	-	-	+	-	-	-
Glu236	-	-	+	-	-	-
Glu279	+	-	+	+	-	-
Asn280	+	+	+	-	+	-
Met282	-	-	+	-	-	-
Asp293	+	+	+	-	+	+
Phe294	+	+	+	-	+	+
Phe439	-	-	+	-	-	-

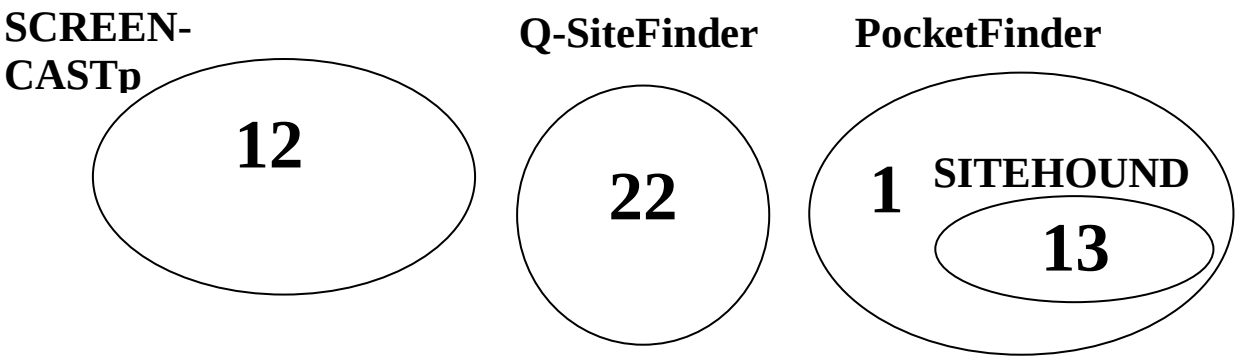

Figure 5.44. Overlap of residues in ligand binding sites (first predicted site) for PH domain using CASTp, SCREEN, Q-SiteFinder, SITEHOUND and Pocket-Finder.

For pleckstrin homology domain, the largest pocket (374 $Å^3$) is predicted by Q-SiteFinder and it is formed by 22 residues that are mainly Leucine, Proline and Tyrosine. All identified residues by CASTp and SCREEN are same. Q-SiteFinder and PocketFinder detect different residues in their first predicted sites. However, PocketFinder includes all residues which are predicted by SITEHOUND and their amino acid composition is also same (Figure 5.44). Additionally, there are not any common residues among the ligand binding sites predicted by geometric and energetic approaches. A summary of the methods is given in Table 5.15.

Table 5.15. The comparison of ligand binding site identification methods for pleckstrin homology domain of Akt2.

	CASTp	SCREEN	SplitPocket	Q-SiteFinder	Pocket-Finder	SITEHOUND
Number of Predicted Pockets	23	10	22	10	10	10
Number of Residues-1st site	12	12	39	22	14	13
Area- 1st site (Å^2)	211	145.7	N.A.	N.A	N.A.	N.A.
Volume-1st site(Å^3)	348.2	N.A.	1080.19	374	168	42
Site Volume /Domain Volume-1st site (%)	3.2	N.A	4.1	3.4	1.5	0.4
AA Composition 1st site	LEU PRO TYR	LEU PRO TYR	PHE THR GLU ASP GLY LYS	ARG GLU HIS PHE PRO TYR VAL	CYS GLU VAL	CYS GLU

5.5. Analysis of The Physicochemical Properties of Binding Sites

5.5.1. Geometry

Classic geometric approaches give basic information about the pockets like size, shape, surface and atoms. CASTp, SCREEN and SplitPocket are the methods that predict the ligand binding sites by using geometric approach. Although CASTp's output page only shows the area and volume of the pockets, SCREEN gives many geometric properties such as the surface area, the diameter, the largest and second largest moment of inertia (MOI), the average curvature, average depth, and the maximum depth (Tables 5.16 and 5.17). Moreover, SplitPocket computes accessible surface area and molecular volume of the pockets (Table 5.18). For example, 22nd pocket is the functional surface, and this volume of the functional surface is the largest one among all other ligand binding prediction sites.

Table 5.16. The geometric features of the pockets given by CASTp (Top part kinase domain, bottom part PH domain).

Pocket ID	Area (Å^2)	Volume (Å^3)
46	1302.4	1693.3
45	220.3	261.6
44	176.9	195.8
43	120.5	122
42	154.4	169.3

Pocket ID	Area (Å^2)	Volume (Å^3)
23	211	348.1
22	242.9	287.8
21	108.6	111.6
20	163.3	122
19	93.4	50.2

Table 5.17. The geometric properties of the cavities identified by SCREEN.

	1st Rank Cavity		2nd Rank Cavity	
	Kinase Domain	**PH Domain**	**Kinase Domain**	**PH Domain**
Area (Å^2)	508.1	145.7	187.4	116.7
Diameter (Å)	24.6	13.0	13.2	9.1
Largest MOI	48.52	15.22	18.67	8.67
Second Largest MOI	39.71	13.16	12.88	8.45
Average Curvature	0.0	0.0	0.0	0.0
Average Depth (Å)	5.2	3.7	4.0	5.9
Maximum Depth (Å)	10.2	6.4	7.1	9.1

Table 5.18. The implementation of SplitPocket to assess geometric properties of kinase domain (PDB 2jdr).

Pocket ID	Solvent Accessible Area (Å^2)	Volume (Å^3)
22	876.98	1080.19
21	148.95	122.58
20	173.92	289.85
19	154.86	218.24
18	89.43	70.52

The energy based servers, Q-SiteFinder, Pocket Finder and SITEHOUND also display the volumes of the pockets and binding box coordinates around the selected pockets (Table 5.19). Energy based servers predict lower volumes for ligand binding sites of Akt2 protein. Protein kinase domain has larger pockets compared to those of PH domain and the largest pocket is predicted by Pocket-Finder.

Table 5.19. Comparison of volumes of predicted ligand binding sites for kinase domain and PH domain of Akt2 protein.

Predicted Site	Volume (Å^3)					
	Q-SiteFinder		**Pocket-Finder**		**SITEHOUND**	
	Kinase Domain	**PH Domain**	**Kinase Domain**	**PH Domain**	**Kinase Domain**	**PH Domain**
1	356	374	592	168	86	42
2	271	320	394	134	76	48
3	255	97	241	70	59	43
4	169	113	188	47	42	36
5	140	117	78	30	43	27

5.5.2. Amino Acid Residue Composition

CASTp, SCREEN, Q-SiteFinder, Pocket-Finder, SITEHOUND and SplitPocket, all predict ligand binding sites of proteins and give the residues of the pockets. The ligand binding sites are often conserved, and these conserved residues are very significant since the functionally important residues are known to be conserved within protein families.

ConSurf (http://consurf.tau.ac.il) accessed freely, aims to analyze amino acid residue composition of the domains. Each domain's conservation score is computed by ConSurf, and protein kinase domain's and PH domain's scores are 5.51 and 5.16, respectively. Furthermore, the first predicted binding sites' conservation scores are also calculated by ConSurf (Table 5.20). The first predicted pockets of protein kinase domain have higher conservation scores than those belonging to PH domain. The first predicted site identified by Q-SiteFinder has the highest conservation score. Additionally, the lowest conservation score belongs to the pocket identified by Pocket-Finder.

Table 5.20. Conservation scores of the first predicted binding sites.

Ligand Binding Site Prediction Methods	**Conservation Scores**	
	Protein Kinase Domain	**PH Domain**
CASTp	7.67	3.92
SCREEN	7.76	4.17
Q-SiteFinder	8.32	5.18
Pocket-Finder	7.07	5.93
SITEHOUND	8.00	5.84
SplitPocket	7.56	-

5.5.3. Solvation

The characterization of the binding properties of a protein's binding pocket requires the identification of the sites at which ordered water molecules bind. The binding of a ligand requires the displacement of these water molecules and these effects are described by desolvation energy (energy to break the molecule-solvent interaction at the binding

site). Solvation energy is the energy released when ions associate with molecules (proteins) in a solvent (water).

Solvation energy is only computed by SCREEN. The highest solvation value of protein kinase domain is obtained by the first ranked pocket although the highest solvation value of PH domain is obtained by the second ranked pocket (Table 5.21).

Table 5.21. Solvation energy values belonging to protein kinase domain and PH domain of Akt2 protein.

Ranked of Pocket	**Solvation Energy (kcal/mol)**	
	Protein Kinase Domain	**PH Domain**
1	1.688	0.982
2	-1.067	1.111
3	-0.092	0.119
4	0.932	0.766
5	-0.195	0.573

The solvation energy of protein tyrosine phosphatase 1B (PDB 1l8g) and human factor Xa complexed with inhibitor RPR128515 (PDB 1ezq) are obtained by SCREEN and the first ranked pocket of these proteins have the highest solvation energy (Table 5.22). The solvation energy values of these proteins and Akt2 domains change between -1.067 and 1.982 kcal/mol.

Table 5.22. Solvation energy values belonging to protein tyrosine phosphatase 1B (PDB 1l8g) and human factor Xa complexed with inhibitor RPR128515 (PDB 1ezq).

Ranked of Pocket	**Solvation Energy (kcal/mol)**	
	1l8g	**1ezq**
1	0.989	1.981
2	0.799	1.657
3	0.890	0.234
4	0.415	0.596
5	0.625	0.196

5.5.4. Electrostatics

The average hydrophobicity of a protein core is positive whereas the protein surface hydrophobicity is negative. The polar and charged residues are rich in interfaces. Moreover, the electric field around proteins, which is caused by the shape of the dielectric boundary between the protein and aqueous phase, is related with protein-protein or protein-ligand association rates, and the charge distribution of proteins also affects the association rates. The electrostatics of proteins affects the stability of protein, so they are important to investigate.

The electrostatic potential of Akt2 protein is computed by SCREEN only and given for protein kinase and PH domains in Table 5.23. The average charge and average electric potential of the first ranked pocket of kinase domain are -0.070 and -10.77, respectively, and they are the lowest values among other pockets. The average electric field of the first ranked pocket of kinase domain is 11.63 and it is the second highest value. The average charge and average electric potential of the first ranked pocket of PH domain are -0.062 and -7.14, respectively, they are the lowest values among other pockets. The average electric field value (11.51 mV/nm) of PH domain is highest for the first ranked pocket.

Table 5.23. Average charge, average electric potential and average electric field of protein kinase domain and PH domain of Akt protein.

Pocket ID	**Average Charge (c)**		**Average Electric Potential (mV)**		**Average Electric Field (mV/nm)**	
	Kinase Domain	**PH Domain**	**Kinase Domain**	**PH Domain**	**Kinase Domain**	**PH Domain**
1	-0.070	-0.062	-10.77	-7.14	11.63	11.51
2	0.020	0.005	1.99	-5.56	9.95	5.71
3	0.089	0.048	3.60	5.99	5.48	6.56
4	-0.017	-0.004	-3.81	-4.52	5.63	5.15
5	-0.111	-0.031	-10.72	-3.67	14.37	7.59

The average charge, average electric potential and average electric field of protein tyrosine phosphatase 1B (PDB 1l8g) and human factor Xa complexed with inhibitor RPR128515 (PDB 1ezq) are also computed by SCREEN (Table 5.24). The first ranked pockets of both proteins have the lowest average charge. However, the average electric potential and electric field of proteins vary and are not related with the ranks of pockets. Additionally, the values of average charge of protein tyrosine phosphatase 1B (PDB 1l8g), human factor Xa complexed with inhibitor RPR128515 (PDB 1ezq) and Akt2 protein are between -0.070 and 0.089. The average electric potential of these proteins are computed between -10.77 and 18.21 mV and the average electric fields are calculated between 5.15 and 16.80 mV/nm.

Table 5.24. Average charge, average electric potential and average electric field of protein tyrosine phosphatase 1B (PDB 1l8g) and human factor Xa complexed with inhibitor RPR128515 (PDB 1ezq).

Pocket ID	**Average Charge (c)**		**Average Electric Potential (mV)**		**Average Electric Field (mV/nm)**	
	1l8g	**1ezq**	**1l8g**	**1ezq**	**1l8g**	**1ezq**
1	-0.040	-0.018	0.22	-10.29	12.52	12.46
2	0.065	0.063	18.21	-1.74	14.31	9.22
3	0.039	0.002	0.21	-4.41	11.49	14.53
4	-0.038	0.026	-9.41	2.48	16.80	12.23
5	-0.017	0.024	-4.39	-5.97	11.65	13.17

5.5.5. Chemical Fragment Interactions

Chemical fragment interactions correspond to druggability index and it can be given by SCREEN. Druggability Index (*DI*) changes from 0 to 1. Zero describes non-drug binding cavity and 1 describes drug binding cavity. Figure 5.45 shows the druggability index of pockets of protein kinase domain and PH domain. The indexes of first ranked pockets of protein kinase and PH domains are 0.8003 and 0.4375, respectively.

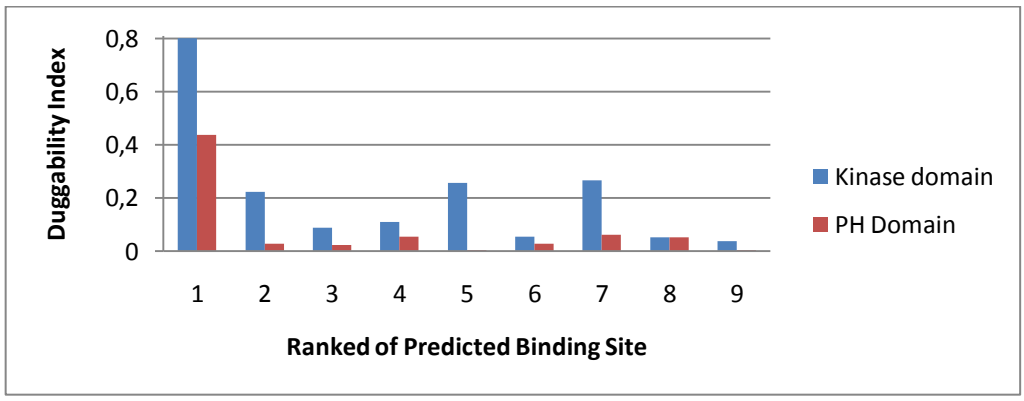

Figure 5.45. Druggability index of protein kinase and PH domain of Akt protein.

6. CONCLUSIONS AND RECOMMENDATIONS

6.1. Conclusions

The following conclusions were drawn from the present study:

- The map of the insulin signaling pathway which is categorized in Organismal Systems and in the subgroup of Endocrine Systems was obtained from KEGG database. The homologs of the proteins involved in *Homo sapiens'* insulin signaling pathway were found in *Saccharomyces cerevisiae* by using Basic Local Alignment Search Tool (BLAST).

- After the homologs of insulin signaling components of *Homo sapiens* were determined in *S.cerevisiae*, it was investigated which of these proteins have roles in sphingolipid pathway. Pkh1, Ypk1 and Ypk2 were selected for investigation of the relationship between insulin and sphingolipid signaling pathways.

- The wild type and three homozygous deletion mutant strains , and were used in batch experiments. The growth curve of yeast cells were obtained by optical density measurements at different initial glucose concentrations and samples are taken for glucose and lipid analysis at different phases of growth i.e. exponential and stationary phases.

- The initial concentration of the glucose in F1 medium was changed (20g/l, 30g/l and 40g/l) and the effects of the glucose concentration on glucose uptake by the cells were investigated. The wild type yeast cells consume more glucose than the deletion mutant strains at different initial glucose concentrations. Moreover, the remaining glucose concentrations in the medium are highest for the deletion mutant of and lowest for the deletion mutant of .

- The retention times of complex sphingolipids in yeast IPC, MIPC and M $(IP)_2$ C are 4.3, 4.0 and 3.8 minutes, respectively. The amount of IPC is highest in wild type. The

deletion mutants of , and have 87.75, 88.04 and 90.62% IPC at 30g/l initial glucose concentration and 92.23, 87.93 and 85.65 % IPC at 40g/l initial glucose concentration, respectively.

- The deletion mutants at 30g/l initial glucose concentration have reduced IPC percentages compared to wild type strain in agreement with the literature information. However, at 40 g/l initial glucose concentration, the deletion mutants result in higher percentages of lipid composition compared to wild type strain as well as higher amounts of remaining glucose in the medium as expected. When the initial glucose concentration in the medium is increased, the effect of other proteins having roles in glucose signal reception and transduction might be dominant. Nevertheless, the experimental results on the relation between glucose consumption and complex sphingolipid production are found to be in agreement with the literature.

- In order to get further insight about the crosstalk between the sphingolipid and insulin signaling networks, the individual physical and genetic interactions of Pkh1, Ypk1 and Ypk2 are investigated through databases and by OSPREY. Pkh1, Ypk1 and Ypk2 interact physically with 15, 18 and 13 proteins, respectively and genetically with 18, 30 and 5 proteins, respectively. Moreover, Pkh1, Ypk1 and Ypk2 interact with each other physically but not genetically.

- Pkh1 interacts with Sch9 (Akt/Protein Kinase B) directly whereas Ypk2 interacts with Sch9 via Snf1, and Ypk1 interacts with Sch9 through Ypk2 and Snf1. It is here important to note that Snf1p has a primary role in glucose sensing and transduction and upon glucose depletion, Snf1p is activated. The results from glucose analysis also indicate that the glucose uptake is lowest in the deletion mutant of Ypk11. On the other hand, the amounts of complex sphingolipids are lowest for the deletion mutant of Pkh1. This stiuation can be explained by the interaction of Pkh1 with Lcb1 via Bmh2.

- Akt/PKB (Sch9p in yeast) is the most significant protein that affects GLUT4 translocation, and Akt is also defined as a critical target protein for anticancer drug discovery. Thus Akt2 protein is further investigated from the aspect of drug discovery.

The ligand binding sites of Akt2 are found by using geometry-based and energy-based methods. CASTp, SCREEN and SplitPocket are geometry-based web servers and Q-SiteFinder, PocketFinder and SITEHOUND are energy-based web servers to identify pockets.

- CASTp predicts 46 different pockets for protein kinase domain and the largest one is 1302.4 $Å^3$. SplitPocket detects 22 pockets and the largest one being the functional surface of kinase domain has a volume of 1080.19 $Å^3$. The first predicted cavities of energy based methods (Q-SiteFinder, Pocket-Finder and SITEHOUND) are smaller than those identified by geometry based servers.

- CASTp, SCREEN, Q-SiteFinder, Pocket Finder, SITEHOUND and SplitPocket have only one common residue which is the active site residue, Asp-275 for the protein kinase domain of Akt2 protein. CASTp has the largest first predicted binding site which is formed by 51 residues. It has 34 common residues with SCREEN, and 23 and 18 common residues with Pocket Finder and SplitPocket, respectively. Moreover, the first ranked pocket of CASTp (geometry based method) covers all the residues also identified by Q-SiteFinder and SITEHOUND (energy based method) for protein kinase domain of Akt2 protein.

- Although the first ranked cavities of protein kinase domain predicted by CASTp, SCREEN, Q-SiteFinder, Pocket-Finder and SITEHOUND, are composed of mainly Valine and Leucine, SplitPocket's functional surface is formed mainly by Phenylalanine, Glutamic Acid and Threonine.

- The ligand binding site residues of Akt2 reported in the literature are compared with the residues identified by different ligand binding site prediction methods used here. SplitPocket predicts all the binding residues of the pocket belonging to protein kinase whereas Q-SiteFinder finds only one binding residue from the literature. Furthermore, CAStp, SCREEN, SITEHOUND and Pocket-Finder predict 9, 8, 6 and 8 residues in their first ranked pockets of protein kinase domain in agreement with the literature.

- For pleckstrin homology domain, the largest pocket (374 $Å^3$) is predicted by Q-SiteFinder and it is formed by 22 residues that are mainly Leucine, Proline and Tyrosine. All residues identified by CASTp and SCREEN are same. Q-SiteFinder and PocketFinder detect different residues in their first predicted sites. However, PocketFinder includes all residues which are predicted by SITEHOUND. Additionally, there are not any common residues among the ligand binding sites predicted by geometric and energetic approaches.

- The physicochemical properties of binding sites which are geometry, amino acid residue composition, solvation, electrostatics and chemical fragment interaction are also analyzed.

- The functionally important residues are known to be conserved within protein families. Protein kinase and pleckstrin homology domains' conservation scores are computed as 5.51 and 5.16 by ConSurf, respectively. The first predicted pockets of protein kinase domain have higher conservation scores compared to those of PH domain.

- Solvation energy is computed by SCREEN. The highest solvation value of protein kinase domain is obtained by the first ranked pocket (1.688 kcal/mol) although the highest solvation value of PH domain is obtained by the second ranked pocket (1.111 kcal/mol).

- Chemical fragment interactions correspond to druggability index and are given by SCREEN. Druggability Index (*DI*) changes from 0 to 1. 0 describes a non-drug binding cavity and 1 describes a drug binding cavity. The indexes of the first ranked pockets of protein kinase domain and PH domain are 0.8003 and 0.4375, respectively.

6.2. Recommendations

- One of the aims of this study is to clarify the relationship between the sphingolipid and insulin signaling pathways. The results of the physical interactions of Ypk1, Ypk2 and Pkh1 indicated some key genes to explain the association of these signaling pathways. The experimental research may continue with the deletion mutants of Snf1, Bmh2 and Ubi4 genes.

- Akt2 is known to have roles in both insulin signaling and tumor progression; it is a target protein for anticancer drug discovery. The first step of the drug design is to detect the significant residues to which ligands bind with high affinity and specificity. The pockets of Akt2 are identified by using both geometric and energetic approaches in this study. These results can be used as a starting point for docking suitable ligands.

APPENDIX A: ANNOTATION-COLLECTION TABLES

A. Process

Table A.1.1. Biological process terms of the significant proteins in insulin signaling pathway.

Protein Name	Isoforms of Proteins	Biological Process
PDK 1/2		actin cytoskeleton organization
		activation of protein kinase B activity
		cellular response to insulin stimulus
		intracellular signaling cascade
		negative regulation of protein kinase activity
		peptidyl-threonine phosphorylation
		regulation of establishment of protein localization
Akt	Akt3	protein amino acid phosphorylation
		signal transduction
	Akt1	anagen
		apoptotic mitochondrial changes
		blood vessel development
		cell projection organization
		germ cell development
		glucose transport
		glycogen biosynthetic process
		inflammatory response
		insulin receptor signaling pathway
		negative regulation of cell size
		peptidyl-serine phosphorylation
		placenta development
		positive regulation of multicellular organism growth
		positive regulation of proteasomal ubiquitin-dependent protein catabolic process
		protein amino acid phosphorylation
		protein kinase B signaling cascade
		protein ubiquitination
		regulation of survival gene product expression
		response to food
		response to hormone stimulus
	Akt2	cellular response to insulin stimulus
		glucose metabolic process
		insulin receptor signaling pathway

Table A.1.1. Biological process terms of the significant proteins in insulin signaling pathway (Continued).

Protein Name	**Isoforms of Proteins**	**Biological Process**
	Akt2	negative regulation of plasma membrane long-chain fatty acid transport
		positive regulation of fatty acid beta-oxidation
		positive regulation of glucose import
		positive regulation of glycogen biosynthetic process
		protein amino acid phosphorylation
JNK	MAPK8	JUN phosphorylation
		activation of pro-apoptotic gene products
		cell motion
		negative regulation of apoptosis
		response to UV
	MAPK10	JNK cascade
		protein amino acid phosphorylation
aPKC	PRKCI	cell-cell junction organization Ref.8
		cellular response to insulin stimulus
		establishment or maintenance of epithelial cell apical/basal polarity
		intracellular signaling cascade
		positive regulation of glucose import
		protein amino acid phosphorylation
		protein targeting to membrane
		regulation of establishment of protein localization
		secretion
	PRKCZ	microtubule cytoskeleton organization
		protein amino acid phosphorylation
AMPK	PRKAA1	activation of MAPK activity
		fatty acid biosynthetic process
		negative regulation of glucosylceramide biosynthetic process
		positive regulation of anti-apoptosis
		positive regulation of cholesterol biosynthetic process
		response to hypoxia
	PRKAA2	cholesterol biosynthetic process
		fatty acid biosynthetic process
		protein amino acid phosphorylation
		regulation of fatty acid oxidation
		signal transduction
PYK	PKLR	glycolysis
	PKM2	glycolysis
FBP	FBP1	fructose metabolic process Ref.4
		gluconeogenesis
TC10		GTP catabolic process

Table A.1.1. Biological process terms of the significant proteins in insulin signaling pathway (Continued).

Protein Name	**Isoforms of Proteins**	**Biological Process**
TC10		cellular response to insulin stimulus
		cortical actin cytoskeleton organization
		insulin receptor signaling pathway
		negative regulation of glucose import
		positive regulation of filopodium assembly
		positive regulation of specific transcription from RNA polymerase II promoter
		regulation of actin cytoskeleton organization
		regulation of establishment of protein localization
		small GTPase mediated signal transduction
GSK-3b		ER overload response
		Wnt receptor signaling pathway through beta-catenin
		glycogen metabolic process
		peptidyl-serine phosphorylation
		positive regulation of protein complex assembly
		positive regulation of protein export from nucleus
PP1	PPP1CA	
	PPP1CB	protein amino acid dephosphorylation
	PPP1CC	cell cycle
		cell division
		glycogen metabolic process
PKA	PRKACA	hormone-mediated signaling
		protein kinase cascade
	PRKACB	protein amino acid phosphorylation
	PRKACG	hormone-mediated signaling
		male gonad development
		protein amino acid phosphorylation
		protein kinase cascade
		spermatogenesis
	PRKX	protein amino acid phosphorylation
	PRKY	protein amino acid phosphorylation
Raptor		
p70s6k	RPS6KB1	protein amino acid phosphorylation
		signal transduction Ref.1
	RPS6KB2	protein amino acid phosphorylation
		protein kinase B signaling cascade
MEK1/2	MAP2K1	cell proliferation
		keratinocyte differentiation
		mitosis
		neuron differentiation
		positive regulation of MAP kinase activity
		positive regulation of cell differentiation

Table A.1.1. Biological process terms of the significant proteins in insulin signaling pathway *(Continued)*.

Protein Name	**Isoforms of Proteins**	**Biological Process**
		protein amino acid phosphorylation
		response to glucocorticoid stimulus
		response to oxidative stress
	MAP2K2	Ras protein signal transduction
		protein amino acid phosphorylation
ERK1/2	MAPK1	B cell receptor signaling pathway
		MAPKKK cascade
		T cell receptor signaling pathway
		cytosine metabolic process
		lipopolysaccharide-mediated signaling pathway
		negative regulation of cell differentiation
		organ morphogenesis
		protein amino acid phosphorylation
		response to DNA damage stimulus
		response to exogenous dsRNA
		response to lipopolysaccharide
	MAPK3	protein amino acid phosphorylation
PFK	PFKM	fructose 6-phosphate metabolic process
		glycogen metabolic process
		glycolysis
		muscle maintenance
		protein oligomerization
	PFKP	glycolysis
PFK	PFKL	glycolysis
		negative regulation of insulin secretion
		response to glucose stimulus
mTOR		cell growth
		protein amino acid autophosphorylation
		protein catabolic process
		response to nutrient
		signal transduction
ACC	ACACA	fatty acid biosynthetic process
	ACACB	fatty acid biosynthetic process
		regulation of fatty acid oxidation
GYS	GYS1	glycogen biosynthetic process
	GYS2	glycogen biosynthetic process
		response to glucose stimulus
PYG	PYGB	glycogen catabolic process
	PYGL	glucose homeostasis
		glycogen metabolic process

Table A.1.2. Biological process terms of the proteins in yeast found by BLAST.

Protein Name	**Biological Process**
Pkh1	MAPKKK cascade involved in cell wall biogenesis
	endocytosis
	protein amino acid phosphorylation
Ypk1	cellular cell wall organization
	endocytosis
	protein amino acid autophosphorylation
	sphingolipid metabolic process
Hog1	hyperosmotic response
	negative regulation of transcription from RNA polymerase II promoter by pheromones
	osmosensory signaling pathway
	positive regulation of transcription from RNA polymerase II promoter
	protein amino acid phosphorylation
	response to arsenic
	transcription
Pkc1	actin filament organization
	cell cycle
	fungal-type cell wall organization
	intracellular protein kinase cascade
	protein amino acid phosphorylation
Snf1	cellular response to glucose starvation
	invasive growth in response to glucose limitation
	protein amino acid phosphorylation
	regulation of protein complex assembly
	replicative cell aging
	signal transduction
Pyk2	glycolysis
	pyruvate metabolic process
Rim11	ascospore formation
	protein amino acid phosphorylation
	proteolysis
Glc7	chromosome segregation
	regulation of phosphoprotein phosphatase activity
Tpk2	Ras protein signal transduction
	invasive growth in response to glucose limitation
	protein amino acid phosphorylation
Kog1	TOR signaling pathway

Table A.1.2. Biological process terms of the proteins in yeast found by BLAST *(Continued).*

Protein Name	**Biological Process**
	regulation of cell growth
Ypk2	cellular cell wall organization
	protein amino acid phosphorylation
	regulation of cell shape
Pbs2	N-terminal peptidyl-methionine acetylation
	actin filament organization
	activation of MAPK activity involved in osmosensory signaling pathway
	hyperosmotic response
	negative regulation of transposition, RNA-mediated
	nuclear translocation of MAPK involved in osmosensory signaling pathway
	response to antibiotic
Fus3	cell cycle arrest
	cell division
	invasive growth in response to glucose limitation
	mitosis
	negative regulation of MAPKKK cascade
	pheromone-dependent signal transduction involved in conjugation with cellular fusion
	protein amino acid phosphorylation
Pfk2	glycolysis
	proton transport
Tor2	G1 phase of mitotic cell cycle
	Rho protein signal transduction
	TOR signaling pathway
	actin filament reorganization during cell cycle
	establishment or maintenance of actin cytoskeleton polarity
	positive regulation of endocytosis
	regulation of cell cycle
	regulation of cell growth
	ribosome biogenesis
Acc1	fatty acid biosynthetic process
	nuclear envelope organization
	protein import into nucleus
Gys2	glycogen biosynthetic process
Gph1	glycogen catabolic process

Table A.1.3. Biological process terms of the proteins that interact physically with Pkh1.

Protein Name	**Biological Process**
Ypk1	cellular cell wall organization
	endocytosis
	protein amino acid autophosphorylation
	sphingolipid metabolic process
Ypk2	cellular cell wall organization
	protein amino acid phosphorylation
	regulation of cell shape
Sch9	age-dependent response to oxidative stress during chronological cell aging
	positive regulation of transcription from RNA polymerase I promoter
	positive regulation of transcription from RNA polymerase III promoter
	protein amino acid phosphorylation
	regulation of cell size
	regulation of protein localization
	regulation of response to osmotic stress
	regulation of transcription from RNA polymerase II promoter in response to oxidative stress
	replicative cell aging
Myo5	actin cortical patch localization
	bipolar cellular bud site selection
	exocytosis
	fungal-type cell wall organization
	receptor-mediated endocytosis
	response to salt stress
Lsp1	endocytosis
	response to heat
Pil1	endocytosis
	protein localization
	response to heat
Ssb1	'de novo' cotranslational protein folding
	response to stress
Hsp82	'de novo' protein folding
	positive regulation of telomere maintenance via telomerase
	proteasome assembly
	protein refolding
	protein targeting to mitochondrion
	response to osmotic stress
Bmh2	DNA damage checkpoint
	DNA replication initiation

Table A.1.3. Biological process terms of the proteins that interact physically with Pkh1 *(Continued).*

Protein Name	**Biological Process**
	Ras protein signal transduction
	ascospore formation
	cell wall chitin biosynthetic process
	glycogen metabolic process
	negative regulation of ubiquitin-protein ligase activity during mitotic cell cycle
	pre-replicative complex assembly
	pseudohyphal growth
	signal transduction during filamentous growth
Reb1	regulation of transcription from RNA polymerase II promoter
	termination of RNA polymerase I transcription
Aep3	mRNA metabolic process
Tpk3	Ras protein signal transduction
	mitochondrion organization
	protein amino acid phosphorylation
Yrf1-4	telomere maintenance via recombination

Table A.1.4. Biological process terms of the proteins that interact physically with Ypk1.

Protein Name	**Biological Process**
Tor1	G1 phase of mitotic cell cycle
	TOR signaling pathway
	fungal-type cell wall organization
	meiosis
	mitochondrial signaling pathway
	regulation of cell cycle
	regulation of cell growth
	response to DNA damage stimulus
	ribosome biogenesis
	transcription of nuclear rRNA large RNA polymerase I transcript
Tor2	G1 phase of mitotic cell cycle
	Rho protein signal transduction
	TOR signaling pathway
	actin filament reorganization during cell cycle
	establishment or maintenance of actin cytoskeleton polarity
	positive regulation of endocytosis
	regulation of cell cycle
	regulation of cell growth
	ribosome biogenesis
Ypk2	cellular cell wall organization
	protein amino acid phosphorylation
	regulation of cell shape
Pkh1	MAPKKK cascade involved in cell wall biogenesis
	endocytosis
	protein amino acid phosphorylation
Pkh2	protein amino acid phosphorylation
Hsp82	'de novo' protein folding
	positive regulation of telomere maintenance via telomerase
	proteasome assembly
	protein refolding
	protein targeting to mitochondrion
	response to osmotic stress
Bmh2	DNA damage checkpoint
	DNA replication initiation
	Ras protein signal transduction
	ascospore formation
	cell wall chitin biosynthetic process
	glycogen metabolic process
	negative regulation of ubiquitin-protein ligase activity during mitotic cell cycle

Table A.1.4. Biological process terms of the proteins that interact physically with Ypk1 *(Continued).*

Protein Name	**Biological Process**
Hsc82	proteasome assembly
	protein folding
	response to stress
	telomere maintenance
Tec1	invasive growth in response to glucose limitation
	positive regulation of transcription from RNA polymerase II promoter
	pseudohyphal growth
	transcription
Leu9	leucine biosynthetic process
Avo2	TOR signaling pathway
	establishment or maintenance of actin cytoskeleton polarity
	fungal-type cell wall organization
	regulation of cell growth
Ubi4	DNA repair
	protein ubiquitination
	ribosome biogenesis
	translation
Crn1	actin cortical patch localization
	actin filament organization
	microtubule-based process
	negative regulation of Arp2/3 complex-mediated actin nucleation
Rpn3	regulation of protein catabolic process
	ubiquitin-dependent protein catabolic process
Inp52	endocytosis
	phosphoinositide dephosphorylation
	protein transport
Ncs2	invasive growth in response to glucose limitation
	protein urmylation
	pseudohyphal growth
	wobble position uridine thiolation
Sac6	actin filament organization
	bipolar cellular bud site selection
	endocytosis
	response to osmotic stress
Slm1	TOR signaling pathway
	actin filament bundle assembly
	establishment or maintenance of actin cytoskeleton polarity
	regulation of cell growth

Table A.1.5. Biological process terms of the proteins that interact physically with Ypk2.

Protein Name	**Biological Process**
Tor2	G1 phase of mitotic cell cycle
	Rho protein signal transduction
	TOR signaling pathway
	actin filament reorganization during cell cycle
	establishment or maintenance of actin cytoskeleton polarity
	positive regulation of endocytosis
	regulation of cell cycle
	regulation of cell growth
	ribosome biogenesis
Ypk1	cellular cell wall organization
	endocytosis
	protein amino acid autophosphorylation
	sphingolipid metabolic process
Pkh1	MAPKKK cascade involved in cell wall biogenesis
	endocytosis
	protein amino acid phosphorylation
Arg81	arginine metabolic process
	negative regulation of calcium ion-dependent exocytosis
	regulation of transcription, DNA-dependent
	transcription
Pet112	glutaminyl-tRNAGln biosynthesis via transamidation Ref.6
	mitochondrial translation
Myo5	actin cortical patch localization
	bipolar cellular bud site selection
	exocytosis
	fungal-type cell wall organization
	receptor-mediated endocytosis
	response to salt stress
Prb1	cellular response to starvation
	negative regulation of catalytic activity
	proteolysis
	sporulation resulting in formation of a cellular spore
	vacuolar protein catabolic process
Ubi4	DNA repair
	protein ubiquitination
	ribosome biogenesis
	translation
Tfp1	ATP synthesis coupled proton transport
	cellular protein metabolic process
	intein-mediated protein splicing

Table A.1.5. Biological process terms of the proteins that interact physically with Ypk2 *(Continued).*

Protein Name	**Biological Process**
	intron homing
	vacuolar acidification
Cdc33	nuclear-transcribed mRNA catabolic process, nonsense-mediated decay
	regulation of cell cycle
	regulation of translation
	translational initiation
Snf1	cellular response to glucose starvation
	invasive growth in response to glucose limitation
	protein amino acid phosphorylation
	regulation of protein complex assembly
	replicative cell aging
	signal transduction

Table A.1.6. Biological process terms of the proteins that interact genetically with Pkh1.

Protein Name	**Biological Process**
Ypk1	cellular cell wall organization
	endocytosis
	protein amino acid autophosphorylation
	sphingolipid metabolic process
Ypk2	cellular cell wall organization
	protein amino acid phosphorylation
	regulation of cell shape
Sch9	age-dependent response to oxidative stress during chronological cell aging
	positive regulation of transcription from RNA polymerase I promoter
	positive regulation of transcription from RNA polymerase III promoter
	protein amino acid phosphorylation
	regulation of cell size
	regulation of protein localization
	regulation of response to osmotic stress
	regulation of transcription from RNA polymerase II promoter in response to oxidative stress
	replicative cell aging
Tos3	glucose metabolic process
	protein amino acid phosphorylation
	response to stress
Sgv1	phosphorylation of RNA polymerase II C-terminal domain
	positive regulation of histone H3-K4 methylation
	transcription
Sip1	protein amino acid phosphorylation
	regulation of protein complex assembly
	signal transduction
Mnn11	cell wall mannoprotein biosynthetic process
	protein amino acid glycosylation
Cup2	regulation of transcription, DNA-dependent
	response to copper ion
	transcription initiation from RNA polymerase II promoter
Hsp82	'de novo' protein folding
	positive regulation of telomere maintenance via telomerase
	proteasome assembly
	protein refolding
	protein targeting to mitochondrion
	response to osmotic stress
Slm1	TOR signaling pathway

Table A.1.6. Biological process terms of the proteins that interact genetically with Pkh1 *(Continued).*

Protein Name	**Biological Process**
	establishment or maintenance of actin cytoskeleton polarity
	regulation of cell growth
Ypt6	intracellular protein transport
	retrograde transport, endosome to Golgi
	small GTPase mediated signal transduction
Cdc8	DNA repair
	DNA-dependent DNA replication
	dTDP biosynthetic process
	dTTP biosynthetic process
	dUDP biosynthetic process
	plasmid maintenance
Mck1	ascospore formation
	double-strand break repair via nonhomologous end joining
	meiosis
	mitotic sister chromatid segregation
	protein amino acid phosphorylation
Ncs2	invasive growth in response to glucose limitation
	protein urmylation
	pseudohyphal growth
	wobble position uridine thiolation
Hsc82	proteasome assembly
	protein folding
	response to stress
	telomere maintenance
Myo5	actin cortical patch localization
	bipolar cellular bud site selection
	exocytosis
	fungal-type cell wall organization
	receptor-mediated endocytosis
	response to salt stress
Ras2	Ras protein signal transduction
	activation of adenylate cyclase activity
	ascospore formation
	positive regulation of transcription by galactose
	pseudohyphal growth
	replicative cell aging

Table A.1.7. Biological process terms of the proteins that interact genetically with Ypk1.

Protein Name	**Biological Process**
Ypk2	cellular cell wall organization
	protein amino acid phosphorylation
	regulation of cell shape
Pkh1	MAPKKK cascade involved in cell wall biogenesis
	endocytosis
	protein amino acid phosphorylation
Pkh2	protein amino acid phosphorylation
Tor1	G1 phase of mitotic cell cycle
	TOR signaling pathway
	fungal-type cell wall organization
	meiosis
	mitochondrial signaling pathway
	regulation of cell cycle
	regulation of cell growth
	response to DNA damage stimulus
	ribosome biogenesis
	transcription of nuclear rRNA large RNA polymerase I transcript
Pkc1	actin filament organization
	cell cycle
	fungal-type cell wall organization
	protein amino acid phosphorylation
	protein kinase cascade
Hsp82	'de novo' protein folding
	positive regulation of telomere maintenance via telomerase
	proteasome assembly
	protein refolding
	protein targeting to mitochondrion
	response to osmotic stress
Bmh2	DNA damage checkpoint
	DNA replication initiation
	Ras protein signal transduction
	ascospore formation
	cell wall chitin biosynthetic process
	glycogen metabolic process
	negative regulation of ubiquitin-protein ligase activity during mitotic cell cycle
	pre-replicative complex assembly
	pseudohyphal growth
	signal transduction during filamentous growth
Bmh1	DNA damage checkpoint

Table A.1.7. Biological process terms of the proteins that interact genetically with Ypk1 *(Continued).*

Protein Name	**Biological Process**
	Ras protein signal transduction
	ascospore formation
	cell wall chitin biosynthetic process
	glycogen metabolic process
	negative regulation of ubiquitin-protein ligase activity during mitotic cell cycle
	pseudohyphal growth
	signal transduction during filamentous growth
Knh1	1,6-beta-glucan biosynthetic process
	cell wall biogenesis
	cellular cell wall organization
Skt5	cell wall chitin biosynthetic process
	cytokinesis
	response to osmotic stress
Exg1	cellular cell wall organization
	cellular glucan metabolic process
Cts2	chitin catabolic process
	sporulation resulting in formation of a cellular spore
Rps6b	maturation of SSU-rRNA from tricistronic rRNA transcript (SSU-rRNA, 5.8S rRNA, LSU-rRNA)
	translation
Srb4	regulation of transcription
	transcription from RNA polymerase II promoter
Smp1	positive regulation of transcription from RNA polymerase II promoter
	regulation of response to osmotic stress
Ypc1	transcription
	ceramide biosynthetic process
	ceramide catabolic process
Frq1	regulation of signal transduction
Sli1	alcohol metabolic process
	response to drug
Clb6	G1/S transition of mitotic cell cycle
	cell division
	positive regulation of DNA replication
	premeiotic DNA synthesis
	regulation of S phase of mitotic cell cycle
Avo2	TOR signaling pathway
	establishment or maintenance of actin cytoskeleton polarity

Table A.1.7. Biological process terms of the proteins that interact genetically with Ypk1 *(Continued).*

Protein Name	**Biological Process**
	regulation of cell growth
Tsc11	TOR signaling pathway
	establishment or maintenance of actin cytoskeleton polarity
	fungal-type cell wall organization
	regulation of cell growth
	sphingolipid biosynthetic process
Hlj1	ER-associated protein catabolic process
	protein folding
Hsc82	proteasome assembly
	protein folding
	response to stress
	telomere maintenance
Sac7	actin filament reorganization involved in cell cycle
	small GTPase mediated signal transduction
Jnm1	nuclear migration
Got1	ER to Golgi vesicle-mediated transport
	Golgi to endosome transport
	protein transport
Ymr291w	protein amino acid phosphorylation

Table A.1.8. Biological process terms of the proteins that interact genetically with Ypk2.

Protein Name	**Biological Process**
Tor2	G1 phase of mitotic cell cycle
	Rho protein signal transduction
	TOR signaling pathway
	actin filament reorganization during cell cycle
	establishment or maintenance of actin cytoskeleton polarity
	positive regulation of endocytosis
	regulation of cell cycle
	regulation of cell growth
	ribosome biogenesis
Ypk1	cellular cell wall organization
	endocytosis
	protein amino acid autophosphorylation
	sphingolipid metabolic process
Avo2	TOR signaling pathway
	establishment or maintenance of actin cytoskeleton polarity
	fungal-type cell wall organization
	regulation of cell growth
Tsc11	TOR signaling pathway
	establishment or maintenance of actin cytoskeleton polarity
	fungal-type cell wall organization
	regulation of cell growth
	sphingolipid biosynthetic process
Myo5	actin cortical patch localization
	bipolar cellular bud site selection
	exocytosis
	fungal-type cell wall organization
	receptor-mediated endocytosis
	response to salt stress

A.2. Component

Table A.2.1. Cellular component terms of the significant proteins in insulin signaling pathway.

Protein Name	**Isoforms**	**Cellular Component**
PDK 1/2		cytosol
		plasma membrane
Akt	Akt3	cytoplasm
		membrane
	Akt1	cytoplasm
		lamellipodium
		spindle
	Akt2	cytosol
JNK	MAPK8	cytosol
	MAPK10	cytoplasm
aPKC	PRKCI	cytosol
		endosome
		membrane
		nucleus
		polarisome
	PRKCZ	apical cortex
		tight junction
AMPK	PRKAA1	intracellular
	PRKAA2	cytosol
		nucleoplasm
	PKM2	cytosol
FBP	FBP1	cytosol
		mitochondrion
TC10		actin filament
		cytoplasm
		plasma membrane
GSK-3b		Axin-APC-beta-catenin-GSK3B complex
		beta-catenin destruction complex
		cytosol
		nucleus
	PPP1CC	nucleus
		protein complex
PKA	PRKACA	cAMP-dependent protein kinase complex
		nucleus
Raptor		cytosol
p70s6k	RPS6KB1	cell junction
		cytosol

Table A.2.1. Cellular component terms of the significant proteins in insulin signaling pathway *(Continued).*

Protein Name	**Isoforms**	**Cellular Component**
		synapse
		synaptosome
	RPS6KB2	ribosome
MEK1/2	MAP2K1	Golgi apparatus
		cytosol
	MAP2K2	extracellular region
ERK1/2	MAPK1	cytoplasm
		nucleus
	MAPK3	cytoskeleton
		nucleus
PFK	PFKM	6-phosphofructokinase complex
		endoplasmic reticulum
	PFKP	6-phosphofructokinase complex
PFK	PFKL	6-phosphofructokinase complex
		soluble fraction
mTOR		TORC1 complex
		TORC2 complex
		membrane
		phosphoinositide 3-kinase complex
ACC	ACACA	cytoplasm
	ACACB	Golgi apparatus
		cytosol
		endomembrane system
		membrane
GYS	GYS1	cytosol
	GYS2	cortical actin cytoskeleton
		cytosol
		ectoplasm
		insoluble fraction
		soluble fraction
PYG	PYGB	cytoplasm
	PYGL	cytoplasm
		nucleus
		plasma membrane
		soluble fraction

Table A.2.2. Cellular component terms of the proteins in yeast found by BLAST.

Protein Name	**Cellular component**
Pkh1	cytosol
Ypk1	cellular bud neck
	cytosol
	plasma membrane
Hog1	cytoplasm
	nucleus
Pkc1	cytoplasm
	cytoskeleton
	nucleus
	plasma membrane enriched fraction
	site of polarized growth
Snf1	AMP-activated protein kinase complex
	cytoplasm
	plasma membrane
Pyk2	mitochondrion
Rim11	cytoplasm
Glc7	cytoplasm
Tpk2	cAMP-dependent protein kinase complex
	nucleus
Kog1	TORC1 complex
	fungal-type vacuole membrane
	membrane fraction
	mitochondrion
	plasma membrane
Ypk2	cytoplasm
	nucleus
Pbs2	NatB complex
	cellular bud neck
	cellular bud tip
Fus3	mating projection tip
	mitochondrion
	nucleus
	periplasmic space
Pfk2	6-phosphofructokinase complex

Table A.2.2. Cellular component terms of the proteins in yeast found by BLAST *(Continued).*

Protein Name	**Cellular component**
	mitochondrion
Tor2	TORC1 complex
	TORC2 complex
	extrinsic to internal side of plasma membrane
	membrane fraction
	mitochondrion
	vacuolar membrane
Acc1	endoplasmic reticulum membrane
	mitochondrion
Gys2	cytoplasm
Gph1	cytoplasm

Table A.2.3. Cellular component terms of the proteins that interact physically with Pkh1.

Protein Name	**Cellular Component**
Ypk1	cellular bud neck
	cytosol
	plasma membrane
Ypk2	cytoplasm
	nucleus
Sch9	fungal-type vacuole membrane
	nucleus
Myo5	actin cortical patch
	mating projection tip
	myosin complex
Lsp1	eisosome
	mitochondrial outer membrane
	plasma membrane enriched fraction
Pil1	eisosome
	lipid particle
	mitochondrial outer membrane
	plasma membrane enriched fraction
Ssb1	cytoplasm
	plasma membrane enriched fraction
	polysome
	soluble fraction
Set5	cytoplasm
	nucleus
Hsp82	cytoplasm
Bmh2	cytoplasm
	nucleus
	plasma membrane enriched fraction
Reb1	nucleus
Aep3	extrinsic to membrane
	mitochondrial inner membrane
Tpk3	cAMP-dependent protein kinase complex
	cytoplasm
	nucleus
Yrf1-4	nucleus

Table A.2.4. Cellular component terms of the proteins that interact physically with Ypk1.

Protein Name	**Cellular Component**
Tor1	Golgi membrane
	TORC1 complex
	endosome membrane
	extrinsic to internal side of plasma membrane
	membrane fraction
	nucleus
	vacuolar membrane
Tor2	TORC1 complex
	TORC2 complex
	extrinsic to internal side of plasma membrane
	membrane fraction
	mitochondrion
	vacuolar membrane
Ypk2	cytoplasm
	nucleus
Pkh1	cytosol
Hsp82	cytoplasm
Bmh2	cytoplasm
	nucleus
	plasma membrane enriched fraction
Hsc82	mitochondrion
	plasma membrane enriched fraction
Tec1	nucleus
Leu9	mitochondrion
Avo2	TORC2 complex
	plasma membrane
	vacuolar membrane
Ubi4	cytosolic large ribosomal subunit
	mitochondrion
	nucleus
Crn1	actin cortical patch
Rpn3	proteasome regulatory particle, lid subcomplex
Inp52	actin cortical patch
	mating projection tip
	vesicular fraction
Ncs2	cytosol
Sac6	actin cortical patch
	actin filament bundle
	mating projection tip
Slm1	mitochondrion

Table A.2.5. Cellular component terms of the proteins that interact physically with Ypk2.

Protein Name	**Cellular Component**
Tor2	TORC1 complex
	TORC2 complex
	extrinsic to internal side of plasma membrane
	membrane fraction
	mitochondrion
	vacuolar membrane
Ypk1	cellular bud neck
	cytosol
	plasma membrane
Pkh1	cytosol
Arg81	cytoplasm
	nucleus
Pet112	glutamyl-tRNA(Gln) amidotransferase complex Ref.6
	mitochondrion
Myo5	actin cortical patch
	mating projection tip
	myosin complex
Prb1	fungal-type vacuole lumen
Ubi4	cytosolic large ribosomal subunit
	mitochondrion
	nucleus
Tfp1	endomembrane system
	fungal-type vacuole membrane
	vacuolar proton-transporting V-type ATPase, V1 domain
Cdc33	eukaryotic translation initiation factor 4F complex
	nucleus
	ribosome
	stress granule
Snf1	AMP-activated protein kinase complex
	cytoplasm
	plasma membrane

Table A.2.6. Cellular component terms of the proteins that interact genetically with Pkh1.

Protein Name	**Cellular Component**
Ypk1	cellular bud neck
	cytosol
	plasma membrane
Ypk2	cytoplasm
	nucleus
Sch9	fungal-type vacuole membrane
	nucleus
Tos3	cytoplasm
Sgv1	cyclin-dependent protein kinase holoenzyme complex
	nucleus
Sip1	AMP-activated protein kinase complex
	fungal-type vacuole
	vacuolar membrane
Mnn11	alpha-1,6-mannosyltransferase complex
	integral to membrane
Cup2	nucleus
Hsp82	cytoplasm
Slm1	mitochondrion
	plasma membrane
	plasma membrane enriched fraction
Ypt6	Golgi apparatus
	plasma membrane
Cdc8	cytoplasm
	nucleus
Mck1	soluble fraction
Ncs2	cytosol
Hsc82	mitochondrion
	plasma membrane enriched fraction
Myo5	actin cortical patch
	mating projection tip
	myosin complex
Ras2	intracellular
	plasma membrane
	plasma membrane enriched fraction

Table A.2.7. Cellular component terms of the proteins that interact genetically with Ypk1.

Protein Name	**Cellular Component**
Ypk2	cytoplasm
	nucleus
Pkh1	cytosol
Pkh2	
Tor1	Golgi membrane
	TORC1 complex
	endosome membrane
	extrinsic to internal side of plasma membrane
	membrane fraction
	nucleus
	vacuolar membrane
Pkc1	cytoplasm
	cytoskeleton
	nucleus
	plasma membrane enriched fraction
	site of polarized growth
Hsp82	cytoplasm
Bmh2	cytoplasm
	nucleus
	plasma membrane enriched fraction
Bmh1	nucleus
	plasma membrane enriched fraction
Knh1	extracellular region
	fungal-type cell wall
Skt5	cellular bud neck
	incipient cellular bud site
	plasma membrane
Exg1	extracellular region
	fungal-type cell wall
Cts2	cytoplasm
	extracellular region
Rps6b	90S preribosome
	cytosolic small ribosomal subunit
	nucleolus
	small-subunit processome
Srb4	mediator complex
Smp1	cytoplasm
	nucleus
Ypc1	
	Golgi membrane

Table A.2.7. Cellular component terms of the proteins that interact genetically with Ypk1 *(Continued).*

Protein Name	**Cellular Component**
	endoplasmic reticulum membrane
	integral to membrane
Frq1	Golgi membrane
	cellular bud membrane
Sli1	endoplasmic reticulum
Clb6	nucleus
Avo2	TORC2 complex
	plasma membrane
	vacuolar membrane
Tsc11	TORC2 complex
	membrane fraction
	plasma membrane
	vacuolar membrane
Hlj1	endoplasmic reticulum membrane
Hsc82	mitochondrion
	plasma membrane enriched fraction
Sac7	cytoplasm
	cytoskeleton
Jnm1	cytoplasm
	dynactin complex
	dynein complex
Got1	ER to Golgi transport vesicle
	Golgi membrane
	endoplasmic reticulum
	integral to membrane
Ymr291w	cytoplasm
	nucleus

Table A.2.8. Cellular component terms of the proteins that interact genetically with Ypk2.

Protein Name	**Cellular Component**
Tor2	TORC1 complex
	TORC2 complex
	extrinsic to internal side of plasma membrane
	membrane fraction
	mitochondrion
	vacuolar membrane
Ypk1	cellular bud neck
	cytosol
	plasma membrane
Avo2	TORC2 complex
	plasma membrane
	vacuolar membrane
Tsc11	TORC2 complex
	membrane fraction
	plasma membrane
	vacuolar membrane
Myo5	actin cortical patch
	mating projection tip
	myosin complex

A.3. Function

Table A.3.1. Molecular function terms of the significant proteins in insulin signaling pathway.

Protein Name	Isoforms	Molecular Function
PDK 1/2		3-phosphoinositide-dependent protein kinase activity
		ATP binding
		protein binding
Akt	Akt3	ATP binding
		protein binding
		protein serine/threonine kinase activity
	Akt1	ATP binding
		protein serine/threonine kinase activity
	Akt2	ATP binding
		protein binding
		protein serine/threonine kinase activity
JNK	MAPK8	ATP binding
		JUN kinase activity
		protein binding
	MAPK10	ATP binding
		JUN kinase activity
		MAP kinase kinase activity Ref.1
aPKC	PRKCI	ATP binding
		diacylglycerol binding
		phospholipid binding
		protein binding
		protein kinase C activity
		zinc ion binding
	PRKCZ	ATP binding
		protein binding
		protein serine/threonine kinase activity
AMPK	PRKAA1	ATP binding
		cAMP-dependent protein kinase activity
		magnesium ion binding
		protein binding
	PRKAA2	ATP binding
		magnesium ion binding
		protein binding
		protein serine/threonine kinase activity
PYK	PKLR	magnesium ion binding
		potassium ion binding
		pyruvate kinase activity
	PKM2	magnesium ion binding
		potassium ion binding

Table A.3.1. Molecular function terms of the significant proteins in insulin signaling pathway *(Continued).*

Protein Name	**Isoforms**	**Molecular Function**
FBP	FBP1	fructose 1,6-bisphosphate 1-phosphatase activity
		fructose-2,6-bisphosphate 2-phosphatase activity
		identical protein binding
		magnesium ion binding
TC10		GBD domain binding
		GTP binding
		GTPase activity
		profilin binding
GSK-3b		ATP binding
		NF-kappaB binding
		beta-catenin binding
		glycogen synthase kinase 3 activity
		p53 binding
		protein kinase A catalytic subunit binding
		tau-protein kinase activity
PP1	PPP1CA	phosphoprotein phosphatase activity
	PPP1CB	protein binding
		protein serine/threonine phosphatase activity
	PPP1CC	iron ion binding
		manganese ion binding
		protein kinase binding
		protein serine/threonine phosphatase activity
PKA	PRKACA	ATP binding
		cAMP-dependent protein kinase activity
		protein kinase binding
	PRKACB	ATP binding
		protein serine/threonine kinase activity
	PRKACG	ATP binding
		cAMP-dependent protein kinase activity
	PRKX	ATP binding
		cAMP-dependent protein kinase activity
	PRKY	ATP binding
		protein serine/threonine kinase activity
Raptor		binding
p70s6k	RPS6KB1	ATP binding
		protein serine/threonine kinase activity
	RPS6KB2	ATP binding
		protein serine/threonine kinase activity
MEK1/2	MAP2K1	ATP binding
		MAP kinase kinase activity
		protein serine/threonine kinase activity

Table A.3.1. Molecular function terms of the significant proteins in insulin signaling pathway *(Continued).*

Protein Name	**Isoforms**	**Molecular Function**
	MAP2K2	ATP binding
		protein binding
		protein serine/threonine kinase activity
		protein tyrosine kinase activity
ERK1/2	MAPK1	ATP binding
		MAP kinase 2 activity
		MAP kinase activity
		phosphotyrosine binding
	MAPK3	ATP binding
		MAP kinase activity
PFK	PFKM	6-phosphofructokinase activity
		ATP binding
		fructose-6-phosphate binding
		identical protein binding
		kinase binding
		magnesium ion binding
		protein C-terminus binding
	PFKP	6-phosphofructokinase activity
		ATP binding
		magnesium ion binding
		protein binding
PFK	PFKL	6-phosphofructokinase activity
mTOR		phosphoprotein binding
		protein serine/threonine kinase activity
ACC	ACACA	ATP binding
		acetyl-CoA carboxylase activity
		biotin binding
		biotin carboxylase activity
		manganese ion binding
		protein binding
	ACACB	ATP binding
		acetyl-CoA carboxylase activity
		biotin binding
		biotin carboxylase activity
		manganese ion binding
GYS	GYS1	glycogen (starch) synthase activity
		protein binding
	GYS2	glycogen (starch) synthase activity
		protein homodimerization activity
PYG	PYGB	glycogen phosphorylase activity

Table A.3.1. Molecular function terms of the significant proteins in insulin signaling pathway *(Continued).*

Protein Name	**Isoforms**	**Molecular Function**
		bile acid binding
		drug binding
		glucose binding
		glycogen phosphorylase activity
		protein homodimerization activity
		purine binding
		pyridoxal phosphate binding
	PYGM	glycogen phosphorylase activity
		nucleotide binding
		protein binding
		pyridoxal phosphate binding

Table A.3.2. Molecular function terms of the proteins found by BLAST.

Protein Name	**Molecular Function**
Pkh1	ATP binding
	protein binding
	protein serine/threonine kinase activity
Ypk1	ATP binding
	protein binding
	protein serine/threonine kinase activity
Hog1	ATP binding
	MAP kinase activity
	identical protein binding
Pkc1	ATP binding
	metal ion binding
	protein binding
	protein kinase C activity
Snf1	protein binding
Pyk2	ATP binding
	magnesium ion binding
	potassium ion binding
	pyruvate kinase activity
Rim11	ATP binding
	identical protein binding
	protein serine/threonine kinase activity
Glc7	protein phosphatase 1 binding
	protein phosphatase type 1 regulator activity
Tpk2	ATP binding
	cAMP-dependent protein kinase activity
	protein binding
Kog1	protein binding
Ypk2	ATP binding
	protein binding
	protein serine/threonine kinase activity
Pbs2	ATP binding
	MAP kinase kinase activity
	MAP-kinase scaffold activity
	peptide alpha-N-acetyltransferase activity

Table A.3.2. Molecular function terms of the proteins in yeast found by BLAST (Continued).

Protein Name	**Molecular Function**
Fus3	ATP binding
	MAP kinase activity
	protein binding
Pfk2	6-phosphofructokinase activity
	ATP binding
	protein binding
Tor2	1-phosphatidylinositol 4-kinase activity
	ATP binding
	protein binding
	protein serine/threonine kinase activity
Acc1	ATP binding
	acetyl-CoA carboxylase activity
	biotin binding
	biotin carboxylase activity
	metal ion binding
Gys2	glycogen (starch) synthase activity
	identical protein binding
Gph1	glycogen phosphorylase activity
	protein binding
	pyridoxal phosphate binding

Table A.3.3. Molecular function terms of the proteins that interact physically with Pkh1.

Protein Name	**Molecular Function**
Ypk1	ATP binding
	protein binding
	protein serine/threonine kinase activity
Ypk2	ATP binding
	protein binding
	protein serine/threonine kinase activity
Sch9	ATP binding
	protein binding
	protein serine/threonine kinase activity
Myo5	ATP binding
	actin binding
	identical protein binding
	microfilament motor activity
Lsp1	protein binding
	protein kinase inhibitor activity
Pil1	protein binding
	protein kinase inhibitor activity
Ssb1	ATP binding
	ATPase activity
	calmodulin binding
	unfolded protein binding
Set5	methyltransferase activity
Hsp82	ATP binding
	ATPase activity, coupled
	unfolded protein binding
Bmh2	DNA replication origin binding
	protein domain specific binding
Reb1	RNA polymerase I transcription termination factor activity
	RNA polymerase II transcription factor activity
	sequence-specific DNA binding
Tpk3	ATP binding
	cAMP-dependent protein kinase activity
	protein binding
Yrf1-4	ATP binding
	ATP-dependent helicase activity
	DNA helicase activity
	nucleic acid binding
	protein binding

Table A.3.4. Molecular function terms of the proteins that interact physically with Ypk1.

Protein Name	**Molecular Function**
Tor1	ATP binding
	protein binding
	protein serine/threonine kinase activity
Tor2	1-phosphatidylinositol 4-kinase activity
	ATP binding
	protein binding
	protein serine/threonine kinase activity
Ypk2	ATP binding
	protein binding
	protein serine/threonine kinase activity
Pkh1	ATP binding
	protein binding
	protein serine/threonine kinase activity
Pkh2	ATP binding
	protein serine/threonine kinase activity
Hsp82	ATP binding
	ATPase activity, coupled
	unfolded protein binding
Bmh2	DNA replication origin binding
	protein domain specific binding
Hsc82	ATP binding
	unfolded protein binding
Tec1	sequence-specific DNA binding
	specific RNA polymerase II transcription factor activity
	transcription factor activity
Leu9	2-isopropylmalate synthase activity
	protein binding
Avo2	protein binding
Ubi4	protein binding
	structural constituent of ribosome
Crn1	actin filament binding
	microtubule binding
	protein binding, bridging
Rpn3	enzyme regulator activity
	protein binding
Inp52	phosphatidylinositol-3,5-bisphosphate 5-phosphatase activity
	phosphatidylinositol-3-phosphatase activity
	phosphatidylinositol-4,5-bisphosphate 5-phosphatase activity
	phosphatidylinositol-4-phosphate phosphatase activity
	protein binding

Table A.3.4. Molecular function terms of the proteins that interact physically with Ypk1 *(Continued).*

Protein Name	**Molecular Function**
Ncs2	protein binding
	tRNA binding
Sac6	actin filament binding
	calcium ion binding
	protein binding, bridging
Slm1	identical protein binding
	phosphoinositide binding

Table A.3.5. Molecular function terms of the proteins that interact physically with Ypk2.

Protein Name	**Molecular Function**
Tor2	1-phosphatidylinositol 4-kinase activity
	ATP binding
	protein binding
	protein serine/threonine kinase activity
Ypk1	ATP binding
	protein binding
	protein serine/threonine kinase activity
Pkh1	ATP binding
	protein binding
	protein serine/threonine kinase activity
Arg81	transcription cofactor activity
	transcription factor activity
	zinc ion binding
Pet112	ATP binding
	glutaminyl-tRNA synthase (glutamine-hydrolyzing) activity
Myo5	ATP binding
	actin binding
	identical protein binding
	microfilament motor activity
Prb1	identical protein binding
	serine-type endopeptidase activity
Ubi4	protein binding
	structural constituent of ribosome
Tfp1	ATP binding
	DNA binding
	endodeoxyribonuclease activity
	hydrogen ion transporting ATP synthase activity, rotational mechanism
	protein binding
	proton-transporting ATPase activity, rotational mechanism
Cdc33	RNA binding
	phosphatidylinositol-3-phosphate binding
	protein binding
	translation initiation factor activity
Snf1	protein binding

Table A.3.6. Molecular function terms of the proteins that interact genetically with Pkh1.

Protein Name	**Molecular Function**
Ypk1	ATP binding
	protein binding
	protein serine/threonine kinase activity
Ypk2	ATP binding
	protein binding
	protein serine/threonine kinase activity
Sch9	ATP binding
	protein binding
	protein serine/threonine kinase activity
Tos3	ATP binding
	protein serine/threonine kinase activity
Sgv1	ATP binding
	RNA polymerase II carboxy-terminal domain kinase activity
	cyclin-dependent protein kinase activity
	protein binding
Sip1	protein binding
Mnn11	alpha-1,6-mannosyltransferase activity
	protein binding
Cup2	copper ion binding
	ligand-regulated transcription factor activity
	protein binding
	transcription factor activity
Hsp82	ATP binding
	ATPase activity, coupled
	unfolded protein binding
Slm1	identical protein binding
	phosphoinositide binding
Ypt6	GTP binding
	GTPase activity
	protein binding
Cdc8	ATP binding
	identical protein binding
	thymidylate kinase activity
	uridylate kinase activity
Mck1	ATP binding
	protein binding
	protein serine/threonine kinase activity
	protein serine/threonine/tyrosine kinase activity
Ncs2	protein binding
	tRNA binding

Table A.3.6. Molecular function terms of the proteins that interact genetically with Pkh1 *(Continued).*

Protein Name	**Molecular Function**
Hsc82	ATP binding
	unfolded protein binding
Myo5	ATP binding
	actin binding
	identical protein binding
	microfilament motor activity
Ras2	GTP binding
	GTPase activity
	protein binding

Table A.3.7. Molecular function terms of the proteins that interact genetically with Ypk1.

Protein Name	**Molecular Function**
Ypk2	ATP binding
	protein binding
	protein serine/threonine kinase activity
Pkh1	ATP binding
	protein binding
	protein serine/threonine kinase activity
Pkh2	ATP binding
	protein serine/threonine kinase activity
Tor1	ATP binding
	protein binding
	protein serine/threonine kinase activity
Pkc1	ATP binding
	metal ion binding
	protein binding
	protein kinase C activity
Hsp82	ATP binding
	ATPase activity, coupled
	unfolded protein binding
Bmh2	DNA replication origin binding
	protein domain specific binding
Bmh1	DNA replication origin binding
	protein domain specific binding
Skt5	binding
	enzyme activator activity
Exg1	cation binding
	glucan 1,3-beta-glucosidase activity
Cts2	cation binding
	chitinase activity
Rps6b	structural constituent of ribosome
Srb4	RNA polymerase II transcription mediator activity
	protein binding
Smp1	DNA bending activity
	sequence-specific DNA binding
Ypc1	transcription factor activity
	phytoceramidase activity
	protein binding
	sphingosine N-acyltransferase activity
Frq1	calcium ion binding
	enzyme activator activity
	identical protein binding

Table A.3.7. Molecular function terms of the proteins that interact genetically with Ypk1 *(Continued).*

Protein Name	**Molecular Function**
Sli1	N-acetyltransferase activity
	alcohol O-acetyltransferase activity
Clb6	cyclin-dependent protein kinase regulator activit
	protein binding
Avo2	protein binding
Tsc11	guanyl-nucleotide exchange factor activity
	protein binding
Hlj1	ATPase activator activity
	heat shock protein binding
	unfolded protein binding
Hsc82	ATP binding
	unfolded protein binding
Sac7	Rho GTPase activator activity
	protein binding
Jnm1	motor activity
	protein binding
	structural constituent of cytoskeleton
Got1	protein binding
Ymr291w	ATP binding
	protein serine/threonine kinase activity

Table A.3.8. Molecular function terms of the proteins that interact genetically with Ypk2.

Protein Name	**Molecular Function**
Tor2	1-phosphatidylinositol 4-kinase activity
	ATP binding
	protein binding
	protein serine/threonine kinase activity
Ypk1	ATP binding
	protein binding
	protein serine/threonine kinase activity
Avo2	protein binding
Tsc11	guanyl-nucleotide exchange factor activity
	protein binding
Myo5	ATP binding
	actin binding
	identical protein binding
	microfilament motor activity

APPENDIX B: THE CONSUMPTION OF GLUCOSE IN THE MEDIUM

Table B.1. The consumption of glucose in the medium (at 20 g/l initial concentration).

Time (Hour)	The Concentration of Glucose (g/l)			
	Wild Type	**Ypk1**	**Ypk2**	**Pkh1**
16	1,91	6,16	0,59	2,52
18	0,9	5,26	0,16	1,88
20	0,06	4,97	0,23	1,21
23	0,15	4,34	0,15	0,1
26	0,3	3,23	0,25	0

Table B.2. The glucose consumption in the medium (at 30g/l initial glucose concentration).

Time (Hour)	The Concentration of Glucose (g/l)			
	Wild Type	**Ypk1**	**Ypk2**	**Pkh1**
16	14,83	26,98	16,23	17,08
18	9,96	18,69	13,36	15,72
20	7,94	8,96	11,33	13,18
24	5,41	12,16	6,34	8,44
26	3,51	9,77	4,49	6,43

Table B.3. The glucose consumption in the medium (at 40g/l initial glucose concentration).

Time (Hour)	The Concentration of Glucose (g/l)			
	Wild Type	**Ypk1**	**Ypk2**	**Pkh1**
24	2.74	8.78	4.54	3.07
26	0.63	5.46	2.21	0.71
28	0.58	4.03	1.43	0.69

REFERENCES

Bartlett, G. J., C. T. Porter, N. Borkakoti and J. M. Thornton, 2002, "Analysis of Catalytic Residues in Enzyme Active Sites", Journal of Molecula Biology, Vol. 324, pp. 105–121, November.

Bryant, N. J., R. Govers and D. E. James, 2002, "Regulated transport of the glucose transporter GLUT4", Vol. 3, pp. 267-277, April.

Carlson, H. A., R. D. Smith, N. A. Khazanov, P. D. Kirchhoff, J. B. Dunbar and M. L. Benson, 2008, "Differences between High- and Low-Affinity Complexes of Enzymes and Nonenzymes", *Journal* of Medicinal Chemistry, Vol. 51, pp. 6432-6441, October.

Cheng, J. Q., C. W. Lindsley, G. Z. Cheng, H. Yang, S. V. Nicosia, 2005, "The Akt/PKB pathway: molecular target for cancer drug discovery", Oncogene, Vol. 24, pp. 7482-7492, July.

Cho, H., J. L. Thorvaldsen, Q. Chu, F. Feng, M. J. Birnbaum, 2001, "Akt1/PKB is required for normal growth but dispensable for maintenance of glucose homeostasis in Mice", Journal of Biological Chemistry, Vol. 276, pp. 38349-38352, October.

Cho, C. R., M. Labow, M. Reinhardt, J. V. Oostrum, M. C. Peitsch, 2006, "The Application of systems biology to drug discovery", Current Opinion in Chemical Biology, Vol. 10, pp. 294-302, July.

Cowart, L.A. and L. M Obeid, 2006, "Yeast sphingolipids: Recent developments in understanding biosynthesis, regulation and function", Biochimica et Biophysica Acta, Vol. 1771, pp.421-431, August.

deHart, A.K. A., J. D. Schnell, D. A. Allen, and L. Hicke, 2002, "The Conserved Pkh-Ypk Kinase Cascade is Required for Endocytosis in Yeast", Journal of Cell Biology, Vol. 156, pp. 241-248, January.

Dickson, R. C., C. Sumanasekera and R. L. Lester, 2006, "Function and metabolism of sphingolipids in Saccharomyces cerevisiae", Progress in Lipid Research, Vol. 45, pp. 447-465, November.

Dickson, R. S., 2008 "*Thematic Review Series: Sphingolipids.* New insights into Sphingolipid Metabolism and Function in Budding Yeast", Journal of Lipid Research, Vol. 49, pp. 909-921, May.

Dundas, J., Z. Ouyang, J. Tseng, A. Binkowski, Y. Turpaz, J, Liang, 2006, "CASTp: Computed Atlas of Surface Topography of Proteins with Structural and Topographical Mapping of Functionally Annotated Residues", Nucleic Acids Research, Vol. 34, pp. 116-118, April.

Dyatlovitskaya, E. V., 1999, "The Interrelation between the Biological Functions of Sphingolipids and Their Chemical Structure", Russian Journal of Bioorganic Chemistry, Vol. 26, pp. 9-15, August.

Easton, R. M., H. Cho, K. Roovers, D. W. Shineman, M. Mizrahi, M. S. Forman, V. M. Lee, M. Szabolcs, R. D. Jong, T. Oltersdorf, T. Ludwig, A. Efstratiadis, M. J. Birnbaum, 2005, " Role of Akt3/Protein Kinase B in attainment of normal brain size", Molecular and Cellular Biology, Vol. 25, pp. 1869-1878, March.

Fahy, E., S. Subramaniam, H. A. Brown, C. K. Glass, A. H. Merrill Jr., R. C. Murphy, C. R.H. Raetz, D. W. Russell, Y. Seyama, Wç Shaw, T. Shimizu, F. Spener, G. Meer, M. S. VanNieuwenhze, S. H. White, J. Witztum, and E. A. Dennis, 2005, "A Comprehensive Classification System for Lipids", Journal of Lipid Research, Vol. 46, pp. 839-861, February.

Friant, S., R. Lombardi, T. Schmelzle, M. N. Hall and H. Riezman, 2001, "Sphingoid Base Signaling via Pkh Kinases is Required for Endocytosis in Yeast", EMBO Journal, Vol. 20, pp. 6783-6792, October.

Ginzburg, L., Y. Kacher and A. H. Futerman, 2004, "The pathogenesis of glycosphingolipid storage disorders", Seminars in Cell and Developmental Biology, Vol. 15, pp. 417-431, August.

Grosshans, B.L., H. Grötsch, D. Mukhopadhyay, I. M. Fernández, J. Pfannstiel, F. Z. Idrissi, J. Lechner, H. Riezman and M. I. Geli, 2006, "TEDS Site Phosphorylation of the Yeast Myosins I Is Required for Ligand-induced but Not for Constitutive Endocytosis of the G Protein-coupled Receptor Ste2p", Journal of Biological Chemistry, Vol. 281, pp. 11104-11114, April.

Hernandez, M., D. Ghersi and R. Sanchez, 2009, "SITEHOUND-web: a Server for Ligand Binding Site Identification in Protein Structures", Nucleic Acids Research, Vol.37, pp. 413-416, April.

Henrich, S., O. M. H. Salo-Ahena, B. Huang, F. F. Rippmann, G. Cruciani, R. C. Wade, 2009, "Computational Approaches to Identifying and Characterizing Protein Binding Sites for Ligand Design", Journal of Molecular Recognition, Doi:10.1002/jmr.984, July.

Hirabayashi, Y., Y. Igarashi and A. H. Merrill, 2006, Sphingolipid Biology, Springer, New York.

Hannun, Y. A. and L. M Obeid, 2002, "The Ceramide-centric Universe of Lipid-mediated Cell Regulation: Stress Encounters of the Lipid Kind", The Journal of Biological Chemistry, Vol. 227, pp. 25847-25850, July.

Hannun, Y. A. and L.M. Obeid, 2008, "Principles of bioactive lipid signaling: lessons from sphingolipids", Molecular Cell Biology, Vol. 9, pp. 139-150, February.

Holland, W. L. and S. A. Summer, 2008, "Sphingolipids, Insulin Resistance, and Metabolic Disease: New Insights from *in Vivo* Manipulation of Sphingolipid Metabolism", Endocrine Reviews, Vol. 29, No. 4, pp. 381-402, June.

Jiang, Z. Y., Q. L. Zhou, K. A. Coleman, M. Chouinard, Q. Boese, M. P. Czech, 2003, "Insulin signaling through Akt/protein kinase B analyzed by small interfering RNA-mediated gene silencing", Proceedings of the National Academy of Sciences, Vol. 100, pp. 7569-7574, June.

Kamada, Y., Y. Fujioka, N. N. Suzuki, F. Inagaki, S. Wullschleger, R. Loewith, M. N. Hall, and Y. Ohsumi, 2005, "Tor2 Directly Phosphorylates the AGC Kinase Ypk2 To Regulate Actin Polarization", Molecular and Cellular Biology, Vol. 25, pp. 7239-7248, August.

Kanehisa, M., S. Goto, M. Furumichi, M. Tanabe and M. Hirakawa, 2009, "KEGG for Representation and Analysis of Molecular Networks Involving Diseases and Drugs", Nucleic Acids Research, Vol. 38, pp. 355-360, October.

Landau, M., I. Mayrose, Y. Rosenberg, F. Glaser, E. Martz, T. Pupko and N. Ben-Tal, 2005, "ConSurf 2005: The Projection of Evolutionary Conservation Scores of Residues on Protein Structures", Nucleic Acids Research, Vol. 33, pp.299-302, February.

Sanschagrin, P. C. and L. A. Kuhn, 1998, "Cluster Analysis of Consensus Water Sites in Thrombin and Trypsin Shows Conservation between Serine Proteases and Contributions to Ligand Specificity" Protein Science, Vol. 7, pp. 2054-2064, October.

Langeveld, M. and J. Aerts, 2009, "Glycosphingolipids and insulin resistance", Progress in Lipid Research, Vol.48; No. 3-4, pp. 196-205, May-July.

Laurie, A. T. R. and R. M. Jackson, 2005, "Q-SiteFinder: an energy-based method for the prediction of protein–ligand binding sites", Structural Bioinformatics, Vol. 21, pp.1908-1916, February.

Liang, J., H. Edelsbrunner and C. Woodward, 1998, "Anatomy of protein pockets and cavities: Measurement of Binding Site Geometry and Implications for Ligand Design", Protein Science, Vol. 7, pp. 1884-1897, April.

Lindsley C. W., Z. Zhao, W. H. Leister, R. G. Robinson, S. F. Barnett, D. Defeo-Jones, R. E. Jones, G. D. Hartman, J. R. Huff , H. E. Hubera, M. E. Duggan, 2005, "Allosteric Akt (PKB) inhibitors: discovery and SAR of isozyme selective inhibitors", Bioorganic and Medicinal Chemistry Letters, Vol. 15, pp. 761-764, February.

*Liu,*K., *X. Zhang, R. L. Lester* and *R. C. Dickson,* 2005 "The Sphingoid Long Chain Base Phytosphingosine Activates AGC-type Protein Kinases in Saccharomyces *cerevisiae* Including Ypk1, Ypk2, and Sch9", Journal of Biological Chemistry, Vol. 280, pp. 22679-22687, June.

Luo, G., A. Gruhler, Y. Liu, O. N. Jensen and R. C. Dickson, 2008, "The Sphingolipid Long-chain Base-Pkh1/2-Ypk1/2 Signaling Pathway Regulates Eisosome Assembly and Turnover", Journal of Biological Chemistry, Vol. 283, pp. 10433-10444, April.

Medina-Franco, J. L., M. A. Giulianotti, Y. Yu, L. Shen, L. Yao, N. Singh, 2009, "Discovery of a novel protein kinase B inhibitor by structure-based virtual screening", Bioorganic and Medicinal Chemistry Letters, Vol. 19, pp. 4634-4638, August.

Nayal, M. and B. Honig, 2009, "On the Nature of Cavities on Protein Surfaces: Application to the Identification of Drug-Binding Sites", PROTEINS: Structure, Function and Bioinformatics, Vol. 63, pp. 892-906, February.

Ogretmen, B. and Y. Hannun, 2004, "Biologically Active Sphingolipids in Cancer Pathogenesis and Treatment", Nature Reviews Cancer, Vol. 4, pp. 604-616, August.

Ogretmen, B., 2006, "Sphingolipids in Cancer: Regulation of Pathogenesis and Therapy", FEBS Letter, Vol. 580, pp. 5467-5476, August.

Park, T. S., R. L. Panek, M. D. Rekhter, S. B. Mueller, W. S. Rosebury, A. Robertson, J. C. Hanselman, E. Kindt, R. Homan and S. K. Karathanasis, 2006, "Modulation of lipoprotein metabolism by inhibiton of sphingomyelin synthesis in ApoE knockout mice", Atherosclerosis, Vol. 189, pp. 264-272, December.

Payne, S. G., S. Milstien and S. Spiegel, 2002, "Sphingosine-1-phosphate: dual messenger functions", Lipid Signaling: Cellular Events and their Biophysical Mechanisms, Vol. 531, pp. 54-57, October.

Pupko, T., R. E. Bell, I. Mayrose, F. Glaser and N. Ben-Tal, 2002, "Rate4Site: An Algorithmic Tool for The Identification of Functional Regions in Proteins by Surface Mapping of Evolutionary Determinants Within Their Homologues", Bioinformatics, Vol. 18, pp. 71–77, April.

Roelants, F. M., P. D. Torrance, N. Bezman, and J. Thorner, 2002, "Pkh1 and Pkh2 Differentially Phosphorylate and Activate Ypk1 and Ykr2 and Define Protein Kinase Modules Required for Maintenance of Cell Wall Integrity", Molecular Biology of the Cell, Vol.13, pp. 3005-3028, September.

Saltiel, A. R. and J. E. Pessin, 2002, "Insulin Signaling Pathways in Time and Space", Trends in Cell Biology, Vol. 12, pp. 65-71, February.

Sawai, H., N. Domae and T. Okazaki, 2005, "Current status and perspectives in ceramide targeting molecular medicine", Current Pharmaceutical Design, Vol. 15, pp. 2479-2487, July.

Saxty, G., S. J. Woodhead, V. Berdini, T. G. Davies, M. L. Verdonk, P. G. Wyatt, R. G. Boyle, D. Barford, R. Downham, M. D. Garrett, R. A. Carr, 2007, "Identification of Inhibitors of Protein Kinase B Using Fragment-Based Lead Discovery", Journal of Medicinal Chemistry, Vol. 50, pp. 2293-2296, January.

Schmelzle, T., S. B. Helliwell, and M. N. Hall, 2002, "Yeast Protein Kinases and the RHO1 Exchange Factor TUS1 are Novel Components of the Cell Integrity Pathway in Yeast", Molecular and Cellular Biology, Vol. 22, pp. 1329-1339, March.

Schmitz-Peiffer, C., 2000, "Signaling aspects of insulin resistance in skeletal muscle: mechanisms induced by lipid oversupply", Cellular Signaling, Vol. 12, pp. 583-594, July.

Seco, J., F. J. Luque and X. Barril, 2009, “Binding Site Detection and Druggability Index from First Principles”, Journal of Medicinal Chemistry, Vol. 52, pp. 2363–2371, March.

Soga, S., H. Shirai, M. Kobori and N. Hirayama, 2007, “Use of Amino Acid Composition to Predict Ligand-Binding Sites” Journal of Chemical Information and Modeling, Vol. 47, pp. 400–406, January.

Stratford, S., K. L. Hoehn and S. A. Summers, 2004, “Regulation of insulin action by ceramide: dual mechanisms linking ceramide accumulation of Akt/protein kinase B”, Journal of Biological Chemistry, Vol. 279, pp. 36608-36615, August.

Summers, S. A., L. A. Garza, H. Zhou, M. J. Birnbaum, 1998, “Regulation of insulin stimulated glucose transporter GLUT4 translocation and Akt kinase activity by ceramide”, Molecular and Cell Biology, Vol. 18, pp. 57-64, September.

Summers, S. A., 2006, “Ceramides in insulin resistance and lipotoxicity”, Progress in Lipid Research, Vol. 45, pp. 42-72, January.

Ozbayraktar, F. B. K and K. Ulgen, 2010, “Drug target identification in sphingolipid metabolism by computational systems biology tools: Metabolic control analysis and metabolic pathway analysis”, Journal of Biomedical Informatics, doi:10.1016/j.jbi.2010.03.006.

Taniguchi, C. M., B. Emanuelli, C. R Kahn, 2006, “Critical nodes in signaling pathways: insight into insulin action”, Molecular Cell Biology, Vol. 7, pp. 85-96, February.

Tseng, Y. Y., C. Dupree, Z. J. Chen, W. H. Li, 2009, “SplitPocket: identification of protein functional surfaces and characterization of their spatial patterns”, Nucleic Acids Research, Vol. 37, pp. 384-389, April.

Wade, R. C. and P. J. Goodford, 1993, “Further Development of Hydrogen Bond Functions for Use in Determining Energetically Favorable Binding Sites on Molecules of

Known Structure. 2. Ligand Probe Groups with the Ability to Form Two Hydrogen Bonds" Journal of Medicinal Chemistry, Vol. 36, pp. 140-147, January.

Yücel, E., A. Cankorur, E. Dereli, F. Alazi, I. Aslandag, B. Kavun, S. D. Tekir, K. Y. Arga and K. O. Ulgen, 2008, "Deciphering the Cross-talk Between Sphingolipid Mechanism and Signaling Pathways in Baker's Yeast", Journal of Engineering and Natural Sciences, Vol. 26, pp. 162-174, May.